# Characterization of the immune system-drug interactions during anti-filarial treatment in the *Litomosoides sigmodontis* mouse model

Dissertation

zur Erlangung des Doktorgrades (Dr. rer. nat.)
der Mathematisch-Naturwissenschaftlichen Fakultät
der Rheinischen Friedrich-Wilhelms-Universität Bonn

vorgelegt von
**Frederic Risch**
aus
Bonn

Bonn, 2023

Angefertigt mit Genehmigung der Mathematisch-Naturwissenschaftlichen Fakultät der Rheinischen Friedrich-Wilhelms-Universität Bonn.

Prof. Dr. Marc P. Hübner

**Erster Gutachter**

Prof. Dr. Oliver Gruß

**Zweiter Gutachter**

Tag der Promotion: 30.11.2023

Erscheinungsjahr: 2024

**Erklärung**

Die hier vorgelegte Dissertation habe ich eigenständig und ohne unerlaubte Hilfsmittel angefertigt. Die Dissertation wurde in der vorgelegten oder in ähnlicher Form noch bei keinem anderen Institut eingereicht.

Es wurden keine vorherigen oder erfolglosen Promotionsversuche unternommen.

Bonn,

Teile dieser Arbeit wurden vorab veröffentlicht in folgenden Publikationen:

**Risch, F.*,** Ritter, M.*, Hoerauf, A., & Hübner, M. P. (2021). Human filariasis-contributions of the *Litomosoides sigmodontis* and *Acanthocheilonema viteae* animal model. *Parasitology research*, *120*(12), 4125–4143. https://doi.org/10.1007/s00436-020-07026-2

*gemeinsame Erstautoren

**Risch, F.,** Koschel, M., Lenz, B., Specht, S., Hoerauf, A., Hübner, M. P. & Scandale, I. (2022). Comparison of the macrofilaricidal efficacy of oxfendazole and its isomers against the rodent filaria *Litomosoides sigmodontis*. *Frontiers in Tropical Diseases*, 3. https://doi.org/10.3389/fitd.2022.982421

**Risch, F.,** Scheunemann, J. F., Reichwald, J. J., Lenz, B., Ehrens, A., Gal, J., Fercoq, F., Koschel, M., Fendler, M., Hoerauf, A., Martin, C., & Hübner, M. P. (2023). The efficacy of the benzimidazoles oxfendazole and flubendazole against *Litomosoides sigmodontis* is dependent on the adaptive and innate immune system. *Frontiers in Microbiology,* 14. https://doi.org/10.3389/fmicb.2023.1213143

## Table of Contents

## Summary

Filarial nematodes can cause debilitating diseases such as lymphatic filariasis and onchocerciasis. Both diseases are included in the list of neglected tropical diseases as defined by the World Health Organization (WHO) and targeted for elimination. There are currently no approved drugs available that can effectively clear the adult worms (= macrofilaricide) in a timely manner. Potential macrofilaricidal compounds that are in development include both directly acting drugs such as the benzimidazole oxfendazole (OXF) as well as indirectly acting drugs like corallopyronin A (CorA). OXF is currently under preparation for phase 2 clinical trials in filariasis patients while CorA is under preparation for phase 1 clinical trials.

This thesis aimed to investigate the immune system's role during treatment with OXF, flubendazole (FBZ) and CorA, and explore the potential to boost the treatment efficacy via stimulation of the immune system (combination therapy) in a rodent model system. Wild type (WT) BALB/c, eosinophil-deficient Δ*dblGata1*, *IL-4r/IL-5*$^{-/-}$, antibody-deficient µMT and B cell, T cell, and ILC-deficient *Rag2/IL-2rγ*$^{-/-}$ mice were infected with the rodent filaria *Litomosoides sigmodontis* and treated with OXF, FBZ and CorA starting at 35 days post infection (dpi). In the second part, WT mice were treated for a reduced duration with a combination of OXF and IL-4, IL-5, or IL-33.

A 5 day-treatment of WT mice reduced the median adult worm burden by up to 94% (OXF, administered orally) and 100% (FBZ, administered subcutaneously) compared to vehicle controls. In contrast, treatment efficacy was lower in all immunodeficient strains with a reduction of up to 90% (OXF) and 75% (FBZ) for Δ*dblGata1*, 50% and 92% for *IL-4r/IL-5*$^{-/-}$, 64% and 78% for µMT or 0% for *Rag2/IL-2rγ*$^{-/-}$ mice. The effect of OXF on microfilaremia and embryogenesis displayed a similar pattern, while FBZ's ability to prevent microfilaremia was independent of the host's immune status. Furthermore, flow cytometric analysis revealed strain- and treatment-specific immunological changes. Treatment with CorA did not result in the clearance of adult worms in either WT or immunodeficient mice and the depletion of *Wolbachia* was unaffected by the lack of eosinophils, IL-4 receptor or IL-5.

The efficacy of a shortened, suboptimal 3-day treatment of OXF (-33% adult worms vs. vehicle) could be boosted to a 91% median worm burden reduction via combination with IL-5, but not IL-4 or IL-33. The combination of OXF with IL-5 for 3 days reached a comparable efficacy as a standard 5-day OXF treatment. In addition, the number of microfilariae-positive animals was reduced in mice that received the combination of OXF with IL-5. A combination therapy for only two days, however, had no discernable effect on the adult worm burden.

Overall, this thesis demonstrates that various components of both the innate and adaptive immune system support the filaricidal efficacy of benzimidazoles *in vivo*. In addition, targeted stimulations of the immune system present an opportunity to boost the treatment efficacy or reduce the treatment duration required for worm clearance and thus present a novel therapeutic approach against filariae with OXF.

## Zusammenfassung

Filarien können die Auslöser schwerwiegender Krankheiten wie der lymphatischen Filariose und Onchozerkose sein. Beide Krankheiten werden von der Weltgesundheitsorganisation (WHO) als vernachlässigte Tropenkrankheiten definiert und sollen nach Willen der WHO eliminiert werden. Momentan gibt es keine Medikamente, die in der Lage sind, die adulten Filarien in einem realistischen Behandlungszeitraum von 1-2 Wochen im Menschen abzutöten (= makrofilarizid). Bei den potentiell makrofilariziden Substanzen, die sich momentan in der Entwicklung befinden, gibt es sowohl direkt wirkende Substanzen wie Oxfendazole (OXF) aus der Substanzklasse der Benzimidazole als auch indirekt wirkende Medikamente wie Corallopyronin A (CorA). Bei der Entwicklung von OXF werden momentan klinische Studien der Phase II vorbereitet während sich CorA noch in der präklinischen Entwicklung befindet.

In der vorliegenden Doktorarbeit wurde zunächst die Rolle des Immunsystems während der Behandlung mit OXF, FBZ und CorA untersucht. Darauf aufbauend wurde das Potential einer Kombinationstherapie erörtert, in der die Behandlungseffizienz durch die Stimulation des Immunsystems gesteigert werden sollte. Beide Ansätze wurden in einem Mausmodell untersucht. Hierfür wurden Wildtyp (WT) BALB/c Mäuse sowie Linien ohne Eosinophile (Δ*dblGata1*), ohne den IL-4 Rezeptor und IL-5 (*IL-4r/IL-5*$^{-/-}$), ohne T Zellen, B Zellen und ILCs (*Rag2/IL-2rγ*$^{-/-}$) und ohne reife B Zellen und Antikörper (μMT) mit der Nagetierfilarie *Litomosoides sigmodontis* infiziert und mit OXF, FBZ oder CorA behandelt. Im zweiten Teil wurde eine Kombinationstherapie getestet, bei der eine verkürzte Therapie von OXF zusammen mit einem von drei Zytokinen (IL-4, IL-5 oder IL-33) zur Behandlung eingesetzt wurde.

Eine fünf-tägige Behandlung in WT Mäusen führte zu einer Reduktion der Zahl der adulten Würmer um bis zu 94% im Falle von OXF (orale Behandlung) und 100% bei FBZ (subkutane Behandlung). In den Mauslinien mit eingeschränkter Immunantwort war die Behandlungseffizienz generell niedriger. In den Δ*dblGata1* Mäusen lag sie bei bis zu 90% (OXF) und 75% (FBZ), bei den *IL-4r/IL-5*$^{-/-}$ Mäusen bei 50% und 92%, bei den μMT Mäusen bei 64% und 78% und bei den *Rag2/IL-2rγ*$^{-/-}$ Mäusen bei 0%. Der Einfluss auf die Mikrofilarämie folgte bei der Behandlung mit OXF einem ähnlichen Muster während

die Behandlung mit FBZ uneingeschränkt in allen Linien die Entwicklung einer Mikrofilarämie verhinderte. Zusätzlich hierzu konnte die Analyse per Durchflusszytometrie sowohl linien- als auch behandlungsspezifische Muster in der Änderung der Frequenz und Anzahl von Immunzellen aufdecken. Die Behandlung mit CorA führte weder in den WT noch in den immundefizienten Linien zu einer Reduktion der Anzahl der erwachsenen Würmer und die Reduktion der *Wolbachia* war in allen Linien vergleichbar.

Im zweiten Teil konnte gezeigt werden, dass die Behandlung mit OXF für nur drei Tage lediglich zu einer Reduktion der Anzahl der erwachsenen Würmer von 33% reicht. Die Kombination mit IL-5 hingegen konnte die Reduktion auf 91% steigern und erreichte somit eine Effizienz, die mit einer Standardtherapie von 5 Tagen vergleichbar war. Die Kombinationen von OXF mit IL-4 oder IL-33 waren hierzu nicht in der Lage. Zusätzlich zu der Reduktion der adulten Würmer führte die Kombination von OXF mit IL-5 zu einer Verringerung der Anzahl der Mäuse, bei denen Mikrofilarien im Blut nachgewiesen werden konnte.

Insgesamt konnte in dieser Doktorarbeit gezeigt werden, dass Komponenten der angeboren und adaptiven Immunantwort die filarizide Wirkung von Benzimidazolen *in vivo* unterstützen. Zusätzlich konnte gezeigt werden, dass die gezielte Stimulation des Immunsystems zu einer Steigerung der Behandlungseffizienz bzw. möglichen Verkürzung der nötigen Behandlungsdauer eingesetzt werden kann, und somit neue therapeutische Ansätze basierend auf OXF für Filarien darstellt.

## List of Abbreviations

AB-PAS ……... Alcian Blue – Periodic Acid Schiff

ADLA ……... acute dermatolymphangioadenitis

AFL ……. acute filarial lymphangitis

ALB …… albendazole

A-WOL …… Anti-*Wolbachia* Consortium

BCE …….. before common era

BSA …….. bovine serum albumin

CD …….. cluster of differentiation

cDC1 ……. conventional dendritic cell 1

cDC2 ……. conventional dendritic cell 2

CeMIM ……. Centre de Microscopie et d'IMagerie numerique

CorA …… corallopyronin A

DEC ……... diethylcarbamazine

DC ……. dendritic cell

d$H_2O$ …….. distilled water

dpi …… days post infection

EDTA ……...… ethylenediaminetetraacetic acid

EPO ……... eosinophil peroxidase

FBS ……..…….... fetal bovine serum

FBZ …… flubendazole

FDA ……. Food and Drug Administration

Fig …….. figure

G-CSF ……. granulocyte-colony stimulating factor

γ-TuRC ……. γ-tubulin ring complex

H&E ……..... Hematoxylin and Eosin

IFN-$\alpha$ …….. interferon-$\alpha$

IFN-γ …… interferon-γ

IgG …….. immunoglobulin G

IL ……..……. interleukin

ILC ……. innate lymphoid cell

IMMIP …….. Institute for Medical Microbiology, Immunology and Parasitology

IVM …… ivermectin

MΦ ……. macrophage

MDA ……. mass drug administration

MF …….. microfilariae

MNHN ……. Muséum national d'Histoire naturelle

MPK …….. mg/kg

MTOC …….. microtubule organizing center

NK cells ……. natural killer cells

NTD …… neglected tropical disease

OAE ……... onchocerciasis associated epilepsy

OXF …… oxfendazole

PBS …… phosphate buffered saline

pDC ……..… plasmacytoid dendritic cell

PEG400 ……. polyethylene glycol 400

PVS …… perivascular adventitial spaces

RT ……. room temperature

RT-PCR …… real time polymerase chain reaction

spp …… species pluralis

syn ……... synonym

Th1 ……. T helper cell subset 1

Th2 ……. T helper cell subset 2

Th17 ……. T helper cell subset 17

Treg ……. regulatory T cell

TRP ……... transient receptor potential

WHO ……. World Health Organization

WSP ……... *Wolbachia* surface protein

WT …… wild type

## List of Figures

## List of Tables

# 1. Introduction

## 1.1 Filarial helminths and a brief description of our history

Loiasis, lymphatic filariasis (LF), mansonellosis and onchocerciasis are infectious diseases caused by filarial helminths (worms) that affect hundreds of millions of humans worldwide. Symptoms range from localized dermal swelling (‘Calabar swelling’) and subconjunctival migration of adult worms in the case of loiasis, lymphedema up to elephantiasis as well as hydrocele and chyluria for lymphatic filariasis, severe dermatitis and blindness for onchocerciasis and generally unspecific symptoms for mansonellosis [1-3]. These diseases can – with certain limitations that will be discussed later – be diagnosed, treated, to some extent cured and even potentially eliminated. According to our current classification, filarial helminths or filariae for short are parasitic organisms that belong to the phylum Nematoda or colloquially roundworms based on their typical cylindrical form [4,5].

Filariae share a common life cycle with a vertebrate definite and arthropod indefinite host, illustrated in figure 1 [6]. In general, arthropod vectors such as mosquitoes or flies take up the first larval stage known as microfilariae (MF) during a blood meal. The larvae develop inside the invertebrate host into the infective third larval stage (L3). During a second blood meal, infective L3 larvae are transmitted to the definite host where they migrate through the skin, tissues and vessels and ultimately develop into adult worms. The precise migration and eventual location of adult worms depend on the filarial species and will be discussed in more detail in later sections. Adult worms may then mate and produce MF, which are finally released into the surrounding tissue or bloodstream and can be taken up by a vector during another blood meal [6].

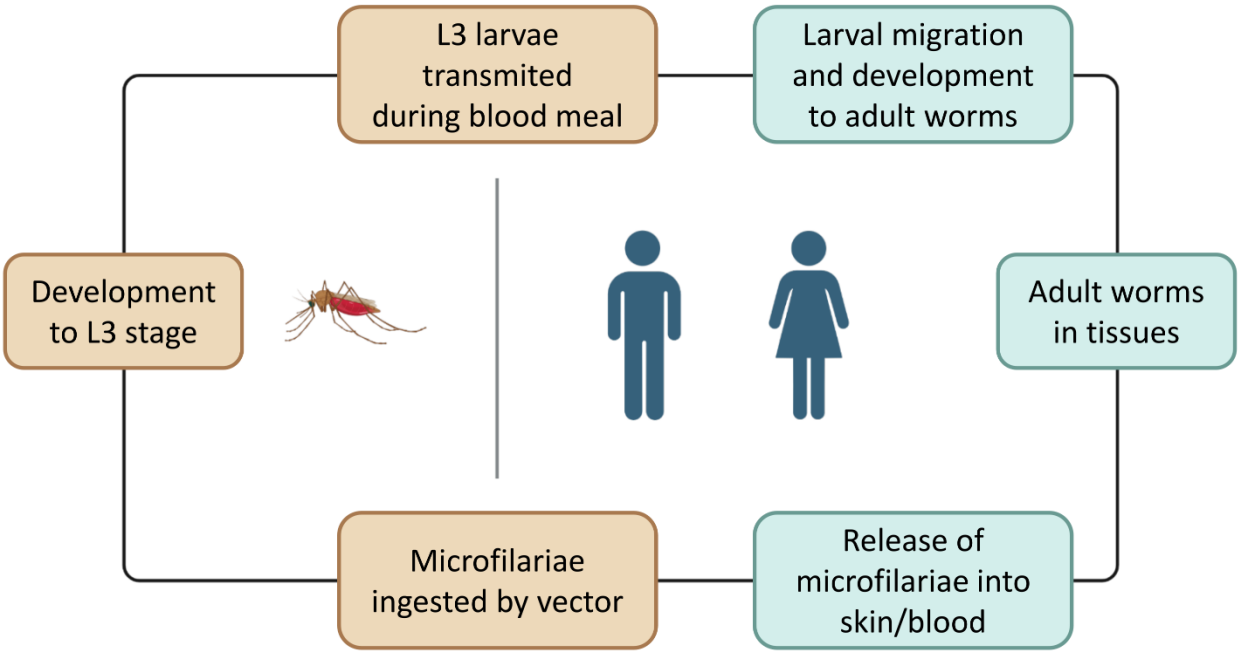


**Fig. 1: General filarial life cycle.** Infective L3 larvae are transmitted by an arthropod vector during a blood meal. L3 larvae then migrate through the skin and tissues where they molt into adult worms. Adult filariae are able to mate and release microfilariae into the blood circulation or skin (onchocerciasis) from where they can be taken up by another vector during a second blood meal. Inside the mosquito, microfilariae shed their sheaths, migrate from the midgut and molt into L3 larvae after which they can be released again during another blood meal thus completing the life cycle (image modified from [6] via biorender.com).

Biological and medical research in the late 20$^{th}$ and early 21$^{st}$ century concerning filariae has largely focused on two main avenues: 1) The development of diagnostic tools, treatment strategies and public health initiatives to cure filarial diseases on a patient level and eliminate the diseases as a general public health problem, and 2) understanding as well as utilizing the inherent ability of filariae in particular and more broadly helminths in general to modulate the host's immune system [3,7-15]. On the one hand, filariae are responsible for debilitating diseases. Yet, they have co-existed with humans since time immemorial and have been an integral factor in the evolution of our immune system [6,16,17]. Numerous studies have described the inverse correlation of infectious diseases, particularly the declining prevalence of parasitic infections and the rise of metabolic and autoimmune diseases over the last few decades culminating in modifications to the original *hygiene hypothesis* [18,19]. The elimination of filarial and helminth infections in much of the developed world and the loss of immunomodulation

may have played an integral part in this development [20,21]. As such, understanding our shared history is necessary to recognize the relationship with these parasites and realize that the aftereffects of any elimination will linger for a long time after the filariae are gone.

Archeological evidence for filarial worms is scarce in comparison to intestinal helminths as filariae do not deposit eggs that can be preserved and later identified in fossilized feces (=coprolites) [22]. However, an investigation into the mummy of Natsef-Amun, a priest in the temple of Amun at Karnak who lived during the reign of Ramesses XI of the late 20$^{th}$ dynasty (reign 1107-1078/77 BCE), revealed the presence of filarial worms in samples collected from the groin area [23,24]. In addition, filarial diseases are potentially described in Ancient Egyptian literature and depicted on statues and stelae. The famed Ebers Papyrus, named after German Egyptologist Georg Ebers, is usually dated to around 1550 BCE and may describe manifestations of elephantiasis (indicative of LF) as a type of growth or form of leprosy (which were often conflated in ancient sources) in therapeutic instruction no. 873 [25]. It is, however, important to note that this interpretation is not definitive and alternative explanations include neurofibromatosis for the disease described in this section of the papyrus [26].

Similarly, a statue of the Pharaoh Mentuhotep II, the sixth ruler of the 11$^{th}$ dynasty (reign 2060-2009 BCE), has been interpreted as being depicted with swollen legs indicative of elephantiasis (Fig. 2A) [27]. Another example is the depiction of Ati, commonly referred to as the “Queen of Punt”, in the temple of Pharaoh Hatshepsut at Deir el-Bahri (Fig. 2B, 2$^{nd}$ person from the right) [28]. As is the case for the written record, these depictions are not clear and academic debate about whether Ati is meant to be shown as suffering from elephantiasis continues to this day [29]. Later Roman and Greek medical writers differentiated between leprosy and elephantiasis caused by filarial worms as *Elephantiasis graecorum* and *Elephantiasis arabum*, respectively [16]. However, descriptions of elephantiasis in Roman sources are scarce.

Elephantiasis is also attested in Asia. In Ancient China, the physician Chao Yuanfang (巢元方) who served as court physician from 605-616 CE during the later phase of the Sui dynasty, is traditionally regarded as the author of the *Zhubing yuanhou lun* (諸病源候論) or *General treatise on the cause and symptoms of diseases* which contains descriptions

of symptoms similar to LF including acute lymphadenitis, lymphedema, elephantiasis, chyluria and hydrocele [30]. Depictions of other filarial diseases, e.g., loiasis, mansonellosis or onchocerciasis in ancient sources could not be identified.

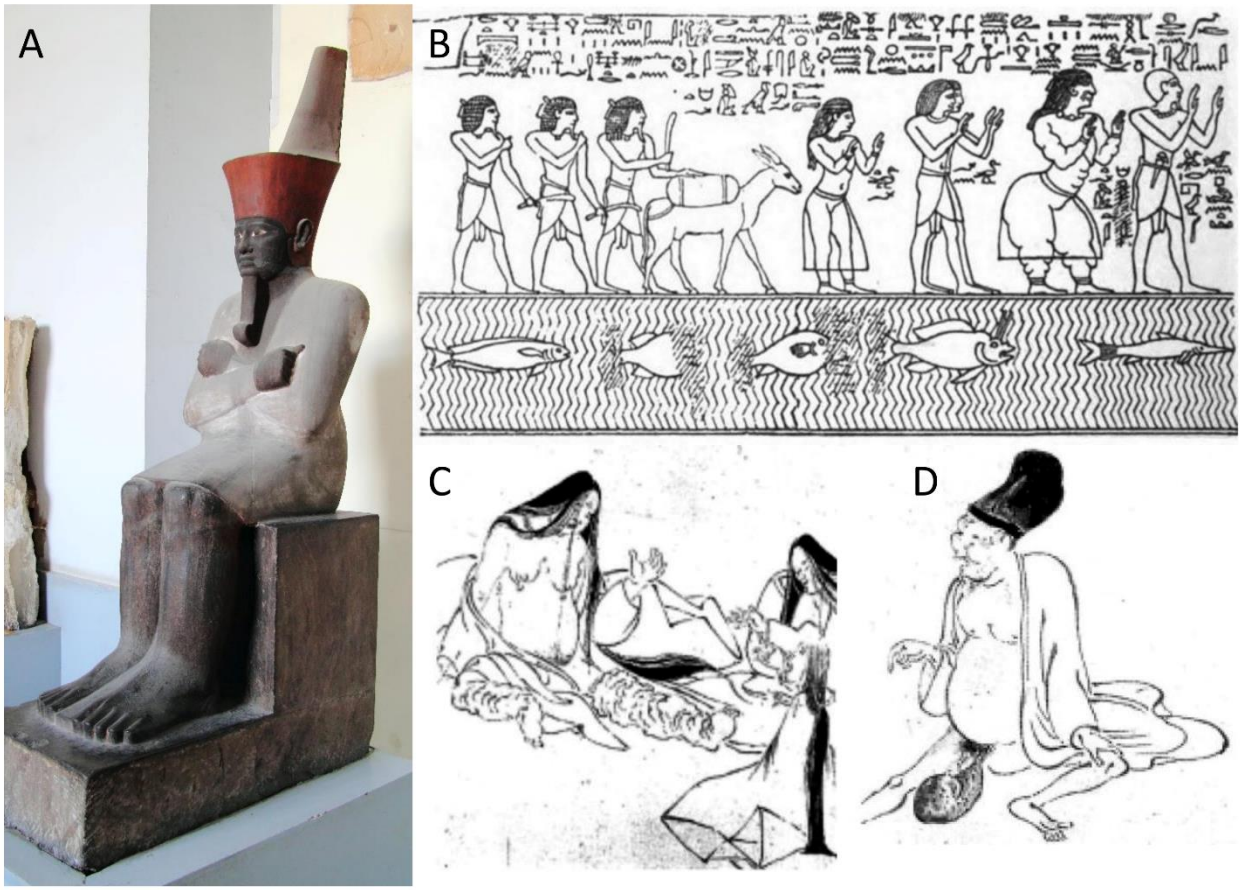


**Fig. 2: Potential ancient depictions of elephantiasis and hydrocele. (A)** Statue of Pharaoh Mentuhotep II (reign 2060-2009 BCE), sixth ruler of the 11th dynasty, presently located in the Egyptian Museum in Cairo (gallery 26, JE 36195) (image: modified from [31]). **(B)** Procession of the Puntite royal family depicted in the temple of Pharaoh Hatshepsut (reign 1478-1458 BCE) (image: modified from [32]). **(C+D)** Likely depiction of elephantiasis **(C)** and hydrocele **(D)** from the *Strange Diseases Picture Scroll* located in the Kyoto National Museum (image modified from [28]).

More definitive descriptions of LF and elephantiasis are known from the second millennium of the Common Era. In Japan, depictions of elephantiasis and hydrocele are included in a picture scroll depicting various diseases that is dated to the 12th century (late Heian or early Kamakura period) and the scroll is now located in the Kyoto National Museum (Fig. 2C+D) [28]. In the 16th century, symptoms of LF and elephantiasis were

described as the “curse of St. Thomas” by European travelers in India [16,33]. Saint Thomas, one of the twelve Apostles, spread the gospel outside the Roman Empire and traveled as far as South India, where he was – according to the Syrian Christian tradition – killed with a spear in 72 CE [34]. LF was highly endemic in India during the 16th century and the cause was unknown to both locals and European travelers [16,28]. Accounts by the Dutch explorer Jan Hughen van Linschoten based on his travels to Goa from 1588-1592 popularized the “curse of St. Thomas” as an explanation for the prevalence of lymphedema and elephantiasis in India as a form of punishment for the legendary death of St. Thomas one and half millennia earlier [16].

Modern scientific descriptions of filarial diseases began in the 18th century. The first definitive description of loiasis is from 1770 [16]. A French surgeon, Mongin, described the passage of a worm in the eye of a female patient and unsuccessful attempts to remove said worm [16]. The first successful removal of *Loa loa*, the causative agent of loiasis, from the eye of an affected patient was recorded in 1781 by the French surgeon Francois Guyot [35]. Additionally, a causative relationship between Calabar swellings, a common symptom of loiasis, and infections with *L. loa* was postulated only in 1910 by Patrick Manson and transmission via flies of the genus *Chrysops* was identified in 1912 by Robert Thompson Leiper [16,36,37]. In the case of onchocerciasis, microfilariae were first identified in skin snips from patients suffering from what was then called *craw craw* in Ghana by the Irish surgeon John O’Neill in 1874 [16,38]. Adult worms were discovered almost twenty years later in 1890 in skin nodules of patients by Patrick Manson [39]. For lymphatic filariasis, MF were first identified in hydrocele fluid and urine in 1863 and 1866 by Jean-Nicolas Demarquay and Otto Henry Wucherer, respectively, while adult worms were first described in 1876 by Joseph Bancroft [16,28]. The complete life cycle was then established by Patrick Manson in 1877/1878 [40,41].

These discoveries set the stage for much of the scientific discoveries in the 20th century in which diagnostic and therapeutic tools were discovered and later utilized in large-scale public health campaigns to eliminate filarial diseases. In the following chapters, our current understanding of filarial diseases, the availability of medical tools and remaining gaps in our understanding will be examined in more detail.

## 1.2 Filarial diseases

As touched upon before, filariae are the cause of various diseases that can range from mostly asymptomatic in the case of mansonellosis, uncomfortable but not life-threatening in the case of loiasis to severely limiting for the affected patients as can be the case for LF and onchocerciasis. Current models estimate that more than 200 million people are infected with at least one filarial disease, and an additional 1 billion people live in affected regions and remain at risk of infection [6,42-44]. Further, one of the commonalities of filarial diseases is their chronic nature. The precise life span of filarial worms is still unclear though estimates put the life span of some filariae at up to 20 years [6]. In addition, as the parasite has evolved to be highly elusive and evade protective immune mechanisms by the host, people in affected regions usually suffer from filarial infections for most of their life unless they receive adequate medical attention.

### 1.2.1 Lymphatic filariasis

LF is caused by three filarial species, *Wuchereria bancrofti*, *Brugia timori* as well as *Brugia malayi,* and they are transmitted by a variety of mosquitoes belonging to the genera *Anopheles*, *Culex*, *Aedes*, and *Mansonia* [6]. The life cycle of all three lymphatic filarial species follows the general life cycle outlined in figure 1. Adult worms reside in lymphatic vessels, often in the lower extremities, hence the name *lymphatic filariae* or *lymphatic filariasis* for the disease itself [3,10]. Adult female worms of *W. bancrofti* measure 80 - 100 x 0.25 mm while adult males are 40 x 0.1 mm and adults from *Brugia* spp. are about half as long [6]. Microfilariae (MF) measure about 0.26 x 0.008 mm [6]. Adult worms may survive and be reproductively active for up to 20 years, however the average lifespan is significantly shorter and estimated at 5-8 years [3,6,8]. The lifespan of MF is estimated to be about 1 year. Natural clearance of the infection for people living in endemic areas is unlikely. A longitudinal study from 2004 surveyed people 26 years apart and found that the majority of infected people (in 1975 and 1991) were also microfilaremic in 2001, indicating that reinfections are common and lead to persistent infections [45].

Precise descriptions of the distribution and disease burden are complicated, however, recent analyses estimated the prevalence as ranging from 51 to 72 million in 2019, mainly

in sub-Saharan Africa (*W. bancrofti*), Southeast Asia and Southwestern India (*B. malayi*) and Eastern Indonesia and Timor Leste (*B. timori*) (Fig. 3) [42,43,46]. *W. bancrofti* is responsible for roughly 90% of cases while the remaining cases are mostly due to infections with *B. malayi* [3,47]. In addition, the WHO estimates that 858.3 million people live in endemic areas and are at risk for infection [43].

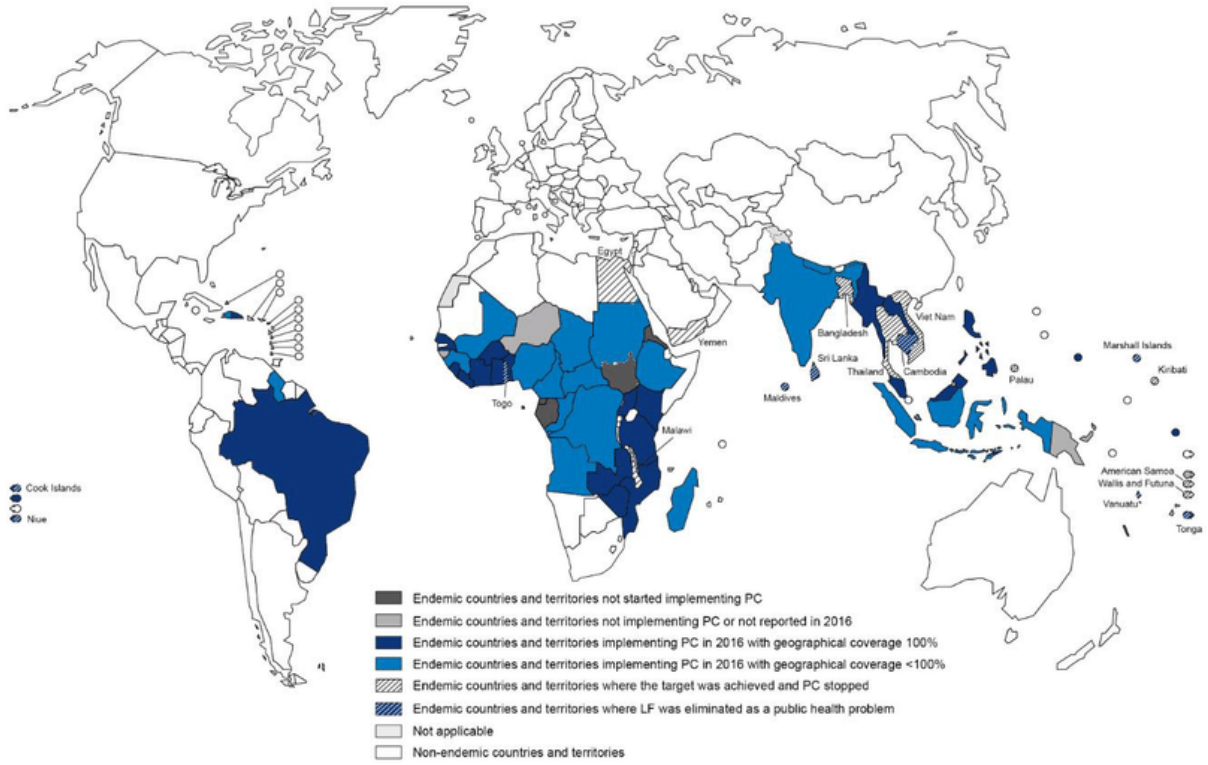


**Fig. 3: Distribution of lymphatic filariasis**. Lymphatic filariasis is a debilitating disease caused by *W. bancrofti*, *B. malayi* and *B. timori* and mainly treated via preventative chemotherapy (PC). Map indicates state of PC implementation for lymphatic filariasis in 2016 (image: modified from [43]).

LF may manifest with a variety of symptoms that are caused by the presence and death of adult worms and MF. The presence of adult worms in the lymphatic vessels is responsible for the most common symptom, i.e., dilation of lymph vessels (lymphangiectasia) [3,6,47]. This dilation impairs the function of lymphatic vessels and precedes the development of swelling of the affected regions (lymphedema) and predisposes the patient for the development of microbial infections (acute dermatolymphangioadenitis, ADLA) [11,13,48]. In addition, the death of adult worms may

trigger acute inflammatory responses in the lymphatic vessels and can cause acute inflammatory symptoms (acute filarial lymphangitis, AFL) [6,48-50]. ADLA and, to a lesser extent, AFL may also lead to the development of chronic swelling of the lower extremities (lymphedema). This may ultimately lead to the previously mentioned severe form of elephantiasis, which is in turn often associated with further bacterial or fungal infections, which in a feed-back loop may further promote the progression of lymphedema development [3,6,51]. Male patients may also develop an accumulation of fluid in the tunica vaginalis surrounding the testicles (hydrocele) while female patients may rarely develop an edema of the labia majora [52,53]. More uncommon symptoms include the development of chyluria, a syndrome caused by the rupture of lymphatic vessels leading into the upper urinary tract which leads to the presence of chyle in the urine (indicated by a milky color), as well as tropical pulmonary eosinophilia during which MF are retained and killed in the lung due to immunological hyperresponsiveness, which leads to excessive inflammation and damage to the lung [54,55]. Overall, the World Health Organization (WHO) estimates that LF was responsible for around 1.6 million disability-adjusted life years (DALYs) in 2019 [42,43].

### 1.2.2 Onchocerciasis

Onchocerciasis, also known as ‘river blindness’, is caused by infections with *Onchocerca volvulus* and transmission occurs via various species of black flies (*Simulium* spp.). Onchocerciasis is almost exclusively found in sub-Saharan Africa and a single transmission locus remains in South America at the border of Venezuela and northern Brazil (Fig. 4) [56]. Current numbers by the WHO estimate that around 21 million people remain infected with a population of 218 million at risk and 1.3 million DALYs [43].

The life cycle follows the general filarial cycle outlined in figure 1 and adult worms reside in subcutaneous nodules that are often palpable. However, migration of adult worms through the skin is possible and male adult worms in particular are known to migrate between different nodules [3,6]. MF are released by the adult worms from the nodules and can mainly be found in the skin where they can be taken up by black flies during feeding. Migration of MF into the blood or other fluids is possible but rare [3]. Adult female

worms are able to release an estimated 500 – 1500 MF per day and remain reproductively active for >10 years [57,58]. In terms of size, adult *O. volvulus* worms are larger than the previously described *W. bancrofti* specimens with adult females being 35 – 70 cm x 0.4 mm and males 2 – 5 cm x 0.2 mm. MF, however, are of a similar length as *W. bancrofti* at 0.3 x 0.008 mm [6].

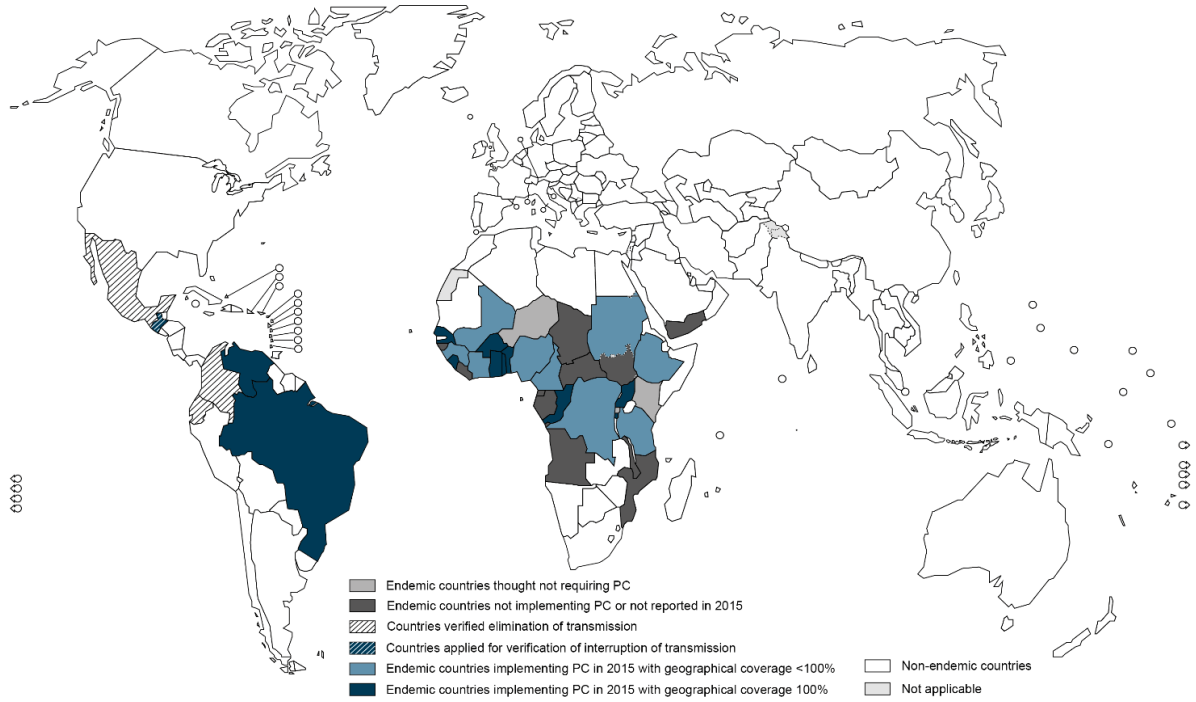


**Fig. 4: Distribution of onchocerciasis**. Onchocerciasis is a disease caused by *O. volvulus* and is mainly treated via preventative chemotherapy (PC). Map indicates state of PC implementation for onchocerciasis in 2015 (image: modified from https://www.afro.who.int/health-topics/onchocerciasis).

The main symptoms associated with onchocerciasis are skin nodules, different forms of dermatitis as well as ocular lesions & keratitis, which may worsen until the development of blindness. As the presence of the vector is limited to a few kilometers surrounding their breeding grounds, i.e., rivers, the disease is also known as 'river blindness'. In terms of pathology, the skin nodules ('onchocercomata') are caused by the presence of the adult worms and an associated immune reaction similar to granuloma formation [3,59]. The nodules have relatively thick and fibrotic walls with an infiltration of various immune cells of which macrophages are usually the most dominant [59]. The nodules themselves are

not painful for the patient though they may be considered uncomfortable or unappealing [6]. The remaining symptoms are mainly caused by the MF of *O. volvulus*.

For dermatitis, the death of MF, either natural or induced via anti-filarial treatment, causes significant inflammatory responses that predominantly attract myeloid cells, e.g., eosinophils, neutrophils and macrophages [60]. This in turn may lead to the formation of lesions and an increased proliferation of dermal fibroblasts which gradually replaces the formerly healthy skin tissue with scar tissue leading to depigmentation as well as thin and wrinkled skin [6,60]. In severe cases, hyperresponsive inflammation (usually limited to one limb) may cause a syndrome termed *sowda,* which is characterized by intense itching, hyperpigmentation and formation of scaly papules [6]. Patients with *sowda* display a strong Th2 immune response with high levels of IgE and eosinophilia and a low amount of regulatory cytokines (TGF-β) or regulatory T cells [61-63].

Ocular symptoms up to and including blindness during onchocerciasis are associated with the migration of MF into the cornea and anterior eye chamber. The migration of live MF can be observed during eye examinations. However – similar to the situation in the skin – it is the death of the MF, be it natural or drug-mediated, which is the cause of clinically relevant symptoms [3,60,64]. Dying MF induce strong inflammatory responses in the eye, particularly the cornea and anterior eye chamber [64]. The inflammatory response due to the death of MF is largely caused by the presence of *Wolbachia* spp. bacteria [65,66]. *Wolbachia* spp. (order: Rickettsiales) are Gram-negative, obligate intracellular endosymbionts that can be found in various filariae as well as a great variety of arthropods [67]. *Wolbachia* exist in a symbiotic relationship inside the cells of nematodes and are involved in various metabolic activities such as hem and vitamin B2 synthesis that support their nematode hosts [66]. As a result, the presence of *Wolbachia* is indispensable for the development and fertility of filarial worms, which also makes them an alternative drug target that will be discussed in detail in a later section [12,68,69]. Studies in a murine model could demonstrate that the adverse events following the demise of MF are indeed due to the presence of *Wolbachia* [3,49,65]. Injection of extract prepared from *O. volvulus* worms caused acute keratitis in mice while injection with extract from worms that were previously treated with antibiotics and depleted of

*Wolbachia* failed to induce pathology [70]. Later studies could also demonstrate that the *Wolbachia*-induced pro-inflammatory response is dependent on Toll-Like receptor (TLR)-2 and TLR-6 signaling leading to a production of type 1 and type 2 interferons in addition to different chemokines which in turn recruit neutrophils. This ultimately leads to corneal haze and eventually blindness [71,72]. In rare cases, onchocerciasis can also manifest as onchocerciasis associated epilepsy (OAE) or nodding syndrome (characterized by specific head seizures). However, the causal relationship and etiology are still unclear, and research is ongoing in this field [73,74].

### 1.2.3 Loiasis

Loiasis is caused by *Loa loa* also known as the *African eye worm* as the adult worms can sometimes be observed migrating through the eye of infected patients. The worm follows the general life cycle outlined in figure 1. Various members of the genus *Chrysops* (deer flies) function as the vector and transmission occurs mainly during the wet season in the rainforest or swamp areas of Central and Western Africa [75]. An estimated 90 million people live in endemic areas and roughly 10 million people are assumed to be infected [75].

The adult worms of *L. loa* migrate through subcutaneous and connective tissues and measure 50 – 70 x 0.5 mm (females) and 30 – 35 x 0.4 mm (males) while MF measure around 0.2 – 0.3 x 0.006 mm [6]. Clinical manifestations of loiasis include hypereosinophilia, angioedema, urticaria, pruritus and the aforementioned migration of adult worms through the eye [6].

### 1.2.4 Mansonellosis

Mansonellosis (or mansonelliasis) is the umbrella term for a set of diseases caused by *Mansonella* spp. [2]. The human pathogenic members of this genus are *Mansonella perstans, Mansonella ozzardi* and *Mansonella streptocerca* [6,76]. Unlike the previously discussed filarial diseases, mansonellosis is usually either asymptomatic or associated with unspecific symptoms including transient swellings, fever, joint pain and pruritus [77].

As such, mansonellosis has often been overlooked from a medical perspective and information about the distribution and biology of the parasite is comparatively scarce. A systematic review from 2010 reported a prevalence of 3-96% for *M. perstans*, 0.5-61% for *M. streptocerca* and 3-61% for *M. ozzardi* in various African countries (*M. perstans* and *M. streptocerca*) and Latin America (*M. ozzardi*) [2]. It is thus believed that mansonellosis is the most common filarial infection in humans with roughly 114 million infections caused by *M. perstans* alone [44].

Adult worms of *M. perstans* reside in the serous cavities and female adult worms measure 70 – 80 x 0.12 mm while male worms are 35 – 45 x 0.06 mm. The other two species are slightly smaller [6]. The lack of significant clinical manifestations despite this size is, however, indicative of a highly evolved capacity to affect and modulate the host's immune response and evade both detection and clearance [76,78].

To summarize, filarial diseases manifest in various forms in human patients and hundreds of millions of people remain infected to this day. In addition, filariae are able to aptly modulate and affect the host's immune response though the precise details and involved pathways are in many cases still unclear. Thus, in order to develop novel treatment strategies and analyze protective or dysfunctional immune responses, animal models have been employed and will be discussed in the following chapter.

## 1.3 Rodent models – *Litomosoides sigmodontis* infection in mice

*L. sigmodontis* (Chandler 1931) has been used as a filarial model organism for almost 80 years now [76,79]. The vector, *Ornithonyssus bacoti,* also known as the tropical rat mite, was identified in 1945 and subsequent studies in the 40s/50s developed appropriate rearing strategies for the vector and clarified the life cycle [80-82]. The initial studies referred to the parasite as *Litomosoides carinii (*Travassos 1919) based on an assessment in 1934 that both species are identical and should be synonymized [83]. It was not until 1989 when the group of the late Odile Bain showed that *L. sigmodontis* and *L. carinii* are in fact two separate species and that previous work had all been done with *L. sigmodontis* [84]. The natural host of *L. sigmodontis* is the cotton rat (*Sigmodon hispidus*) though experimental infections are possible in various hosts including jirds

(*Meriones unguiculatus*), albino rats (*Rattus norvegicus*), natal multimammate mice (*Mastomys nataliensis*) and the house mouse (*Mus musculus*) [76,85-89].

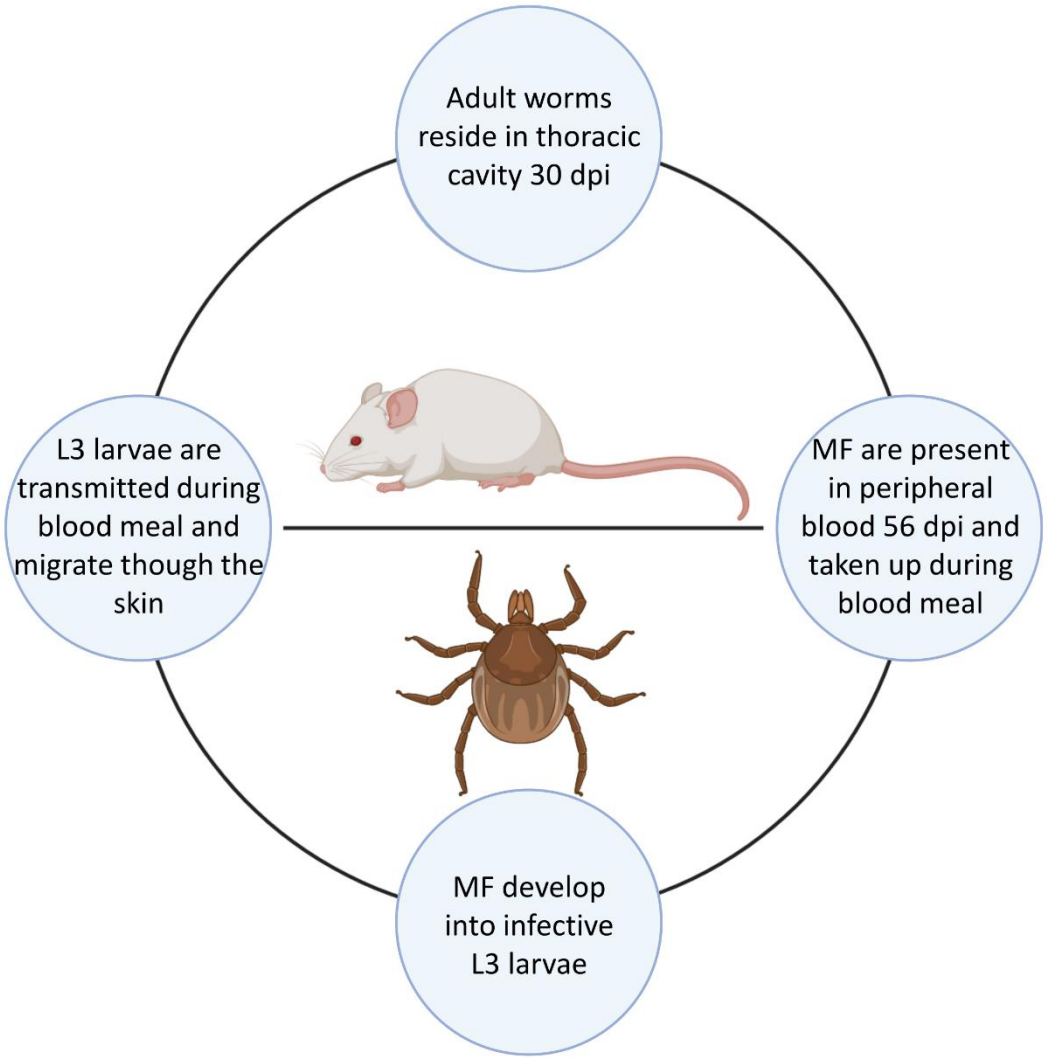


**Fig. 5: Life cycle of *Litomosoides sigmodontis***. Infective L3 larvae are transmitted to the rodent host by the bite of the tropical rat mite *Ornithonyssus bacoti* during a blood meal. L3 larvae then migrate through the skin and via the lymphatic vessels into the thoracic cavity where they molt into adult worms within 28-30 days. Adult filariae are able to mate and release microfilariae into the blood circulation starting 49-56 days after the infection. Microfilariae in the peripheral blood can be taken up by another mite during a second blood meal. Inside the mite, microfilariae molt into L3 larvae and can be transmitted during another blood meal (image created with biorender.com).

The life cycle of *L. sigmodontis* (Fig. 5) is similar to the general filarial life cycle outlined in figure 1. Infective L3 larvae are transmitted via the bite of the vector and the larvae

migrate through the skin and lymphatic vessels to the thoracic cavity within 6-9 days where they molt into later stages. The molting into adult worms is mostly complete within 28-30 days post infection and female worms start releasing MF after 49-56 days. MF then migrate into the peripheral blood vessels where they can be taken up again by the vector during a blood meal. Inside the vector, MF migrate from the midgut and develop into L3 larvae at which point they move to the proboscis to be transmitted during another blood meal. The development within the vector takes 7-10 days [90]. Interestingly, commonly used laboratory mouse strains differ significantly in their response to *L. sigmodontis*. C57BL/6 mice generally do not develop patent infections, i.e., they have no MF detectable in the peripheral blood and clear the infection within ~45 days [89]. BALB/c mice, on the other hand, clear the infection only after >100 days and ca. 50% of female mice develop patent infections with a peak of MF numbers at ~77 dpi [89-91].

In terms of pathology, infection of mice with *L. sigmodontis* is associated with lung damage mainly due to migration of L3 larvae into the thoracic cavity or MF out of the thoracic cavity and thus the infection can be used as model for filariae-mediated lung damage in humans. Entry of L3 larvae into the thoracic cavity induces hemorrhages, formation of granuloma, inflammation and an increase in neutrophil numbers [92,93]. Recent studies highlighted the role of type 2 cytokines, e.g., IL-4 and IL-5 in regulating inflammation in the lung during chronic *L. sigmodontis* infections [94,95]. In addition, Fercoq et al. recently demonstrated MF-mediated morbidity and polyp formation in the thoracic cavity of mice infected with *L. sigmodontis* [96]. Further, the *L. sigmodontis* model has been instrumental in various immunological discoveries including IgE-dependent killing of MF by neutrophils and macrophages, development of a mixed type 1/type 2 immune response in filarial infections and an instrumental role of eosinophils and their release of the major basic protein, eosinophil peroxidase and extracellular DNA traps during protective immune responses (recently reviewed in [7,76,97,98]).

In addition to studies investigating the morbidity and immunological aspects, the *L. sigmodontis* model has also been used as a tool for preclinical development. In the case of diethylcarbamazine (DEC), which is still used as an anti-filarial treatment to this day, the MF-killing (=microfilaricidal) activity was first reported in the *L. sigmodontis* model in

cotton rats [99]. In addition, subsequent studies showed that DEC has no adult worm-killing (=macrofilaricidal) activity and that the activity of DEC against MF is indirect and mediated via the loss of the MF sheath, which in turn allows the MF to be recognized by the immune system, in particular by neutrophils and phagocytes [100,101]. Other examples include the suppression of microfilaremia by emodepside and the macrofilaricidal activity of both flubendazole and oxfendazole [102-105]. Lastly, the *L. sigmodontis* model has been instrumental in the discovery of anti-*Wolbachia* based treatment strategies against filarial infections as will be discussed in more detail in the following chapter [11].

## 1.4 Treatment of filarial diseases

Current treatment options for filarial diseases are limited and the most commonly used drugs are albendazole (ALB), ivermectin (IVM) and the already mentioned DEC [11,43]. Albendazole belongs to the class of benzimidazoles and its mode of action is the inhibition of tubulin polymerization via binding to the β-tubulin subunit [106]. ALB by itself has little anti-filarial activity, but various studies have highlighted that a combination with ALB may boost the efficacy of anti-filarial therapies [11]. Ivermectin (marketed as Mectizan®) belongs to the class of macrocyclic lactones and has a microfilaricidal efficacy [107]. Treatment with IVM leads to a temporary inhibition of embryogenesis of adult female worms [6,107]. In addition, IVM inhibits the release of extracellular vesicles across different life-cycle stages of filarial worms, thus impairing the parasite's ability to modulate and evade the host's immune response [108,109]. DEC, a piperazin derivate, likewise, is predominantly active against the MF stage [100]. Even though DEC has been used since 1947, the precise mode of action is still unknown but recent studies have demonstrated that DEC activates transient receptor potential (TRP) channels in muscle cells of *B. malayi* which induces spastic paralysis and may make the parasite vulnerable to immune responses in addition to encasement in granulomatous nodules [110,111].

Treatment for filarial diseases can be done on an individual patient by patient basis, however management of lymphatic filariasis and onchocerciasis mainly occurs via so called mass drug administrations (MDA). MDA campaigns are large scale public health

initiatives in which the entire population may be treated with anti-filarial compounds regardless of infection status (certain limitations apply). The current treatment recommendations for filarial diseases are outlined in table 1. For LF, a triple therapy with ALB, IVM and DEC was endorsed by the WHO in 2017 and has recently been implemented [14,112-114]. However, this therapy is only partially macrofilaricidal and mainly limits transmission via elimination of MF and the temporary inhibition of filarial embryogenesis. Thus, the treatment needs to be repeated on (bi-)annual basis for at least the reproductive life span of the adult parasites [8]. In addition, IVM and DEC may cause severe adverse events (SAE) in patients with heavy infections of *O. volvulus* or *L. loa* [3]. Therefore, in areas co-endemic for loiasis, a test-and-not-treat strategy may be employed in which people are first screened for *L. loa* before treatment [56,115]. For onchocerciasis, the WHO recommends (bi-)annual MDA with IVM [43].

As the incidence of LF and onchocerciasis decreases in certain regions, a transition from blanket-treatment strategies to individual therapies with the antibiotic doxycycline (DOXY) may become more economic and feasible. Such a transition has been endorsed by the WHO for onchocerciasis in South America [116]. DOXY targets the previously mentioned obligate endobacteria of the genus *Wolbachia* that are present in filariae and essential for their development, survival and fertility [12,66]. For LF, clinical trials have shown that a daily treatment with 200 mg DOXY for 6 weeks is sufficient to reduce *Wolbachia* numbers by 96% and MF levels by 99% one year after the treatment was concluded [12]. A further combination with one dose of IVM and ALB 4 months after doxycycline treatment also reduced the number of adult worms by 86% [117]. Later studies found that a 200 mg DOXY treatment for 4 weeks is enough to reduce viable adult worms by 80% [118]. For onchocerciasis, 100 mg DOXY daily for 6 weeks similarly depleted *Wolbachia*, prevented microfilaremia and severely reduced the number of adult worms [119]. While treatment with DOXY may be curative, i.e., clear the adult worms, the long treatment duration of up to 6 weeks preclude its use in MDA campaigns. In addition, DOXY is contraindicated in pregnant and breast-feeding women, as well as children under the age of eight [11].

Loiasis and Mansonellosis, on the other hand, are not part of any MDA campaigns [43]. Generally speaking, treatment for loiasis is complicated due the risk of severe adverse

events and should be managed by an experienced physician. DEC is only recommended in patients with less than 2000 MF/ml blood, IVM is recommended in patients with less than 8000 MF/ml blood while ALB is recommended for heavy infections with more than 8000 MF/ml [120,121]. DOXY cannot be used to treat loiasis as the parasite does not harbor *Wolbachia* [11]. For mansonellosis, the recommended treatment depends on the species [77,122,123]. For *M. perstans*, diethylcarbamazine can be ineffective and DOXY is curative for some but not all *M. perstans* infections as *Wolbachia* are not always present. IVM is recommended for *M. ozzardi* while DEC is the drug of choice of *M. streptocerca* [123].

**Table 1: Overview of treatment options for filarial diseases.** "+" indicates that the drug is recommended, "-" indicates that the drug is not recommended. "?" indicates that the effect is unknown.

| | ALB | IVM | DEC | DOXY | Recommendation |
|---|---|---|---|---|---|
| *LF* | + | + | + | + | (MDA) Annual triple therapy [113]<br>(Individual) 4-6 weeks DOXY [11] |
| *Onchocerciasis* | - | + | SAE | + | (MDA) (Bi-)annual IVM [43]<br>(Individual) 6 weeks DOXY [11] |
| *Loiasis* | -/+ | SAE[1] | SAE[1] | - | DEC if <2000 MF/ml [121]<br>IVM if <8000 MF/ml [121]<br>ALB if >8000 MF/ml [121] |
| *M. perstans* | - | - | -/+ | -/+ | DEC or DOXY if *Wolbachia*+ [123] |
| *M. ozzardi* | ? | + | - | ? | IVM [123] |
| *M. streptocerca* | ? | + | + | ? | DEC or IVM [123] |

[1] in patients with heavy infections

The MDA campaigns described above are one of the main tools to eliminate LF and onchocerciasis as public health problems. In this context, LF and onchocerciasis are classified by the WHO as part of the neglected tropical diseases (NTDs), and the WHO

has recently published a roadmap for NTDs entitled *Ending the neglect to attain the Sustainable Development Goals – A road map for neglected tropical diseases 2021-2030* [43]. This publication serves as a guideline for further research and implementation of strategies to combat filarial diseases. Onchocerciasis is targeted for elimination via interruption of transmission in 12 out of 38 countries by 2030 while LF is targeted for elimination as a public health problem in 58 out of 72 countries by 2030 [43]. For onchocerciasis, the WHO has outlined the development of novel macrofilaricidal compounds as one of the critical actions required to reach the roadmap's goals [43].

### 1.4.1 Development of macrofilaricidal treatment options

Development of novel treatment options is – generally speaking – difficult and riddled with a high attrition rate. Next to the overall efficacy and safety, preclinical development of anti-filarial compounds needs to address three additional aspects: 1) the choice of life-cycle stage that should be targeted (macro- vs. microfilaricide), 2) the speed at which the filariae should be cleared and 3) whether elimination is actually necessary [76]. A macrofilaricidal compound, i.e., one that targets and clears the adult worms, has the advantage of being curative rather than simply preventing transmission as is the case for microfilaricidal treatments. Further, a treatment that exclusively targets the adult worms may cause fewer adverse events as the MF would be cleared slowly overtime by the immune system.

Rapid killing of the parasite, regardless of the life-cycle stage, however, releases large amounts of both worm and *Wolbachia* antigen and may induce strong inflammatory immune responses as is the case in patients with heavy *L. loa* infections after treatment with DEC or IVM or the previously discussed ocular damage associated with dying MF and release of *Wolbachia* following DEC treatment in onchocerciasis patients [3,6,65,124]. An alternative to the elimination of filariae is the induction of sterility. In the case of onchocerciasis, MF are the main etiological agent and necessary for transmission. Thus, achieving permanent sterilization via the elimination of *Wolbachia* is a potential alternative to the direct clearance of adult worms.

The previous sections have touched upon the role of *Wolbachia* a number of times. To recapitulate, *Wolbachia* are present in most human pathogenic filariae except for *Loa loa* and certain members of the genus *Mansonella*. If present, *Wolbachia* are essential for the development of the filariae, and, thus, *Wolbachia* have been identified as an excellent drug target. *Wolbachia* were described in 1924 in insects as rickettsia-like bacteria by Hertig & Wolbach [125]. It took another 50 years for *Wolbachia* to be described in different nematodes including *Dirofilaria immitis*, *Brugia pahangi*, *B. malayi* and *O. volvulus* [126-129]. Then, in the late 90s, different groups described an inhibitory effect of antibiotics (tetracyclines) on filarial growth and fertility and could correlate this result with the depletion of *Wolbachia* [68,130-132]. First human trials were conducted in the early 2000s demonstrating the sterilizing effect of DOXY treatment against *O. volvulus* and *W. bancrofti* and the macrofilaricidal activity of a 6-week treatment regimen in LF patients [11,12,117,119]. Subsequent clinical trials further optimized the required treatment regimen, leading to the current recommendations of a 4-5 week daily treatment with 100 mg DOXY for LF patients and a 6-week daily treatment with 100 mg DOXY for onchocerciasis patients [6]. However, a 4-6-week long therapy is not feasible for MDA campaigns. As such, a variety of alternative compounds were identified through a collaboration of partners from industry, academia and not-for-profit organizations. Promising candidates include ABBV-4083, AWZ1066S and corallopyronin A (CorA). ABBV-4083 is currently undergoing phase II clinical trials in the Democratic Republic of the Congo as a treatment for onchocerciasis, while AWZ1066S is tested in phase I clinical trials. CorA is still in pre-clinical development and is being prepared for phase I clinical trials in 2024/2025 [11,133-136].

CorA was isolated from culture broth of *Corallococcus coralloides*, a myxobacterium, in the 1980s [136]. CorA inhibits the bacterial DNA-dependent RNA polymerase and, importantly, it binds to the switch region and is therefore a non-competitive inhibitor to another antibiotic, rifampicin [136]. CorA did not receive significant attention until it was found to be highly effective against *Wolbachia* in 2012 [137]. From thereon, CorA was developed as a new anti-*Wolbachia* drug and screened for various microbial infections. CorA was found to be effective against a variety of bacteria including *Chlamydia trachomatis*, *Staphylococcus aureus*, rifampicin-resistant *S. aureus* and *Neisseria*

*gonorrhoeae* [136,138]. In terms of its anti-filarial activity, studies with the *L. sigmodontis* model could demonstrate that a 14-day treatment with CorA immediately after the infection reduced the number of *Wolbachia* by more than 90% and prevented the development of adult worms [139]. In addition, treatment of patently infected animals for 14 days achieved a reduction of *Wolbachia* numbers by more than 99% and resulted in a complete clearance of MF [139]. Lastly, a combination of CorA with ALB for 7 days achieved a significant reduction of the adult worm burden [139].

Next to the *Wolbachia*-targeting drugs, a number of directly acting compounds are also in development. These include auranofin, emodepside and oxfendazole (OXF) [9,11,103-105]. All three are repurposed and have their origin either in veterinary medicine (emodepside & oxfendazole) or have already been used in human patients (auranofin) [11]. Auranofin is approved by the American Food and Drug Administration (FDA) with indications for rheumatoid arthritis [140,141]. Recent studies could demonstrate limited activity of auranofin against MF and adult worms of *Brugia* spp. and *Onchocerca ochengi* (a bovine parasite used as a model for *O. volvulus*) [142].

Emodepside belongs to the group of cyclooctadepsipeptides and has been used in veterinary medicine as a broad-spectrum anthelmintic against gastrointestinal nematodes. Emodepside's mode of action involves opening the $K^+$ channel SLO-1, which in turn induces paralysis [103,143,144]. Recent studies have shown that emodepside is also active against *O. ochengi* with treatment leading to rapid clearance of MF, inhibition of embryogenesis and a reduction of the adult worm burden [145]. Based on extensive *in vitro* studies, emodepside has been demonstrated to inhibit the motility of various filariae including *Acanthocheilonema viteae*, *B. pahangi*, *L. sigmodontis*, *O. gutturosa*, *O. lienalis*, *B. malayi* and *Dirofilaria immitis* [103]. In addition, phase I clinical trials reported that emodepside was safe and well tolerated in humans [11]. Phase II clinical trials for onchocerciasis are currently ongoing in the Democratic Republic of the Congo and in Ghana [146,147]. In addition, separate phase II trials recently demonstrated that a single dose of 5 mg emodepside led to a cure rate of 85% in patients infected with *Trichuris trichiura* and a 30 mg dose to a cure rate of 95% in hookworm patients [148].

OXF belongs to the chemical class of benzimidazoles. Benzimidazoles are broad-spectrum anthelmintics that have been used in both veterinary medicine, e.g., flubendazole (FBZ) and oxfendazole (OXF), and human medicine, e.g., albendazole, and they are potentially macrofilaricidal [9,106,149]. The mode of action for all benzimidazoles is based on the binding to β-tubulins and inhibition of tubulin polymerization [106]. The binding of benzimidazoles to nematode tubulins is relatively specific and their affinity for nematode tubulins is roughly 100-400 times higher than for mammalian β-tubulin [106].

Nevertheless, benzimidazoles are still active against human β-tubulin and as a result FBZ has in recent years become a promising novel cancer drug [150-154]. The development of FBZ for human filarial diseases as a macrofilaricide, on the other hand, has hit a number of roadblocks that are rooted in two main issues: 1) the poor oral bioavailability of FBZ and 2) induction of adverse events after parenteral injections. An initial human study conducted in 1983 showed that while FBZ had excellent activity against *O. volvulus* in human patients, the intramuscular injection caused the formation of painful abscesses and fever [155]. Research in the following decades focused on improving the oral bioavailability and a number of novel formulations based on an amorphous solid dispersion of the compound were created [9]. However, these new formulations did not achieve the desired availability or efficacy [104,156-158]. In combination with reports on the genotoxicity of FBZ, it was concluded that "no flubendazole treatment regimen can be selected that would provide efficacy in humans at safe exposure." [157]. Thus, FBZ currently remains as a potential backup drug that requires additional preclinical research leading to improved formulations and delivery methods before it can be considered for clinical studies.

OXF (syn.: fenbendazole sulfoxide), on the other hand, is a promising macrofilaricidal compound. In veterinary medicine, it has been used as a broad-spectrum drug against both nematodes and cestodes since the 1980s [149]. Studies have demonstrated the efficacy and safety of OXF for the treatment of cysticercosis in pigs (caused by *Taenia solium*), echinococcosis in sheep and goats [159] as well as hydatidosis (*Echinococcus granulosus*) and fascioliasis (*Fasciola hepatica*) in sheep [160,161]. Further studies in animals besides ruminants have demonstrated that OXF is effective against adult worms

of *Onchocerca gutturosa*, young adult stages of *O. volvulus* and adult worms of *L. sigmodontis* [105]. Notably, OXF displays little to no direct effect against MF stages [105]. This makes OXF a particularly interesting drug candidate for the treatment of onchocerciasis, where much of the pathology is caused by the untimely death of MF [65]. Therefore, OXF was selected for further development by the *Drugs for Neglected Diseases initiative* (DNDi) and the *Helminth elimination platform* (HELP, https://eliminateworms.org/), a consortium of research institutes, universities, not-for-profit organizations and pharmaceutical companies [162]. Phase I clinical trials demonstrated that OXF is safe and well tolerated in humans [163] and a field applicable tablet formulation has been tested by the *Swiss Tropical and Public Health Institute* [162]. OXF is currently in the process of being evaluated as a pan-nematode drug for *O. volvulus*, *L. loa*, *M. perstans* and the intestinal human whipworm *T. trichiura* in phase II clinical trials via the recently EU-funded consortium *enabling the WHO Road Map* (eWHORM, https://www.ewhorm.org/) [164].

## 1.5 Microtubules, inhibitors and their potential as anti-filarial drug targets

The previous section covered the role and use of benzimidazoles as broad-spectrum anthelmintic compounds. To better understand their mode of action, it is necessary to briefly discuss the biology of their target, i.e., β-tubulin in particular and microtubules in general. Microtubules, together with actin and intermediate filaments, form the core of the cytoskeletal network that is near ubiquitous in eukaryotic cells. Microtubules and their associated structures and proteins are well-conserved and display significant similarities across different species and phyla, however, advances in imaging techniques and improvements in resolution have highlighted important architectural and potential functional differences [165]. The peculiarities of filarial microtubules, centrosomes and associated proteins are largely unknown as most research on nematode microtubules has only been conducted in *Caenorhabditis elegans* [166].

In general, microtubules consist of cylindrical structures that are based on long polymers of α- and β-tubulin dimers. The polymers grow via addition of GTP-tubulin dimers which form a stabilizing GTP-rich cap while the dimers below are generally hydrolyzed GDP-

dimers due to the GTPase activity of tubulin [167]. Generally, 13 polymers or protofilaments are assembled into one microtubule and stabilized via lateral interactions. In the case of nematodes, however, most cytoplasmic microtubules consist of only 11 protofilaments while those in sensory neurons may have 15 [166]. Based on the rigid dimer structure, microtubules form a polarized structure with a β-tubulin at one end ("+end") and an α-tubulin at the other ("-end"). The growth and shrinkage of microtubules, in particular at the +end, is a highly dynamic process mediated via the hydrolyzation of the GTP-cap and it is essential to fulfill their role in intracellular organization, organelle and vesicle trafficking, cellular movement as well as chromosome segregation [167].

Nucleation of microtubules, that is the formation of new microtubules, rarely occurs spontaneously in an unaided fashion [168]. As a result, nucleation *in vivo* is a highly regulated process and is usually mediated via the γ-tubulin ring complex (γ-TuRC) [168-170]. The γ-TuRC forms a conical shape, which serves as a scaffold to which the initial tubulin dimers may bind and begin the process of polymerization [168,171]. The exact shape and composition of the γ-TuRC is still the subject of debate though a number of components have already been identified [169,170]. Interestingly, studies on the structure of γ-TuRC from *Xenopus laevis* recently confirmed the presence of actin co-localized with GCP6, a component of the γ-TuRC [171]. Subsequent studies further clarified that actin is involved in microtubule nucleation and chromosome alignment during mitosis [172]. In eukaryotic cells, the γ-TuRC is often localized near microtubule organizing centers (MTOC) which can take the form of centrosomes if located near the nucleus, basal bodies if located at the base of cilia/flagella, or spindle poles during mitosis [173].

Due to their essential involvement in various cellular processes, microtubules are an attractive drug target. Microtubule-targeting agents can broadly be separated into two categories, i.e., microtubule-stabilizing agents and microtubule-destabilizing agents [174]. Microtubule-stabilizing agents, e.g., the cancer drug paclitaxel (marketed as Taxol) or epothilones, can bind to β-tubulin on the luminal side and stabilize microtubules and thus impair mitotic spindle assembly and chromosome segregation [174,175]. Alternatively, laulimalide and peloruside A bind to two adjacent β-tubulins from the outside and create a "bridging" effect thus stabilizing the microtubules [176].

Microtubule-destabilizing agents, on the other hand, bind to the “colchicine site” (located between the α- and β-subunit within one dimer) or the “vinca site” (between the α- and β-subunit of two dimers within one protofilament) named after the corresponding compounds [174]. Microtubule-destabilizing agents which target the colchicine site prevent the conformational change from curved to straight that occurs during microtubule assembly while vinca site targeting compounds introduce a forced curled structure, thus disrupting the formation of straight protofilaments [177,178]. The aforementioned anthelmintic benzimidazoles are believed to bind near or at the colchicine binding site [166]. Competitive inhibition experiments with colchicine and benzimidazoles have suggested that both target the same region near the N-terminal domain of β-tubulin and modeling studies have supported these results [179,180].

However, our understanding of the broader impact of benzimidazole treatment on filarial worms beyond the cellular level is largely unknown. It remains unclear how the different benzimidazoles damage or alter the filarial worms, and make them susceptible for recognition and clearance by the immune system. One thing that is known, however, is that benzimidazoles as well as other anti-filarial drugs are generally not able to kill the worms by themselves. Essentially all *in vitro* studies for novel anti-filarial compounds have only been able to demonstrate reduced motility or viability of worms whereas the actual death is – with reasonable dosages – never achieved. Thus, the elimination of filariae *in vivo* requires both chemotherapy and a functional immune system, which in turn makes combination therapies particularly attractive treatment options for filarial diseases.

## 1.6 Chemotherapy and stimulation of the immune system

The concept of a combination therapy, a combined application of a specific drug and some compound with immunostimulatory activity is not new. In 1909, Paul Ehrlich postulated that such a combination may yield significantly improved treatment outcomes compared to a therapy with either drug or immunostimulatory compound alone [181]. However, it was not until the second half of the 20$^{th}$ century that rigorous studies started to be conducted that investigated the role of the immune system during the treatment of infectious diseases. Reports from 1948 suggested that acquired immunity was necessary

for the treatment of malaria with quinines in chickens [182]. For schistosomiasis, studies by Doenhoff et al. in the late 70s found that the treatment efficacy of potassium antimony tartrate was reduced in mice with a suppressed T-cell activity [182].

Since then, various groups have investigated potential combination therapy regimens for parasitic infections. Continuing with schistosomiasis, Silva et al. performed a meta-analysis in 2020 in which they identified 17 studies that investigated potential combinations of immunomodulatory compounds with praziquantel (the drug of choice for schistosomiasis) alone [183]. Overall, the meta-analysis revealed somewhat mixed results and only slight improvements in terms of treatment outcomes for combinations with praziquantel [183].

In the case of echinococcosis, ALB has been combined with a number of immunomodulatory compounds [184-186]. Dvorožňáková et al. reported that a combination of ALB with a dialyzable leukocyte extract transfer factor in mice infected with *Echinococcus multilocularis* (also known as the fox tapeworm) led to an increase in the proliferative capabilities of otherwise suppressed T and B cells that was accompanied by an increase of interferon-gamma (IFN-γ) in the serum during the infection. In addition, the combination therapy impaired the growth of larval cysts and reduced cyst weight compared to ALB alone [186]. For infections with *Echinococcus granulosus* (dog tapeworm), Zhang et al. reported that a combination of ALB with interferon-α (IFN-α) in chronically infected mice resulted in a significant reduction of the number, size and weight of cysts in comparison to both ALB or IFN-α alone [184].

Studies with combination therapies for nematodes have been conducted in a variety of models. Murthy et al. demonstrated that a combination of mebendazole and Freund's complete adjuvant led to an increase in parasite-specific antibodies and almost tripled the rate of worm killing from 18.7% (mebendazole alone) to 48.5% in natal multimammate rats (*Mastomys natalensis*) infected with *B. malayi* [187]. Similarly, DEC in conjunction with the tetrapeptide tuftsin (which is naturally formed *in vivo* due to enzymatic cleavage of IgG) has been shown to suppress microfilaremia of *B. malayi* in the southern multimammate rat *Mastomys coucha* for up to 90 days compared to only 60 days after treatment with DEC alone [188]. In the case of *Angiostrongylus cantonensis*, which is the

most common cause of eosinophilic meningitis in Southeast Asia, Du et al. analyzed the combination of mebendazole with IL-12 in a mouse model [189]. They showed that treatment with mebendazole alone or in combination with IL-12 at 4 to 5 dpi resulted in a reduction of recoverable worms of more than 94% [189]. Of note, while IL-12 did not boost the parasite-killing effect of mebendazole, it had a significant impact on the meningitis-associated pathology, i.e., mechanical damage in the brain parenchyma and infiltration of eosinophils and other leukocytes was severely reduced in mice that received mebendazole together with IL-12 [189]. Further, they showed a shift from a type 2 (high levels of IL-4, IL-5) to a type 1 (IFN-γ) immune response in the brain in mice that received the combination therapy [189].

Lastly, for *L. sigmodontis*, Fatma et al. investigated combinations of IVM with four different immunomodulators, i.e., Freund's complete adjuvant, pricoliv, tuftsin and CDRI compound 86/448, in chronically infected cotton rats [190]. They were able to confirm that IVM given by itself causes sterilization of female adult worms and prevents microfilaremia [190]. Interestingly, while IVM alone had, as expected, no lethal effects against adult worms, the combination with any of the tested immunomodulators led to significant reductions of the adult worm burden (mean reduction of 57-78%) in comparison to untreated controls or mice that received IVM alone [190].

Overall, a plethora of studies have highlighted that a combination of chemotherapeutic agents with immunomodulatory or immunostimulatory compounds can improve the treatment efficacy and reduce infection-associated pathology. However, a similar approach with OXF has not been tested previously and will be explored in this thesis.

## 1.7 Aims

The aims of this thesis were 1) to characterize the immune-system drug interactions during anti-filarial treatment and 2) investigate the potential to improve therapeutic options via immunostimulatory combination approaches.

The impact of the immune system on anti-filarial treatment efficacy in general and on treatment with benzimidazoles in particular is not well understood. Benzimidazoles are

potential macrofilaricidal drugs and OXF is a promising drug candidate that is currently advancing through clinical trials as a pan-nematode compound. An improved understanding of the impact and limitations of treatment with OXF and the related compound FBZ may facilitate the development of better therapeutic strategies.

Thus, in a first part, the treatment efficacy of OXF, FBZ and the *Wolbachia*-targeting compound CorA against adult worms, microfilariae and worm fertility were evaluated in different immunodeficient mouse strains in the *L. sigmodontis* rodent model. In addition, immunological changes associated with the treatment were quantified and compared.

In a second part, novel combination therapy approaches were evaluated. Based on the impact of the immune system observed in the first part, immunostimulatory compounds were selected and tested in combination with OXF. The potential to shorten the timeframe needed for effective worm clearance as well as the impact on fertility, microfilariae and the immune system were analyzed. In addition, histopathological changes were assessed to validate the treatment strategy.

In a side project, the efficacy and pharmacokinetic parameters of oxfendazole isomers were compared to see if the development of a treatment based on one specific isomer was warranted. The efficacy was assessed in mice infected with *L. sigmodontis* while the pharmacokinetic profile was evaluated in both mice and dogs.

# 2. Materials & Methods

## 2.1 Maintenance of *Litomosoides sigmodontis* life cycle

The life cycle of *L. sigmodontis* was maintained at the animal facility of the Institute for Medical Microbiology, Immunology and Parasitology (IMMIP), University Hospital Bonn. The tropical rat mite *Ornithonyssus bacoti* was kept at 28°C and 80% humidity in plastic cages containing bedding material. Mites were fed three times a week with fresh blood via exposure to <14 day old baby mice.

To maintain the life cycle, mites were exposed to cotton rats (*Sigmodon hispidus*) that were infected with *L. sigmodontis*. In brief, cotton rats were placed into cages with direct contact to the bedding material containing the mites for 24 hours. During the following blood meals, mites took up MF via ingestion of infected blood from the cotton rats. After 24 hours, bedding material together with the infected mites was collected into Erlenmeyer flasks and incubated at 28°C, 80% humidity for 12-14 days without additional feeding to hunger the mites and allow the MF to mature into infective L3 larvae. The life cycle was maintained according to EU Directive 2010/63/EU and approved by the appropriate state authorities Landesamt für Natur-, Umwelt- und Verbraucherschutz, Recklinghausen, Germany (AZ: 81-02.05.40.18.057).

## 2.2 Animals and ethics

6-8 week old female and male BALB/cJ WT mice were purchased from Janvier Labs, Saint-Berthevin, France. BALB/c Δ*dblGata1*, BALB/c *IL-4r/IL-5*$^{-/-}$, BALB/c µMT and C57BL/6 *Rag2/IL-2rγ*$^{-/-}$ were bred at the animal facility "Haus für Experimentelle Therapie" of the University Hospital Bonn. Δ*dblGata1* and µMT mice were originally obtained from Jackson Laboratory (Bar Harbor, USA), *IL-4r/IL-5*$^{-/-}$ mice from Prof. Dr. Klaus Matthaei (Matthaei, Stem Cell & Gene Targeting Laboratory, ANU College of Medicine, Biology and Environment, Canberra, Australia) and *Rag2/IL-2rγ*$^{-/-}$ mice from Taconic Biosciences Inc. (Cologne, Germany).

For the experiments, mice were housed in individually ventilated cages with access to food and water *ad libitum* and a 12 hour day/night cycle within the animal facility at the

IMMIP. All animal experiments with mice were performed according to EU Directive 2010/63/EU and approved by the appropriate state authorities Landesamt für Natur-, Umwelt- und Verbraucherschutz, Recklinghausen, Germany (AZ: 84-02.04.2015.A507, 81-02.04.2020.A244).

The pharmacokinetic study in beagles was conducted at WuXi AppTec Co., Ltd. in accordance with the WuXi IACUC standard animal procedures along with the IACUC guidelines compliant with the Animal Welfare Act, the Guide for the Care and Use of Laboratory Animals.

### 2.3 Natural infection with *Litomosoides sigmodontis*

6-20 week old male and female mice were naturally infected with *L. sigmodontis* via exposure to *O. bacoti* carrying the infective L3 larvae. In short, mice were placed in steel mesh cages placed on top of bedding material containing infected mites inside a large plastic tub that was placed inside a separate larger plastic tub. The second tub contained disinfectant and served as a “moat” to prevent mites from escaping. After 24 hours, the bedding material containing the mites was removed and the cages were placed on top of the plastic tub with disinfectant. The mice had no direct contact to the disinfectant. After an additional 24 hours, mice were moved into standard cages and the bedding material was exchanged daily for 5 days to remove any remaining mites.

### 2.4 Separation of oxfendazole isomers

Oxfendazole (+) (lot FS00144340) and oxfendazole (-) (lot FS00144342) isomers were obtained by chiral separation from WuXi AppTec (Shanghai) and had the appearance of a white powder. To confirm the separation, the structure of both isomers was evaluated by $^{1}$H NMR and both isomers could be differentiated in 0.1% DMSO solution via specific optical conformation. Oxfendazole (+) had a purity of 99.0% or 99.7% as confirmed by LC-MS or HPLC, respectively. Oxfendazole (-) had a purity of 96.0% or 99.2%, accordingly.

### 2.5 Treatments of mice

For the OXF treatment of *L. sigmodontis* infected immunodeficient strains, a commercially available formulation of oxfendazole (Dolthene®) was used and dissolved in corn oil (Sigma-Aldrich, St. Louis, USA). Vehicle controls received only corn oil. Treatment was performed orally, twice per day, 8 hours apart for 5 days starting 35 dpi. Male and female BALB/cJ WT, BALB/c Δ*dblGata1*, BALB/c *IL-4r/IL-5*$^{-/-}$, BALB/c µMT and C57BL/6 *Rag2/IL-2rγ*$^{-/-}$ mice received either 5 or 12.5 mg/kg OXF in a total volume of 5 ml/kg per treatment for 5 days. Experiments with BALB/c WT mice (n=2-5) were performed 6 times, experiments with BALB/c *IL-4r/IL-5*$^{-/-}$ mice (n=2-6) were performed 3 times and experiments with BALB/c Δ*dblGata1*, BALB/c µMT and C57BL/6 *Rag2/IL-2rγ*$^{-/-}$ (n=2-6) were performed twice.

For the 3-day combination therapy, 6-8 week old female BALB/cJ mice were naturally infected with *L. sigmodontis* and treated orally with 12.5 mg/kg OXF (Dolthene) twice per day starting 35 dpi. For the 2-day combination therapy, mice received either 12.5 or 25 mg/kg OXF per treatment. 2 µg of interleukin-4 (IL-4), IL-5 or IL-33 was given intranasally in a volume of 10 µl in 1xPBS under short anesthesia induced with 2% isoflurane (AbbVie, Wiesbaden, Germany) once per day. Cytokine treatments were performed roughly 45 minutes before the afternoon treatments with OXF. Both combination therapies were performed twice with n=6-7 (3-day therapy) or n=5-10 mice (2-day therapy). Treatment with cytokines alone was performed only once with n=7 mice.

For the FBZ treatment, FBZ (Sigma-Aldrich, St. Louis, USA) was dissolved in distilled water with 0.1% v/v tween80 (Sigma-Aldrich, St. Louis, USA) and 0.5% w/v hydroxyethyl cellulose (Sigma-Aldrich, St. Louis, USA). Vehicle controls received only distilled water with 0.1% v/v tween80 and 0.5% w/v hydroxyethyl cellulose. Male and female BALB/cJ WT, BALB/c Δ*dblGata1*, BALB/c *IL-4r/IL-5*$^{-/-}$, BALB/c µMT and C57BL/6 *Rag2/IL-2rγ*$^{-/-}$ mice were naturally infected with *L. sigmodontis* and treatment was performed 35 dpi for 2 or 5 days once per day via subcutaneous injections into the neck fold. All mice received 2 mg/kg FBZ in a volume of 5 ml/kg per treatment. Experiments with BALB/c WT mice (n=5) were performed 3 (treatment for 5 days) or 5 times (treatment for 2 days and vehicle controls), experiments with BALB/c Δ*dblGata1* and BALB/c *IL-4r/IL-5*$^{-/-}$ mice (n=4-6) were

performed twice and experiments with BALB/c µMT and C57BL/6 *Rag2/IL-2rγ*$^{-/-}$ (n=5) were performed once.

For the CorA treatment, CorA with a purity >90% was produced by the Helmholtz Centre for Infection Research, Department of Microbial Drugs, Braunschweig, using the heterologous producer strain *Myxococcus xanthus*. CorA was formulated 1:1 with polyethylene glycol 400 (PEG400, Carl Roth GmbH & Co. KG, Karlsruhe, Germany) and stored at -80°C until treatment. Before each treatment, vials of CorA were thawed and mixed 1:1 with 1xPBS (Thermo Fisher Scientific, Waltham, USA). Male and female BALB/cJ WT, BALB/c Δ*dblGata1* and BALB/c *IL-4r/IL-5*$^{-/-}$ mice were naturally infected with *L. sigmodontis,* and treatment was performed either once or twice per day via an intraperitoneal injection 35 dpi for 14 days. All mice received 18 mg/kg CorA in a volume of 10 ml/kg per treatment. Vehicle controls were treated once per day with a 1:1 solution of PEG400:PBS. The experiment was performed once with n=3-5 mice.

For the comparison of isomers, 6-8 week old female BALB/c mice were naturally infected with *L. sigmodontis* and treated orally with 25 mg/kg of a racemic mixture of OXF (Dolthene®) or one of two isomers (OXF(+) and OXF(-)) for 5 or 10 days twice per day. OXF (Dolthene®) was dissolved in corn oil (Sigma-Aldrich, St. Louis, USA) while both isomers were suspended in corn oil with 3% sodium carboxymethyl cellulose (Sigma-Aldrich, St. Louis, USA). Vehicle controls received corn oil with 3% sodium carboxymethyl cellulose (Sigma-Aldrich, St. Louis, USA). The experiment was performed once with n=8.

For the pharmacokinetic analysis, 6-8 week old female BALB/c mice were naturally infected with *L. sigmodontis* and treated orally with 12.5 mg/kg of a racemic mixture of OXF (Dolthene®) or one of two isomers (OXF(+) and OXF(-)) for 5 days twice per day. OXF (Dolthene®) was dissolved in corn oil (Sigma-Aldrich, St. Louis, USA) while both isomers were suspended in corn oil with 3% sodium carboxymethyl cellulose (Sigma-Aldrich, St. Louis, USA). Vehicle controls received corn oil with 3% sodium carboxymethyl cellulose (Sigma-Aldrich, St. Louis, USA). The experiment was performed once with n=8 mice.

### 2.6 Pharmacokinetic analysis in mice

To analyze the pharmacokinetic profile of oxfendazole and its isomers, 40 µl of blood was taken from the facial vein of mice (n=8, one experiment) that were naturally infected with *L. sigmodontis* and treated with a racemic mixture of OXF (Dolthene®) or one of its two isomers (see section 2.5). Blood was taken 2 hours after the first and second to last treatment at 35 and 39 dpi, respectively. Blood was collected in EDTA tubes (Sarstedt AG & Co. KG, Nümbrecht, Germany) on ice before centrifugation at 3220xg for 10 min and 4°C to isolate plasma.

Further pharmacokinetic analysis was performed by WuXi AppTec Co., Ltd. In brief, LC-MS analysis was conducted with a Sciex LC-MS Triple Quad 6500-7. 32 µl plasma was mixed with 96 µl of an acetonitrile solution containing 100 ng/ml labetolol, 100 ng/ml tolbutamide and 200 nM nadolol, centrifuged at 4000xg for 10 min and 4°C. 60µl of the supernatant was added to 120 µl water and shaken at 800 rpm for 10min before analysis. A Chiral-AGP 150 x 4.0 mm, 5 µm column (Chrom Tech, Inc./ChiralPak) with a flow rate of 0.7 mL/min was used. The mobile phase consisted of 90% phase A (1% formic acid in water, pH 7.5) and 10% B (isopropyl alcohol). For fenbendazole and fenbendazole sulfone, an ACQUITY UPLC BEH C18 2.1*50 mm, 1.7 µM column with a flow rate of 0.6 ml/min was used. Mobile phase A consisted of 0.1% formic acid in water and phase B consisted of 0.1% formic acid in acetonitrile. Ratio of phases A:B was 85:15 from start until 1.10 min, 2:98 until 1.50 min and 85:15 until 2.00 min. Oxfendazole, fenbendazole and fenbendazole sulfone were then determined via electrospray positive ionization.

### 2.7 Pharmacokinetic analysis in dogs

The Pharmacokinetic study in dogs was performed by WuXi AppTec Co., Ltd, China. In brief, naïve male beagles (n=3) were treated orally with 10 mg/kg of OXF (+) or OXF (-). Both isomers were formulated in a suspension in 3% sodium methylcellulose. Dogs were fed one day before treatment while they had access to water *ad libitum*. To evaluate the pharmacokinetic profile, ca. 0.5 ml of blood was taken 0.083, 0.25, 0.5, 1, 2, 4, 8, 12 and 24 hours after treatment and taken into a tube containing $K_2$-EDTA-2$H_2O$ (Jiangsu Kangjian medical supplies co., LTD, Jiangyan, China). Blood was centrifuged at 12000xg

for 15 min at 4°C and 50 µl of supernatant was used for further analysis with a LCMS-01-SMBA-Triple Quad 6500 Plus with a CHIRALCEL OD-RH 4.6··150 mm column with a flow rate of 0.8 mL/min at 30°C. The mobile phase consisted of phase A (0.1% formic acid and 2mM $HCOONH_4$ in $H_2O$/ACN (95/5) and B (0.1% formic acid and 2mM $HCOONH_4$ in ACN/$H_2O$ (95/5)). Phase B was 25% from start until 11 min, 26% until 11.8 min and 100% until 16 min.

### 2.8 Parasite recovery and quantification

All necropsies of mice infected with *L. sigmodontis* were performed 70 dpi. Adult worm burden was quantified in the thoracic cavity while the number of MF was determined in the peripheral blood. Mice were anesthetized with isoflurane (AbbVie, Wiesbaden, Germany) and 50 µl was taken from the vena facialis via a puncture with a 4 mm animal lancet (Braintree Scientific, Braintree, USA). Blood was drawn into an EDTA tube (Sarstedt AG & Co. KG, Nümbrecht, Germany), mixed with 0.95 ml red blood cell lysis buffer (Thermo Fisher Scientific, Waltham, USA) and incubated for 10 min at room temperature (RT). Blood was then centrifuged at 400xg for 5 min at RT, the supernatant was discarded and MF in the pellet were counted with a bright-field microscope (Zeiss, Göttingen, Germany).

After blood was taken, mice were euthanized with an overdose of isoflurane (AbbVie, Wiesbaden, Germany) to isolate adult worms from the thoracic cavity. In brief, the peritoneal cavity was opened and a small hole was made into the diaphragm. The thoracic cavity was then flushed with 8-10 ml of PBS (Thermo Fisher Scientific, Waltham, USA) and adult worms were collected and transferred to 6-well plates containing PBS. Worms were stored at 4°C and then counted, measured, had their gender determined and intact female worms were further processed to quantify embryonal stages or stored at -20°C for later PCR analysis (see section 2.12).

To quantify the embryonal stages, intact female adult worms were transferred to 4% formaldehyde (Sigma-Aldrich, St. Louis, USA) in PBS (Thermo Fisher Scientific, Waltham, USA) for 24 hours and then stored in 60% v/v ethanol in distilled water at RT until further analysis. Afterward, worms were transferred into 1.5 ml Eppendorf tubes

(Eppendorf SE, Hamburg, Germany) containing 100 µl Hinkelmann solution (0.5% eosin yellow, 0.5% phenol, 0.185% formaldehyde in distilled water) and homogenized completely with a mortar. Embryonal stages (oocyte, morula, pretzel, stretched microfilaria, degenerated early stage [altered oocyte/morula] and degenerated late stage [altered pretzel/microfilaria], see Fig. 6) were then quantified with a bright-field microscope (Zeiss, Göttingen, Germany).

### 2.9 Histology

Histological analysis was performed by Joséphine Gal, Dr. Frédéric Fercoq and Prof. Dr. Coralie Martin (Unité Molécules de Communication et Adaptation des Microorganismes (MCAM, UMR 7245), 10 Sorbonne Université, Muséum national d'Histoire naturelle, CNRS; CP52, Paris, France). Lungs from *L. sigmodontis* infected BALB/cJ WT mice (n = 6-7 per group) were inflated with and fixed in 4% formaldehyde (Sigma-Aldrich, St. Louis, USA) in PBS (Thermo Fisher Scientific, Waltham, USA) for 2 x 24h. Lungs were then dehydrated in ethanol baths of increasing concentrations from 70% to 100% and placed in toluene before paraffin embedding. All sections were cut deep enough to see the main bronchi and perivascular adventitial spaces (PVS). Seven-micron-thick serial sections were prepared and various stainings were performed:

(i) Hematoxylin and eosin staining was used to visualize lung structure and performed as follows: Sections were incubated with Mayer's hematoxylin solution for 5 min, rinsed with tap water for 20 seconds and then incubated with 1% eosin solution for 1 min.

(ii) Alcian Blue - Periodic Acid Schiff (AB-PAS) staining to visualize mucus-producing cells was performed as follows: Sections were incubated with 1% Alcian blue in 3% acetic acid for 20 min, rinsed with tap water and distilled water for 2 min each, incubated with 0.5% periodic acid for 5 min and again rinsed with distilled water. Next, sections were counter stained with Schiff's reagent for 10 min, rinsed with tap water for 5 min and stained with hematoxylin for 1 min. Finally, sections were rinsed again with tap water for 2 min and then differentiated with acid alcohol.

(iii) Luxol Fast Blue staining to visualize eosinophils was performed as follows: Sections were incubated with Luxol blue for 20 min, rinsed with running tap water for 2 min and then counterstained with Mayer's hematoxylin for 10 seconds. The number of Luxol blue positive eosinophils was determined in 15 fields of view with an x100 objective using Olympus BH2.

The sections were scanned at the MNHN light microscopy facility (CeMIM, Centre de Microscopie et d'IMagerie numerique, MNHN Paris) with a NanoZoomer S60 digital slide scanner (Hamamatsu) and images were analyzed with QuPath 0.3 software. For cell infiltration in PVS, 3-5 PVS areas per mouse were segmented manually, Hematoxylin positive nucleus detection was done using the "Cell detection" tool in Qupath and results were expressed as "number of nuclei / $mm^2$ of PVS"; 3) Minimal thickness of bronchial arteries (in micrometer) was measured from 3-6 arteries of similar diameter per mouse.

### 2.10 Preparation of organs for flow cytometry analysis

The thoracic cavity lavage was performed with 8-10 ml of PBS. The lavage was centrifuged at 400xg, for 5 min at 4°C and the supernatant was discarded. The pellet was resuspended in 1 ml red blood cell lysis buffer (Thermo Fisher Scientific, Waltham, USA), washed once with PBS containing 1% v/v FBS (PAN Biotech, Aidenbach, Germany) and 2 mM EDTA (Carl Rohe, Karlsruhe, Germany), resuspended in 2 ml of PBS containing 1% v/v FBS (PAN Biotech, Aidenbach, Germany) and 2 mM EDTA (Carl Rohe, Karlsruhe, Germany) and counted via a CasyR TT Cell Counter (Schärfe Systems, Reutlingen, Germany). The concentration was adjusted to 1 x $10^7$ cells/ml and 100 µl (=1 x $10^6$ cells) were used per flow cytometry staining.

To isolate splenocytes, spleens were perfused with 3 ml of a 0.5 mg/ml collagenase VIII solution (Roche, Basel, Switzerland), minced and incubated at 37°C for 30 min on a shaker at 200 rpm. 5 ml PBS containing 1% v/v FBS (PAN Biotech, Aidenbach, Germany) and 2 mM EDTA (Carl Rohe, Karlsruhe, Germany) was added to stop the collagenase activity and cells were then pushed through a 70 µm metal sieve to obtain single cell suspensions. Splenocytes were then centrifuged (400xg, 5 min, 4°C) and the pellet was incubated with 1 ml of red blood cell lysis buffer (Thermo Fisher Scientific, Waltham, USA)

for 5 min at RT and then washed once with PBS containing 1% v/v FBS (PAN Biotech, Aidenbach, Germany) and 2 mM EDTA (Carl Rohe, Karlsruhe, Germany), resuspended in 5 ml of PBS containing 1% v/v FBS (PAN Biotech, Aidenbach, Germany) and 2 mM EDTA (Carl Rohe, Karlsruhe, Germany) and counted via a CasyR TT Cell Counter (Schärfe Systems, Reutlingen, Germany). The concentration was adjusted to 1 x $10^7$ cells/ml and 100 µl (=1 x $10^6$ cells) were used per flow cytometry staining.

### 2.11 Flow cytometry

Cells from the thoracic cavity and spleen were analyzed with one surface staining to identify lymphoid cells and two intracellular stainings to identify T helper cell subsets and myeloid cells. For the surface staining, cells were incubated for 20 min in a mastermix in PBS with 1% v/v FBS, 0.1% v/v rat IgG (Sigma-Aldrich, St. Louis, USA) containing the antibodies indicated in table 2 on ice. Cells were then washed twice with PBS containing 1% v/v FBS, resuspended in 200 µl PBS containing 1% v/v FBS and 2 mM EDTA and filtered through 70 µm gauze (Labomedic, Bonn, Germany) before measurement with a CytoFLEX S (Beckmann Coulter, Brea, USA) and further analysis with FlowJo V10 (FlowJo, Ashland, USA).

For the intracellular staining, cells were incubated in a fixation/permeabilization buffer (Thermo Fisher, Waltham, USA) for 20 min at RT. Cells were then centrifuged at 400xg for 5 min at 4°C and incubated overnight in PBS containing 1% w/v bovine serum albumin fraction V (PAA Laboratories, Cölbe, Germany) and 0.1% v/v rat IgG (Sigma-Aldrich, St. Louis, USA) at 4°C. The following day, cells were centrifuged at 400xg for 5 min at 4°C and incubated in a permeabilization buffer (Thermo Fisher Scientific, Waltham, USA) for 20 min at RT. Cells were again centrifuged at 400xg for 5 min at 4°C and stained with mastermixes in PBS containing 1% w/v bovine serum albumin fraction V (PAA Laboratories, Cölbe, Germany) and the antibodies indicated in table 3 for 45 min at 4°C in the dark. Cells were then washed twice with PBS containing 1% v/v FBS, resuspended in 200 µl PBS containing 1% v/v FBS and 2 mM EDTA and filtered through 70 µm gauze (Labomedic, Bonn, Germany) before measurement with a CytoFLEX S (Beckmann Coulter, Brea, USA) and further analysis with FlowJo V10 (FlowJo, Ashland, USA).

**Table 2: Antibodies for flow cytometric surface stainings.**

| Antigen | Fluorophore | Clone | Company |
|---|---|---|---|
| CD3 | Al700 | GK1.5 | BioLegend, San Diego, USA |
| CD4 | BV605 | RM4-5 | BioLegend, San Diego, USA |
| CD5 | PerCP-Cy5.5 | 53-7.3 | BioLegend, San Diego, USA |
| CD8a | PE | 53-6.7 | BioLegend, San Diego, USA |
| CD19 | APC | eBio1D3 | Thermo Fisher Scientific, Waltham, USA |

**Table 3: Antibodies for flow cytometric intracellular stainings.**

| Antigen | Fluorophore | Clone | Company |
|---|---|---|---|
| CD3 | BV510 | 145-2C11 | BioLegend, San Diego, USA |
| CD4 | Al700 | 17A2 | BioLegend, San Diego, USA |
| CD8a | PerCP-Cy5.5 | 53-6.7 | BioLegend, San Diego, USA |
| CD11b | Al700 | M1/70 | BioLegend, San Diego, USA |
| CD11c | BV605 | N418 | BioLegend, San Diego, USA |
| CD25 | BV421 | PC61 | BioLegend, San Diego, USA |
| GATA-3 | Al488 | 16E10A23 | BioLegend, San Diego, USA |
| FOXP3 | PE-Cy7 | FJK-16S | Thermo Fisher Scientific, Waltham, USA |
| I-ab | BV421 | M5/114.15.2 | BioLegend, San Diego, USA |
| Ly6C | APC-Cy7 | HK1.4 | BioLegend, San Diego, USA |
| Ly6G | PE-Cy7 | 1A8 | BioLegend, San Diego, USA |
| RELM-$\alpha$ | APC | DS8RELM | Thermo Fisher Scientific, Waltham, USA |
| RORγT | PE | AFKJS-9 | Thermo Fisher Scientific, Waltham, USA |
| Siglec-F | PE | E50-2440 | BD Biosciences, San Jose, USA |
| T-bet | APC | 4B10 | BioLegend, San Diego, USA |

### 2.12 Quantification of *Wolbachia* via RT-PCR

Intact female adult worms isolated from the thoracic cavity were stored at -20°C. DNA was extracted from up to 5 worms per mouse using the QIAamp mini Kit (Qiagen, Hilden, Germany). Worms were taken up in 180 µl ALT buffer and smashed with a mortar. 40 µl proteinase K was then added and the samples were incubated at 56°C and 350 rpm overnight. The next day, 400 µg of RNase A (Thermo Fisher Scientific, Waltham, USA) was added and incubated for 2 min at RT before 200 µl AL buffer was added and the

sample was incubated for an additional 10 min at 70°C and 350 rpm. Next, 200 µl of 100% ethanol was added, applied to a spin column and centrifuged at 6000xg for 1 min. 500 µl AW1 buffer was added next and the samples were centrifuged again at 6000xg for 1min. Subsequently, 500 µl AW2 buffer was added and the column was centrifuged at 20000xg for 1 min and a second time for 3 min. To elute the DNA, the column was transferred to an elution tube, 50 µl AE buffer was added, incubated for 1 min and the column was centrifuged at 6000xg for 1 min. DNA was quantified via NanoVue (Ge Healthcare, Chicago, USA) and stored at -20°C until further analysis.

To quantify *Wolbachia* numbers, a RT-qPCR with primers for the *Wolbachia ftsZ* gene and *L. sigmodontis actin* gene for normalization was performed (Tab. 4). The RT-qPCR was done in triplicates with the mastermix as indicated in table 5. The polymerase was activated at 95°C for 2 min as a first step and DNA was then amplified for 45 cycles of 95° (5 seconds) - 58°C (30 seconds). Copies of *ftsZ* and *actin* were quantified via a standard curve based on plasmids containing the *ftsZ* and *actin* sequences.

**Table 4: Primer sequences.**

| **Primer** | **Sequence** |
|---|---|
| *Wolbachia ftsZ* forward | 5'-cgatgagattatggaacatataa-3' |
| *Wolbachia ftsZ* reverse | 5'-ttgcaattactggtgctgc-3' |
| *L. sigmodontis actin* forward | 5'-atccaagctgtcctgtctct-3' |
| *L. sigmodontis actin* reverse | 5'-tgagaattgatttgagctaatg-3' |

**Table 5: Mastermix for *Wolbachia* quantification via RT-qPCR.**

| **Mastermix (1x)** | **Volume** |
|---|---|
| Water | 4.1 µl |
| *L. sigmodontis actin* forward (10 µM) | 1.0 µl |
| *L. sigmodontis actin* reverse (10 µM) | 1.0 µl |
| *Wolbachia ftsZ* forward (10 µM) | 0.8 µl |
| *Wolbachia ftsZ* reverse (10 µM) | 0.8 µl |
| *ftsZ* taqman probe (5 µM) | 0.1 µl |
| *actin* taqman probe (5 µM) | 0.2 µl |
| Quantinova mastermix | 10 µl |

### 2.13 Isolation of eosinophils from thoracic cavity for next generation sequencing

Eosinophils were isolated from the thoracic cavity of female BALB/c WT mice (n=6 per group) that were naturally infected with *L. sigmodontis* and treated with either 12.5 mg/kg OXF dissolved in corn oil twice per day orally from 35-39 dpi or with 30 mg/kg CorA dissolved in 50% PEG400/50% PBS twice per day intraperitoneally from 35-49 dpi. Treated mice or the corresponding vehicle controls, i.e., corn oil for OXF and 50% PEG400/50% PBS for CorA, were sacrificed one day after the final treatment, i.e., 40 and 50 dpi, respectively, via an overdose of isoflurane. Pleural lavage was performed as described under section 2.10 until the adjustment of the cell concentration to 1 x $10^8$/ml. Cells were then purified with the EasySep™ Mouse PE Positive Selection Kit II (STEMCELL Technologies Inc., Vancouver, Canada) according to the manufacturer's protocol. In brief, cells were transferred to 5 ml polysterene round-bottom tubes and 10 µl/ml FcR blocker as well as 2 µg/ml of an anti-Siglec-F PE antibody (clone E50-2440) were added to the samples, mixed and incubated for 15 min at RT. Afterward, 100 µl/ml of the selection cocktail was added, mixed and incubated for 15 min at RT. Then, 50 µl/ml RapidSpheres™ were added to the sample, mixed and incubated for 10 min at RT. Subsequently, each sample was topped up to 2.5 ml with PBS containing 2% FBS and 1 mM EDTA and placed on the magnet for 5 min at RT. The supernatant was then discarded and the process was repeated an additional 2 times before the sample tubes were removed from the magnet and cells were resuspended in 2 ml PBS containing 2% v/v FBS and 1 mM EDTA. A portion of the isolated cells were analyzed via flow cytometric analysis as described in section 2.11 to validate the purification. Lastly cells were centrifuged at 400xg for 5 min at 4°C, the supernatant was discarded and cells were resuspended in 700 µl TRIzol (QIAGEN, Hilden, Germany) and used for RNA isolation.

### 2.14 Extraction of RNA from eosinophils for next generation sequencing

Eosinophils (for isolation of eosinophils see section 2.13) in 700 µl TRIzol were transferred to Precellys® 2 ml Soft Tissue Homogenizing Ceramic Beads Tubes (Cayman Chemical, Ann Arbor, USA) and homogenized in a Precellys®24 machine (Cayman Chemical, Ann Arbor, USA) with the preset program "6000-3x60-120". The homogenate

was then transferred into a new 1.5 ml reaction tube (Eppendorf SE, Hamburg, Germany) and incubated at RT for 5 min. 70 µl of Bromo-3-chloroproprane (BCP) (Tokyo Chemical Industry, Tokyo, Japan) was then added, mixed and incubated for 2-3 min at RT. Next, the homogenate was centrifuged at 12000xg for 15 min at 4°C and the aqueous phase was transferred into a fresh 2 ml reaction tube (Eppendorf SE, Hamburg, Germany). The RNA isolation was performed with a QIAcube (Qiagen, Hilden, Germany) with the animal tissue and cell protocol according to the RNeasy® Mini kit (QIAGEN, Hilden, Germany). The RNeasy® Mini kit protocol was adjusted to include 100% ethanol instead of 0% ethanol and on-column DNase (QIAGEN, Hilden, Germany) digest was added. The purified RNA was validated via NanoVue (GE Healthcare, Chicago, USA). RNA was then stored at -80°C until further transfer to the NGS core facility of the University Hospital Bonn.

### 2.15 Statistical analysis

Statistical analysis was performed with GraphPad Prism software version 8/9/10 (GraphPad Software, San Diego, USA). The choice of statistical analysis was based on sample size and distribution of samples. Normality was assessed via Shapiro-Wilk test. For normally distributed data a One-Way ANOVA with Dunnet's or Holm-Šídák's multiple comparison test was performed. For non-parametric data Kruskal-Wallis tests followed by Dunn's multiple comparisons test was used to test for significant differences between 3 or more groups or the Mann-Whitney-U test for differences between two groups. p values $< 0.05$ were considered as statistically significant.

# 3. Results

## 3.1 Treatment efficacy of benzimidazoles against *Litomosoides sigmodontis* in immunodeficient mice

The role of the immune system during anti-filarial treatment is largely understudied and it is unclear how different components of both the innate and adaptive immune system contribute to the clearance of filarial worms during and following chemotherapy. The aims of this study were to investigate these immune system – drug interactions and to identify novel and improved treatment strategies based on these interactions.

In a first part, the treatment efficacy of two benzimidazole compounds, OXF and FBZ, was analyzed in the *Litomosoides sigmodontis* rodent model and compared among different immunodeficient mouse strains.

### 3.1.1 Treatment efficacy of oxfendazole is reduced in immunodeficient mice

BALB/c WT mice as well as eosinophil-deficient BALB/c Δ*dblGata1*, BALB/c *IL-4r/IL-5*$^{-/-}$, mature B cell and antibody-deficient BALB/c µMT, as well as T cell, B cell and ILC-deficient C57BL/6 *Rag2/IL-2rγ*$^{-/-}$ were naturally infected with *L. sigmodontis* and treated orally with 5 or 12.5 mg/kg OXF twice per day for 5 days starting 35 dpi. At this point of the infection, *L. sigmodontis* has completed its final molt into adult worms but has not yet started to produce MF. Necropsies were performed to quantify and analyze adult worms and MF 70 dpi (Fig. 6A).

Treatment with 5 or 12.5 mg/kg OXF in BALB/c WT mice led to a statistically significant median reduction of the adult worm burden by 88% ($p = 0.0005$) and 94% ($p < 0.0001$), respectively, when compared to the corresponding vehicle control (Fig. 6B). By contrast, treatment efficacy in all immunodeficient strains was reduced and led to statistically significant differences in Δ*dblGata1* and µMT mice (Fig. 6B). Δ*dblGata1* mice had a reduction of the adult worm numbers by 80% ($p = 0.0433$) and 90% ($p = 0.0136$) while numbers dropped to 64% ($p = 0.0242$) and 35% ($p > 0.05$) in the µMT strain after treatment with 5 or 12.5 mg/kg OXF (Fig. 6B). Treatment in the more severely immunocompromised mice led to a comparatively poor reduction of 50%-20% ($p > 0.05$,

*IL-4r/IL-5*$^{-/-}$) or no reduction of the adult worm burden at all (*Rag2/IL-2rγ*$^{-/-}$) (Fig. 6B). Further, 23% and 44% of BALB/c mice were cleared of adult worms after treatment with 5 or 12.5 mg/kg OXF respectively (Tab. 6). For the immunodeficient mice, there were either no mice cleared of adult worms (*Rag2/IL-2rγ*$^{-/-}$) or only up to one mouse per treatment condition and strain was cured (Tab. 6).

The effect on MF numbers was mostly comparable (Fig. 6C). Treatment in BALB/c mice caused a statistically significant median reduction of MF numbers by 100% after both the low ($p < 0.0021$) and high ($p < 0.0001$) OXF dosage with 85 and 96% of mice identified as MF-negative, respectively (Tab. 6). Treatment in Δ*dblGata1*, *IL-4r/IL-5*$^{-/-}$ and *Rag2/IL-2rγ*$^{-/-}$ mice led to reductions of 0% ($p > 0.05$), 88% ($p > 0.05$) to 97% ($p = 0.0040$) and 74% ($p = 0.0372$) to 82% ($p = 0.0395$), respectively, in comparison to the appropriate vehicle controls (Fig. 6C). In contrast to this reduction of MF numbers, only 7-16% of *IL-4r/IL-5*$^{-/-}$ and 0% of the *Rag2/IL-2rγ*$^{-/-}$ mice were completely negative for peripheral MF (Tab. 6). Interestingly, µMT mice presented with a complete absence of MF 70 dpi after both 5 and 12.5 mg/kg OXF treatments ($p = 0.0040$) (Fig. 6C, Tab. 6). Of note, 70% of Δ*dblGata1* vehicle controls were negative for MF whereas only 54% (5 mg/kg OXF) and 44% (12.5 mg/kg OXF) of treated mice were negative for MF 70 dpi (Tab. 6). This discrepancy in MF-negative animals after treatment is most likely gender related. Female Δ*dblGata1* mice are more prone to develop microfilaremia and have significantly higher MF numbers [191].

In addition to the reduced adult worm and MF numbers, treatment with OXF also affected the remaining worms by reducing the length of adult female (Fig. 6D) and male worms (Fig. 6E). Length of female worms was lower in all treated mice in comparison to the vehicle controls with BALB/c, Δ*dblGata1* and µMT mice presenting mean reductions of 10-23%. *IL-4r/IL-5*$^{-/-}$ mice, on the other hand, had slightly stronger reductions of 21-27% while the effect was highest in *Rag2/IL-2rγ*$^{-/-}$ mice (31-37%, Fig. 6D). The length of male worms was not significantly lower in BALB/c and Δ*dblGata1* mice in the treated groups (Fig. 6E). *IL-4r/IL-5*$^{-/-}$, *Rag2/IL-2rγ*$^{-/-}$ and µMT mice by contrast had significantly shorter male worms with median reductions of 22.7%, 15-20% and 6.2% respectively (Fig 6E).

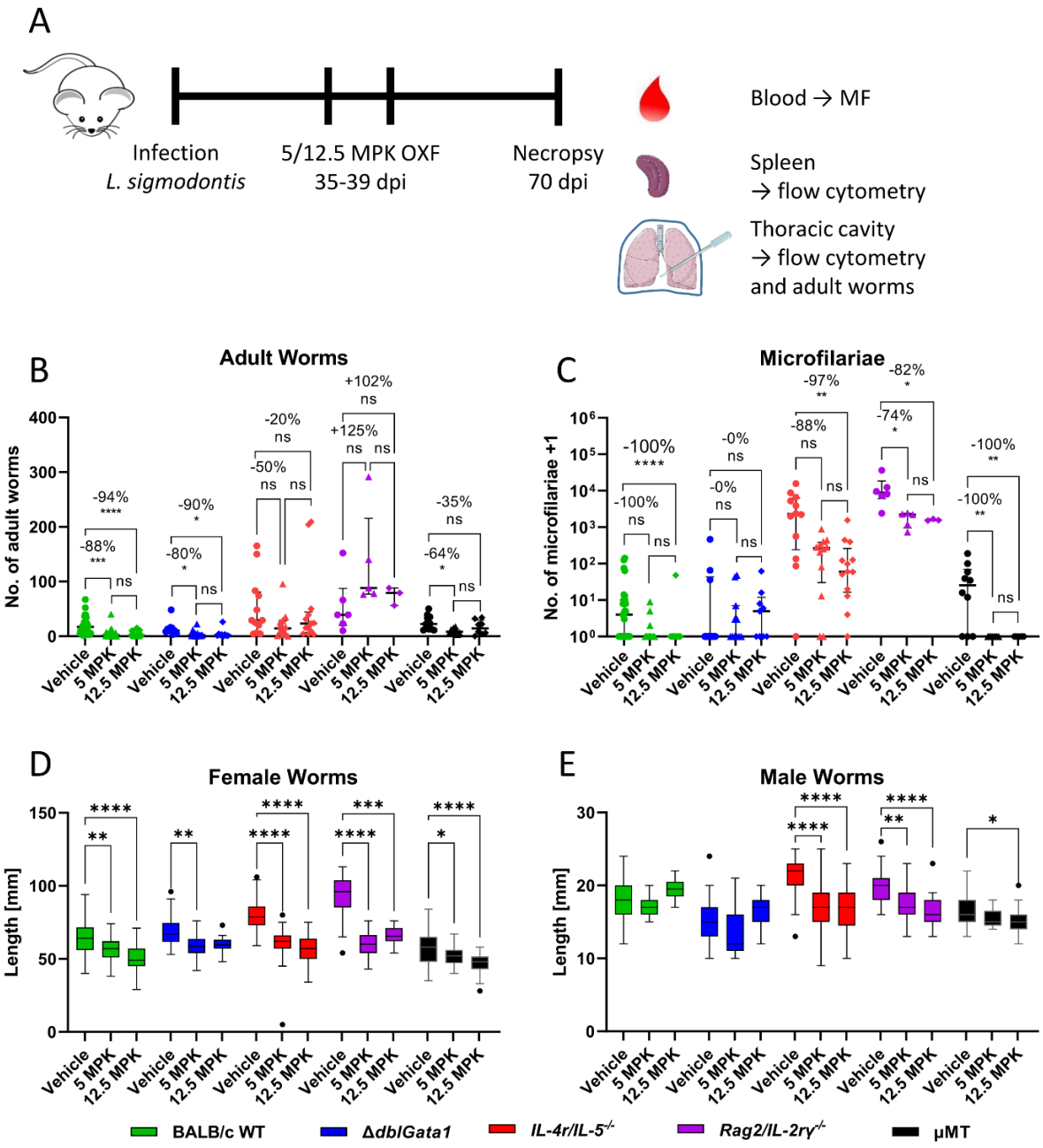


**Fig. 6: Reduced treatment efficacy of oxfendazole in immunodeficient mice**. Different mouse strains were naturally infected with *Litomosoides sigmodontis* and treated orally with 5 or 12.5 mg/kg oxfendazole twice per day for 5 days 35 days after infection. Necropsies were performed 70 days after infection. **(A)** Experimental setup. **(B)** Adult worm burden. **(C)** Microfilariae per 50 µl peripheral blood. **(D)** Length of adult female worms. **(E)** Length of adult male worms. **(B-C)** Data shown as median with interquartile range. Numbers show reduction of median in comparison to corresponding vehicle controls. **(D-E)** Data shown as Tukey box plot. Data for BALB/c (green) pooled from 6 experiments (total n per group = 21-27 mice, 6-154 worms), *IL-4r/IL-5*$^{-/-}$ (red) pooled from 3 experiments (n = 12-13 mice, 68-92 worms), Δ*dblGata1* (blue, n= 9-11 mice, 15-43 worms), *Rag2/IL-2rγ*$^{-/-}$ (purple, n = 3-6 mice, 30-54 worms) and µMT (black, n = 8-10 mice, 9-81 worms) pooled from 2 experiments. Statistical analysis using Kruskal-Wallis with Dunn's post-hoc test, * p<0.05, ** p<0.01, *** p<0.001, **** p<0.0001; MPK = mg/kg

**Table 6: Clearance of adult worms and microfilariae after OXF treatment.** BALB/c WT mice and immunodeficient strains (Δ*dblGata1*, *IL-4r/IL-5*$^{-/-}$, µMT and *Rag2/IL-2rγ*$^{-/-}$) were naturally infected with *Litomosoides sigmodontis* and treated orally with 5 or 12.5 mg/kg OXF twice per day for 5 days starting 35 dpi. The number of adult worms in the thoracic cavity and number of microfilariae per 50 µl blood were quantified 70 dpi. Data for BALB/c pooled from 6 experiments (total n per group = 21-27 mice), *IL-4r/IL-5*$^{-/-}$ pooled from 3 experiments (n = 12-13 mice), Δ*dblGata1* (n = 9-11 mice), *Rag2/IL-2rγ*$^{-/-}$ (n = 3-6 mice) and µMT (n = 8-10 mice) pooled from 2 experiments. Shown is the number and frequency of animals that were free of adult worms and microfilariae 70 dpi.

| | **Adult worm negative mice** | | | **Microfilariae negative mice** | | |
|---|---|---|---|---|---|---|
| | **Vehicle** | **5 mg/kg OXF** | **12.5 mg/kg OXF** | **Vehicle** | **5 mg/kg OXF** | **12.5 mg/kg OXF** |
| **BALB/c** | 0.0% (0/27) | 23.8% (5/21) | 44.4% (12/27) | 44.4% (12/27) | 85.7% (18/21) | 96.2% (26/27) |
| **Δ*dblGata1*** | 0.0% (0/10) | 9.0% (1/11) | 11.1% (1/9) | 70.0% (7/10) | 54.5% (6/11) | 44.4% (4/9) |
| ***IL-4r/ IL-5*$^{-/-}$** | 0.0% (0/12) | 8.3% (1/12) | 0.0% (0/13) | 8.3% (1/12) | 16.6% (2/12) | 7.6% (1/13) |
| ***Rag2/ IL-2rγ*$^{-/-}$** | 0.0% (0/6) | 0.0% (0/5) | 0.0% (0/3) | 0.0% (0/6) | 0.0% (0/5) | 0.0% (0/3) |
| **µMT** | 0.0% (0/10) | 0.0% (0/8) | 12.5% (1/8) | 30.0% (3/10) | 100% (8/8) | 100% (8/8) |

Next, the fertility of the remaining worms was evaluated (Fig. 7). In brief, female worms were fixed, homogenized, stained with Hinkelmann solution and embryonal stages, i.e., oocytes, morulae, “pretzels”, stretched MF as well as degenerated early (altered oocytes or morulae) and degenerated late (altered pretzel or MF) stages were quantified (representative images of the different stages are shown in Fig. 7A). Overall, BALB/c WT, Δ*dblGata1* and µMT vehicle controls had similar numbers per worm while parasites from *IL-4r/IL-5*$^{-/-}$ and *Rag2/IL-2rγ*$^{-/-}$ mice had ~8-10x more embryonal stages overall (Fig. 7B).

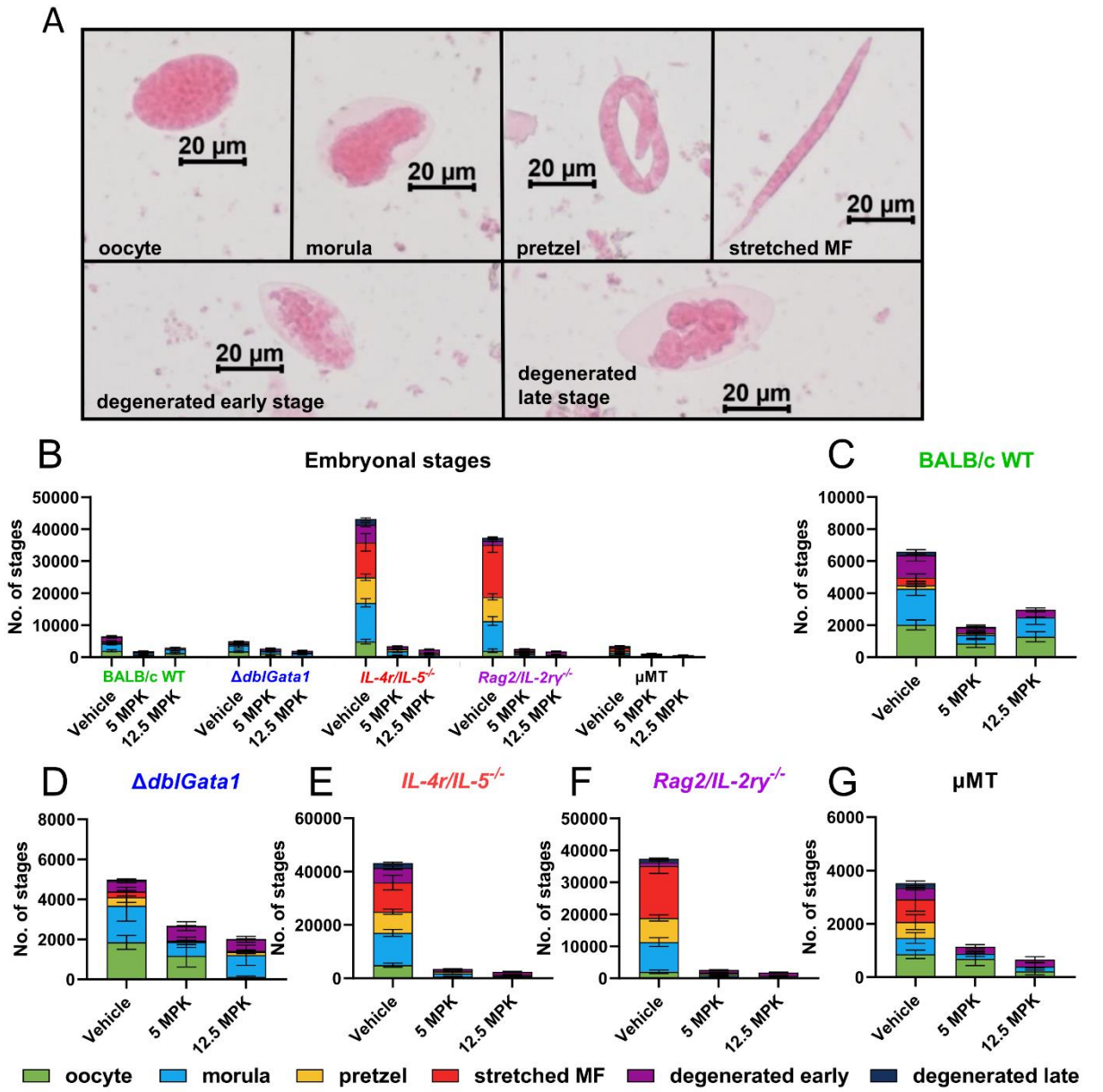


**Fig. 7: Effect of oxfendazole on embryonal development in immunodeficient mice**. Different mouse strains were naturally infected with *Litomosoides sigmodontis* and treated orally with 5 or 12.5 mg/kg oxfendazole twice per day for 5 days 35 days after infection. Necropsies were performed 70 days after infection. Intact female adult worms were fixed in 4% formaldehyde, homogenized, stained with Hinkelmann solution and embryonal stages were quantified under a bright-field microscope. **(A)** Representative images of embryonal stages. **(B-G)** Average number of embryonal stages per female worm in **(B)** all strains, **(C)** BALB/c WT, **(D)** Δ*dblGata1*, **(E)** *IL-4r/IL-5*$^{-/-}$, **(F)** *Rag2/IL-2rγ*$^{-/-}$ and **(G)** µMT mice. **(B-G)** Data shown as mean ± SEM. Data for BALB/c pooled from 6 experiments (total n per group = 29-82 worms), *IL-4r/IL-5*$^{-/-}$ pooled from 3 experiments (n = 47-51 worms), Δ*dblGata1* (n = 12-36 worms), *Rag2/IL-2rγ*$^{-/-}$ (n = 9-16 worms) and µMT (n = 14-26 worms) pooled from 2 experiments; MPK = mg/kg

A closer examination of the embryonal development showed that in BALB/c WT mice the overall number of stages per female worm dropped from 6574 to 1899 (5 mg/kg OXF) and 2958 (12.5 mg/kg OXF) (Fig 7C). Furthermore, the number of oocytes, morulae and degenerated early stages was significantly lower in worms isolated from mice treated with OXF (Tab. 7). Importantly, late stages, i.e., pretzel or stretched MF, were almost completely eliminated after 12.5 mg/kg OXF treatment with an average number of 7.5 ± 4.4 (mean ± SEM) and 0.3 ± 0.3 forms per worm remaining, respectively (Tab. 7). In Δ*dblGata1* mice, the overall reduction of embryonal stages was less pronounced with 2671 (5 mg/kg OXF) and 2018 (12.5 mg/kg OXF) stages per worm in comparison to 4984 stages in the vehicle controls (Fig. 7D). Of note, only the reduction in oocyte numbers was statistically significant and substantial amounts of late stages (157.2 ± 75.0 pretzels and 65.5 ± 43.3 stretched MF) remained after treatment with 12.5 mg/kg OXF (Tab. 7). Treatment in *IL-4r/IL-5*$^{-/-}$ and *Rag2/IL-2rγ*$^{-/-}$ mice led to highest drop-off of overall embryonal forms with a reduction greater than 90% (Fig. 7E+F). In *IL-4r/IL-5*$^{-/-}$ mice, numbers were reduced to 3455 and 2425 after treatment with 5 or 12.5 mg/kg OXF respectively, compared to 43185 stages in vehicle controls (Tab. 7). In *Rag2/IL-2rγ*$^{-/-}$ mice, worms isolated from vehicle controls had 37928 stages on average while worms from treated mice had 2585 (5 mg/kg OXF) or 1775 (12.5 mg/kg OXF) stages (Tab. 7). Importantly, however, worms from both strains still possessed a significant amount of late stages after treatment with 12.5 mg/kg, i.e., worms from *IL-4r/IL-5*$^{-/-}$ mice had an average 469.4 ± 112.0 pretzel stages and 19.2 ± 9.7 stretched MF and worms from *Rag2/IL-2rγ*$^{-/-}$ mice had 355.5 ± 170.8 pretzel stages and 11.1 ± 11.1 stretched MF (Tab. 7). Fitting with the MF numbers from peripheral blood (Fig. 6C), worms isolated from µMT mice had a strong overall reduction of all embryonal stages similar to BALB/c WT mice and a complete absence of late stages after treatment with OXF (Fig. 7G, Tab. 7).

**Table 7: Effect of oxfendazole on embryonal development in immunodeficient mice.** Different mouse strains were naturally infected with *Litomosoides sigmodontis* and treated orally with 5 or 12.5 mg/kg oxfendazole twice per day for 5 days 35 days after the infection. Necropsies were performed 70 days after the infection. Embryonal development was analyzed in up to 5 intact female worms per mouse. Data for BALB/c pooled from 6 experiments (total n per group = 29-82 worms), *IL-4r//IL-5*$^{-/-}$ pooled from 3 experiments (n = 47-51 worms), Δ*dblGata1* (n = 12-36 worms), *Rag2//IL-2rγ*$^{-/-}$ (n = 9-16 worms) and µMT (n = 14-26 worms) pooled from 2 experiments. Statistical analysis using Kruskal-Wallis with Dunn's post-hoc test, * p<0.05, ** p<0.01, *** p<0.001, **** p<0.0001; MPK = mg/kg

| Strain | Treat-ment | Oocyte | | Morula | | Pretzel | | Stretched MF | | Degenerated early | | Degenerated late | |
|---|---|---|---|---|---|---|---|---|---|---|---|---|---|
| | | Mean ± SEM statistics | | Mean ± SEM statistics | | Mean ± SEM statistics | | Mean ± SEM statistics | | Mean ± SEM statistics | | Mean ± SEM statistics | |
| BALB/c | Vehicle | 2019.4 ±303.7 | | 2259.9 ±417.1 | | 216.9 ±78.6 | | 484.8 ±225.7 | | 1390.9 ±355.8 | | 206.1 ±136.7 | |
| | 5 MPK | 853.6 ±249.7 | ** | 540.7 ±205.4 | ** | 111.0 ±54.8 | ns | 15.5 ±9.6 | ns | 334.2 ±161.2 | **** | 46.2 ±25.6 | ns |
| | 12.5 MPK | 1281.2 ±312.7 | * | 1216.1 ±450.9 | ns | 7.5 ±4.4 | ns | 0.3 ±0.3 | * | 453.9 ±126.4 | * | 1.5 ±1.2 | ns |
| Δ*dbl-Gata1* | Vehicle | 1847.5 ±345.0 | | 1829.2 ±762.9 | | 427.7 ±257.6 | | 282.2 ±216.6 | | 531.6 ±96.2 | | 68.8 ±39.7 | |
| | 5 MPK | 1177.9 ±564.2 | ** | 678.7 ±259.3 | ns | 67.0 ±28.3 | ns | 15.0 ±8.5 | ns | 722.5 ±221.1 | ns | 12.9 ±8.4 | ns |
| | 12.5 MPK | 128.1 ±37.2 | **** | 1079.1 ±504.4 | ns | 157.2 ± 75.0 | ns | 65.5 ±43.3 | ns | 570.9 ±149.2 | ns | 19.0 ±10.0 | ns |
| *IL-4r/ IL-5*$^{-/-}$ | Vehicle | 4885.1 ±765.4 | | 12104.0 ±1320.7 | | 7961.7 ±983.8 | | 10902.0 ±2721.1 | | 5561.7 ±662.7 | | 1772.3 ±335.8 | |
| | 5 MPK | 561.2 ±149.4 | **** | 1295.5 ±397.4 | **** | 667.4 ±166.6 | **** | 41.7 ±15.9 | **** | 823.4 ±203.0 | **** | 68.7 ±22.2 | **** |
| | 12.5 MPK | 322.1 ±63.6 | **** | 580.2 ± 21.5 | **** | 469.4 ±112.0 | **** | 19.2 ±9.7 | **** | 1012.0 ±192.4 | **** | 23.5 ±7.4 | **** |
| µMT | Vehicle | 856.9 ±159.2 | | 616.1 ±200.6 | | 596.1 ±287.7 | | 850.0 ±447.6 | | 433.0 ±85.0 | | 173.0 ±82.1 | |
| | 5 MPK | 688.9 ±252.6 | ns | 193.1 ±109.3 | * | 1.5 ±1.5 | * | 0.0 ±0.0 | * | 260.5 ±74.9 | ns | 0.0 ±0.0 | * |
| | 12.5 MPK | 220.0 ±125.0 | *** | 180.0 ±133.61 | * | 0.0 ±0.0 | * | 0.0 ±0.0 | ns | 259.2 ±106.8 | ns | 0.0 ±0.0 | * |
| *Rag2/ IL-2rγ*$^{-/-}$ | Vehicle | 2018.8 ±558.4 | | 9287.5 ±1387.0 | | 7537.5 ±936.9 | | 16256.0 ±2337.3 | | 1250.0 ±263.6 | | 950.0 ±237.0 | |
| | 5 MPK | 473.3 ±136.7 | ns | 573.3 ±181.0 | *** | 540.0 ±148.9 | **** | 226.6 ±94.8 | **** | 720.0 ±125.4 | ns | 53.3 ±23.6 | * |
| | 12.5 MPK | 255.5 ±64.7 | ns | 188.8 ±65.4 | **** | 355.5 ±170.8 | **** | 11.1 ±11.1 | **** | 933.3 ±180.2 | ns | 33.3 ±33.3 | ** |

Overall, the macrofilaricidal treatment efficacy of OXF was reduced in all immunodeficient strains with the least effective treatments achieved in the more severe immunocompromised strains, i.e., *IL-4r/IL-5*$^{-/-}$ and *Rag2/IL-2rγ*$^{-/-}$ mice. The effect on microfilaremia was similarly reduced in most strains, however, treatment in µMT mice led to a complete absence of MF, indicating that the prevention of microfilaremia was B cell or antibody independent. Importantly, analysis of the embryogenesis showed a fitting reduction of late embryonal stages, particularly in worms from BALB/c and µMT mice which suggests that the effect of OXF on microfilaremia was not the result of a direct effect on circulating MF but rather mediated via an impact on fertility of adult female worms.

### 3.1.2 Macrofilaricidal treatment efficacy of flubendazole is reduced in immunodeficient mice

Next, the role of the immune system during treatment with FBZ was analyzed. Similar to the experiments with OXF, BALB/c WT, Δ*dblGata1*, *IL-4r/IL-5*$^{-/-}$, *Rag2/IL-2rγ*$^{-/-}$ and µMT mice were naturally infected with *L. sigmodontis* and treated subcutaneously with 2 mg/kg FBZ once per day for 2 or 5 days starting from 35 dpi. Necropsies were again performed 70 dpi to evaluate parasitological and immunological changes (Fig. 8A).

Treatment with FBZ in BALB/c WT mice led to a median reduction of the adult worm burden by 100% after both 2 ($p < 0.0001$) and 5 ($p < 0.0001$) days of treatment (Fig. 8B). As was the case for OXF, the efficacy against adult worms of FBZ was reduced in all immunodeficient strains. In Δ*dblGata1* and *IL-4r/IL-5*$^{-/-}$ mice the adult worm burden was reduced by 0% or 75% ($p > 0.05$ in both cases) and 32% ($p > 0.05$) or 92% ($p = 0.0099$) after 2 and 5 days of FBZ treatment, respectively (Fig. 8B). Due to a lack of mice, *Rag2/IL-2rγ*$^{-/-}$ and µMT mice were only treated with 2 mg/kg FBZ for 2 days. Treatment in *Rag2/IL-2Rγ*$^{-/-}$ mice led to no reduction of the adult worm burden at all, while µMT mice had 78% ($p = 0.0159$) fewer adult worms (Fig. 8B). The clearance of adult worms followed a similar pattern (Tab. 8). The treatment efficacy was highest in BALB/c WT mice with 56% and 93% of mice cleared after 2 and 5 days of FBZ treatment (Tab. 8). Of the immunodeficient strains, FBZ only led to a partial clearance in Δ*dblGata1* mice (27-30%) whereas all other

strains remained infected with adult worms (Tab. 8). Next, MF numbers in the peripheral blood were quantified. Interestingly, MF numbers were reduced by 100% in all strains after both 2 and 5 days of FBZ. (Fig. 8C). There was only one *IL-4r/IL-5*$^{-/-}$ mouse in which 1 MF was found (Tab. 8).

Similar to OXF, treatment with FBZ affected the remaining worms beyond clearance (Fig. 8D+E). Overall, female adult worms were significantly shorter in all strains in comparison to the corresponding vehicle controls (Fig. 8D). The length of worms from BALB/c mice was significantly reduced by 15% from 65 mm (vehicle controls) to 55 mm ($p = 0.0002$, 2-day FBZ) (Fig. 8D). Worms from BALB/c mice that received 5 days of FBZ were not measured as no intact and undamaged specimens could be isolated from the thoracic or peritoneal cavity. In immunodeficient mice, treatment with FBZ for 2 days led to median reductions of the adult female worm length by 28% ($p < 0.0001$, Δ*dblGata1*), 21% ($p < 0.0001$, *IL-4r/IL-5*$^{-/-}$), 32% ($p = 0.0214$, *Rag2/Il-2rγ*$^{-/-}$) and 18% ($p = 0.0247$, µMT) while treatment for 5 days reduced the worm length by 31% ($p = 0.0005$) and 27% ($p < 0.0001$) in Δ*dblGata1* and *IL-4r/IL-5*$^{-/-}$ mice, respectively (Fig. 8D).

The effect on male worms was less pronounced (Fig. 8E). Length of male worms from BALB/c WT, *Rag2/IL-2rγ*$^{-/-}$ and µMT mice was not significantly reduced when compared to the appropriate vehicle controls with median reductions of less than 5% (Fig. 8E). By contrast, the length of male worms was significantly reduced after the 2-day FBZ treatment in Δ*dblGata1* (27%, $p < 0.0001$) and *IL-4r/IL-5*$^{-/-}$ (9%, $p = 0.0002$) while the difference was not statistically significant for the 5-day treatment group with median reductions of 9 and 14% in Δ*dblGata1* and *IL-4r/IL-5*$^{-/-}$ mice respectively (Fig. 8E).

Overall, the macrofilaricidal efficacy of FBZ was dependent on both the innate and adaptive immune system, while the effect on MF numbers was immune system independent.

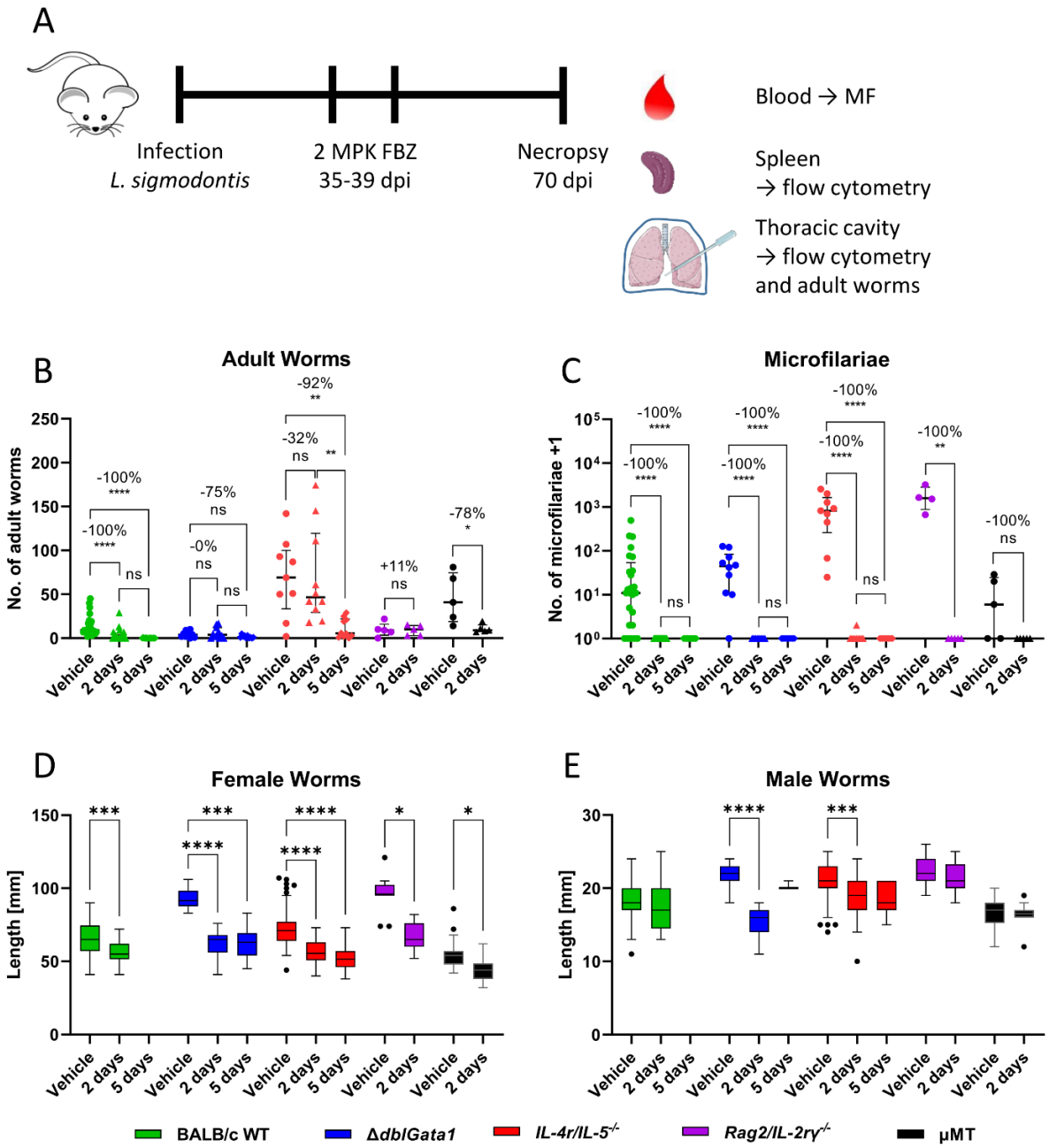


**Fig. 8: Reduced macrofilaricidal treatment efficacy of flubendazole in immunodeficient mice**. Different mouse strains were naturally infected with *Litomosoides sigmodontis* and treated subcutaneously with 2 mg/kg flubendazole once per day for 2 or 5 days 35 days after infection. Necropsies were performed 70 days after infection. **(A)** Experimental setup. **(B)** Adult worm burden. **(C)** Microfilariae per 50 µl peripheral blood. **(D)** Length of adult female worms. **(E)** Length of adult male worms. **(B-C)** Data shown as median with interquartile range. Numbers show reduction of median in comparison to corresponding vehicle controls. **(D-E)** Data shown as Tukey box plot. Data for BALB/c (green) pooled from 5 experiments (total n per group = 15-25 mice, 0-100 worms), Δ*dblGata1* (blue, n = 10-11 mice, 3-31 worms) and *IL-4r/IL-5*$^{-/-}$ (red, n = 9-10 mice, 9-98 worms) pooled from 2 experiments, *Rag2/IL-2rγ*$^{-/-}$ (purple, n = 5 mice, 10-23 worms) and µMT (black, n = 5 mice, 12-46 worms) from 1 experiment. Statistical analysis using Kruskal-Wallis with Dunn's post-hoc test, * p<0.05, ** p<0.01, *** p<0.001, **** p<0.0001.

**Table 8: Clearance of adult worms and microfilariae after FBZ treatment.** BALB/c WT mice and immunodeficient strains (Δ*dblGata1*, *IL-4r/IL-5*$^{-/-}$, µMT and *Rag2/IL-2rγ*$^{-/-}$) were naturally infected with *Litomosoides sigmodontis* and treated with 2 mg/kg FBZ once per day for 2 or 5 days starting 35 dpi. Number of adult worms in the thoracic cavity and number of microfilariae per 50 µl blood were quantified 70 dpi. Data for BALB/c pooled from 5 experiments (total n per group = 15-25 mice), Δ*dblGata1* (n = 10-11 mice) and *IL-4r/IL-5*$^{-/-}$ (n = 9-10 mice) pooled from 2 experiments, *Rag2/IL-2rγ*$^{-/-}$ (n = 5 mice) and µMT (n = 5 mice) from 1 experiment. Shown is the number and frequency of animals that were free of adult worms and microfilariae at 70 dpi.

| | **Adult worm negative mice** | | | **Microfilariae negative mice** | | |
|---|---|---|---|---|---|---|
| | **Vehicle** | **2 days FBZ** | **5 days FBZ** | **Vehicle** | **2 days FBZ** | **5 days FBZ** |
| **BALB/c** | 0.0% (0/25) | 56.0% (14/25) | 93.3% (14/15) | 20.0% (5/25) | 100% (25/25) | 100% (15/15) |
| **Δ*dblGata1*** | 10.0% (1/10) | 27.2% (3/11) | 30.0% (3/10) | 10.0% (1/10) | 100% (11/11) | 100% (10/10) |
| ***IL-4r/ IL-5*$^{-/-}$** | 0.0% (0/9) | 0.0% (0/10) | 10.0% (1/10) | 0.0% (0/9) | 90% (9/10) | 100% (10/10) |
| ***Rag2/ IL-2rγ*$^{-/-}$** | 0.0% (0/5) | 0.0% (0/5) | n/a | 0.0% (0/5) | 100% (5/5) | n/a |
| **µMT** | 0.0% (0/5) | 0.0% (0/5) | n/a | 20.0% (2/5) | 100% (5/5) | n/a |

Next, the state of embryogenesis was assessed (Fig. 9). Similar to the data from the OXF section, vehicle controls from the immunodeficient strains had markedly more overall stages than worms isolated from BALB/c WT mice (Fig. 9A). Of note, female worms isolated form Δ*dblGata1* vehicle controls had significantly more stages overall for the FBZ experiments (36386 stages) than the OXF experiments (4984) (Fig 7B, 9A). This discrepancy is – similar to the previously discussed difference in MF numbers – most likely due to the difference in susceptibility to filarial infections between male and female mice [191]. In the OXF experiments, only 1/10 mice in the vehicle control group were female, while all mice in the Δ*dblGata1* vehicle control group were female.

Beyond this discrepancy, treatment with FBZ induced strong reductions in the overall number of stages in all strains, similar to the treatment with OXF (Fig. 9A). The 2-day FBZ regimen in BALB/c WT reduced the overall number of stages from 9027 (vehicle control) to 4405 stages (Fig 9B). As no intact female worms could be isolated from BALB/c mice that received the high FBZ dose, no data on the potential fertility exists. Closer examination of the distribution of stages shows that worms isolated from the vehicle controls had high numbers of late embryonal stages, i.e., an average of 740.5 ± 258.1 (mean ± SEM) pretzel and 1108.9 ± 303.0 stretched MF stages per worm (Tab. 9). Treatment with FBZ for 2 days led to a strong reduction of pretzel stages down to 3.8 ± 3.8 per worm ($p = 0.0001$) and complete elimination of stretched MF ($p = 0.0004$) (Tab. 9). Fittingly, the percentage of degenerated stages increased to 39.4% in the 2-day FBZ group compared to only 14.1% in the vehicle controls (Tab. 9). For Δ*dblGata1* mice, the reduction of embryonal stages after treatment was even more pronounced than in the WT mice (Fig. 9C). In terms of overall developmental stages, worms from vehicle controls had an average of 36386 stages while treated females had only 182 or 331 stages in the 2- and 5-day FBZ groups (Tab. 9). Importantly, late stages were completely absent in both treatment groups ($p \leq 0.0002$) and the percentage of degenerated stages was increased from 12.8% in the vehicle controls to 74.7% and 82.1% in the 2- and 5-day FBZ groups (Tab. 9). The reduction of embryonal stages in worms isolated from *IL-4r/IL-5*$^{-/-}$ mice showed a similar pattern as worms from Δ*dblGata1* mice with an overall reduction > 90% after treatment (Fig. 9D). Worms from *IL-4r/IL-5*$^{-/-}$ vehicle controls had an average of 51132 developmental stages while the treated worms had only 2895 and 272 stages after 2 and 5 days of FBZ with an accompanying increase in degenerated stages from 11.7% (vehicle) to 26.7% and 81.6%, respectively, as well as a complete absence of late stages in the 5-day FBZ group (Tab. 9). Of note, *IL-4r/IL-5*$^{-/-}$ mice that received the 2-day FBZ treatment still retained some pretzel stages (141.9 ± 141.9, Tab. 9). Likewise, worms isolated from *Rag2/IL-2rγ*$^{-/-}$ and µMT mice had a general reduction of embryonal stages > 90% after the 2-day FBZ treatment while the amount of degenerated stages increased from 6.9 to 15.9% for the *Rag2/IL-2rγ*$^{-/-}$ mice and 17.3 to 38.7% for the µMT mice (Fig. 9E+F, Tab. 9). Similar to the other mice, late stages were fully absent in both strains after treatment (Tab. 9).

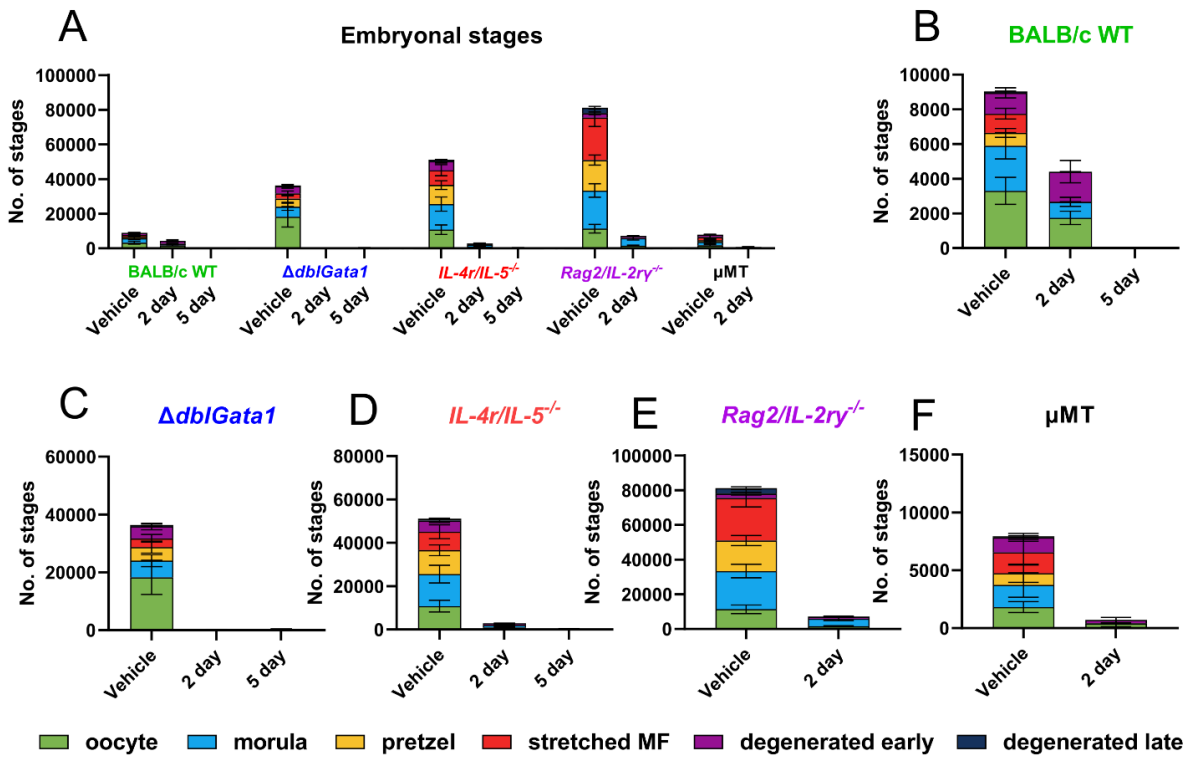


**Fig. 9: Effect of flubendazole on embryonal development in immunodeficient mice**. Different mouse strains were naturally infected with *Litomosoides sigmodontis* and treated subcutaneously with 2 mg/kg flubendazole once per day for 2 or 5 days 35 days after infection. Necropsies were performed 70 days after infection. Intact female adult worms were fixed in 4% formaldehyde, crushed, stained with Hinkelmann solution and embryonal stages were quantified under a bright-field microscope. **(A-F)** Average number of embryonal stages per female worm in **(A)** all strains, **(B)** BALB/c, **(C)** Δ*dblGata1*, **(D)** *IL-4r/IL-5*$^{-/-}$, **(E)** *Rag2/IL-2rγ*$^{-/-}$ and **(F)** μMT mice. **(A-F)** Data shown as mean ± SEM. Data for BALB/c pooled from 5 experiments (total n per group = 0-70 worms), Δ*dblGata1* (n = 11-19 worms) and *IL-4r/IL-5*$^{-/-}$ (n = 22-31 worms) pooled from 2 experiments, *Rag2/IL-2rγ*$^{-/-}$ (n = 9-17 worms) and μMT (n = 14-15 worms) from 1 experiment.

Overall, treatment with FBZ revealed a number of intriguing differences in comparison to the OXF treatment in immunodeficient strains. Similar to OXF, the macrofilaricidal efficacy of FBZ was reduced in all immunodeficient strains. Further, the efficacy was lowest in the more severely immunocompromised lines and treatment in *Rag2/IL-2rγ*$^{-/-}$ did not reduce the adult worm burden at all. However, in contrast to OXF, the effect on microfilaremia was unaffected by the state of the immune system and all mice were cleared of MF after treatment. Supporting these observations, quantification of embryonal stages demonstrated that the fertility of female worms was severely altered after treatment with a complete absence of late stages in all worms of the 5-day FBZ groups as well as stretched MF but not pretzel stages in the 2-day FBZ groups.

**Table 9: Effect of flubendazole on embryonal development in immunodeficient mice.** Different mouse strains were naturally infected with *Litomosoides sigmodontis* and treated subcutaneously with 2 mg/kg flubendazole once per day for 2 or 5 days starting 35 days after the infection. Necropsies were performed 70 days after the infection. Embryonal development was analyzed in up to 5 intact female worms per mouse. Data for BALB/c pooled from 5 experiments (total n per group = 0-70 worms), Δ*dblGata1* (n = 11-19 worms) and *IL-4r/IL-5*$^{-/-}$ (n = 22-31 worms) pooled from 2 experiments, *Rag2/IL-2rγ*$^{-/-}$ (n = 9-17 worms) and µMT (n = 14-15 worms) from 1 experiment. Statistical analysis using Kruskal-Wallis with Dunn's post-hoc test, * p<0.05, ** p<0.01, *** p<0.001, **** p<0.0001.

| Strain | Treat-ment | Oocyte | | Morula | | Pretzel | | Stretched MF | | Degenerated early | | Degenerated late | |
|---|---|---|---|---|---|---|---|---|---|---|---|---|---|
| | | Mean ± SEM | statistics | Mean ± SEM | statistics | Mean ± SEM | statistics | Mean ± SEM | statistics | Mean ± SEM | statistics | Mean ± SEM | statistics |
| BALB/c | Vehicle | 3301.6 ±779.5 | | 2598.3 ±754.8 | | 740.5 ±258.1 | | 1108.9 ±303.0 | | 1201.7 ±289.3 | | 79.5 ± 25.2 | |
| | 2 days | 1748.4 ±380.8 | ns | 917.8 ±258.3 | ns | 3.8 ±3.8 | *** | 0.0 ±0.0 | *** | 1737.7 ±645.8 | ns | 0.3 ± 0.3 | * |
| | 5 days | No worms | | | | | | | | | | | |
| Δ*dbl-Gata1* | Vehicle | 18276.0 ±5901.0 | | 5741.2 ±2084.1 | | 4688.2 ±2061.2 | | 023.5 ±1350.0 | | 4123.5 ±1127.6 | | 535.2 ±332.8 | |
| | 2 days | 46.4 ±32.4 | **** | 0.6 ±0.4 | **** | 0.0 ±0.0 | **** | 0.0 ±0.0 | **** | 131.5 ±49.5 | **** | 5.2 ±5.2 | ns |
| | 5 days | 59.8 ±23.8 | *** | 0.2 ±0.1 | **** | 0.0 ±0.0 | **** | 0.0 ±0.0 | *** | 272.7 ±101.8 | ** | 0.0 ±0.0 | ns |
| *IL-4r/ IL-5*$^{-/-}$ | Vehicle | 10800.0 ±2691.3 | | 14770.0 ±4063.5 | | 11000.0 ±2478.2 | | 8555.6 ±3193.8 | | 5148.1 ±981.7 | | 859.2 ±227.6 | |
| | 2 days | 1005.2 ±205.4 | ** | 975.4 ±716.3 | **** | 141.9 ±141.9 | **** | 0.0 ±0.0 | *** | 771.2 ±147.2 | *** | 3.2 ±3.2 | **** |
| | 5 days | 50.0 ±45.4 | **** | 0.0 ±0.0 | **** | 0.0 ±0.0 | **** | 0.0 ±0.0 | ** | 222.7 ±108.3 | **** | 0.0 ± 0.0 | **** |
| µMT | Vehicle | 1820.0 ±468.5 | | 1913.3 ±1058.4 | | 1006.7 ±780.1 | | 1820.0 ±1110.1 | | 1286.7 ±335.6 | | 93.3 ±57.2 | |
| | 2 days | 389.2 ±264.3 | **** | 37.1 ±35.6 | *** | 0.0 ±0.0 | ns | 0.0 ±0.0 | ns | 270.7 ±240.8 | ** | 0.0 ±0.0 | ns |
| | 5 days | n/a (experiment not performed) | | | | | | | | | | | |
| *Rag2/ IL-2rγ*$^{-/-}$ | Vehicle | 11389.0 ±2474.6 | | 22011.0 ±3870.0 | | 17611.0 ±2927.1 | | 24456.0 ±5159.1 | | 2511.1 ±722.7 | | 3155.6 ±810.8 | |
| | 2 days | 1623.5 ±296.4 | **** | 4370.6 ±1153.7 | *** | 0.0 ±0.0 | **** | 0.0 ±0.0 | **** | 1135.3 ±239.1 | ns | 0.0 ±0.0 | **** |
| | 5 days | n/a (experiment not performed) | | | | | | | | | | | |

### 3.1.3 Immunological changes after benzimidazole treatment

Next, immunological changes associated with the treatment of OXF and FBZ were characterized via flow cytometry. Changes in the composition and numbers of immune cells were analyzed in the thoracic cavity and the spleen. The thoracic cavity is the main site of infection into which L3 larvae migrate within 5-9 dpi and then molt into L4, L5 and adult stages. The adult worms reside within the thoracic cavity for the remainder of the infection. MF, starting at ~50 dpi, are released into the thoracic cavity and migrate into the peripheral blood stream. Prior studies have shown that the spleen in particular is relevant for clearance of MF [192-194]. In order to better understand the immunological changes, broad flow cytometry panels were established to evaluate both lymphoid and myeloid cell populations. The gating strategies are shown in figures 10 and 11, respectively.

As the five different strains used in this project have significant baseline differences in the immune cell composition of both organs and the focus of this project was the impact of treatment with benzimidazoles, changes in the immune cell frequencies and total cell counts are shown as fold changes in comparison to the corresponding vehicle controls in the form of heat maps (Fig. 12+13).

Starting with the situation in BALB/c WT mice: Treatment with OXF induced only limited changes in the frequency of splenocytes (Fig. 12A, green). Lymphocyte numbers were mostly similar or slightly upregulated after treatment while only some myeloid cell frequencies were slightly higher, e.g., monocytes ($CD8^{-/lo}$, $CD11b^{+}$, $Ly6G^{-}$, $Siglec\text{-}F^{-}$, $I\text{-}ab^{-}$) overall, $Ly6C^{lo\text{-}int}$ monocytes in particular and cDC1s ($CD8^{-/lo}$, $CD11b^{-}$, $I\text{-}ab^{+}$, $CD11c^{+}$, $CD8^{+}$) (Fig. 12A, green). Other myeloid cell frequencies were lower after treatment with the strongest differences observed for eosinophils ($CD8^{-/lo}$, $CD11b^{+}$, $Ly6G^{-}$, $Siglec\text{-}F^{+}$), $Ly6C^{hi}$ monocytes and cDC2s ($CD8^{-/lo}$, $CD11b^{-}$, $I\text{-}ab^{+}$, $CD11c^{+}$, $CD8^{-}$) (Fig. 12A, green). There were no significant differences between the mice that received 5 mg/kg OXF and those that received 12.5 mg/kg OXF (Fig. 12A, green). The splenocyte cell count in contrast was either unchanged (Th2/17 cells, $Ly6C^{lo}$ monocytes, cDC1s) or lower after treatment in BALB/c WT mice with a similar pattern for both treatment dosages (Fig. 12B, green).

For the eosinophil-deficient Δ*dblGata1* mice, treatment with OXF induced a slight increase in both cell frequencies and total cell counts for most immune cells (Fig. 12A+B, blue). Only $CD4^+$ and $CD8^+$ T cells, regulatory T cells (Tregs; $CD3^+$, $CD4^+$, $Foxp3^+$, $CD25^+$) and neutrophils ($CD8^{-/lo}$, $CD11b^+$, $Ly6C^+$, $Ly6G^+$) had slightly lower cell frequencies in both treatment groups (Fig. 12A+B, blue). Similarly, the eosinophil and RELM$\alpha^+$ macrophage-deficient *IL-4r/IL-5*$^{-/-}$ mice had only minor changes in immune cell frequencies and cell counts in the spleen with no strong differences between mice that received 5 and 12.5 mg/kg OXF (Fig. 12A+B, red).

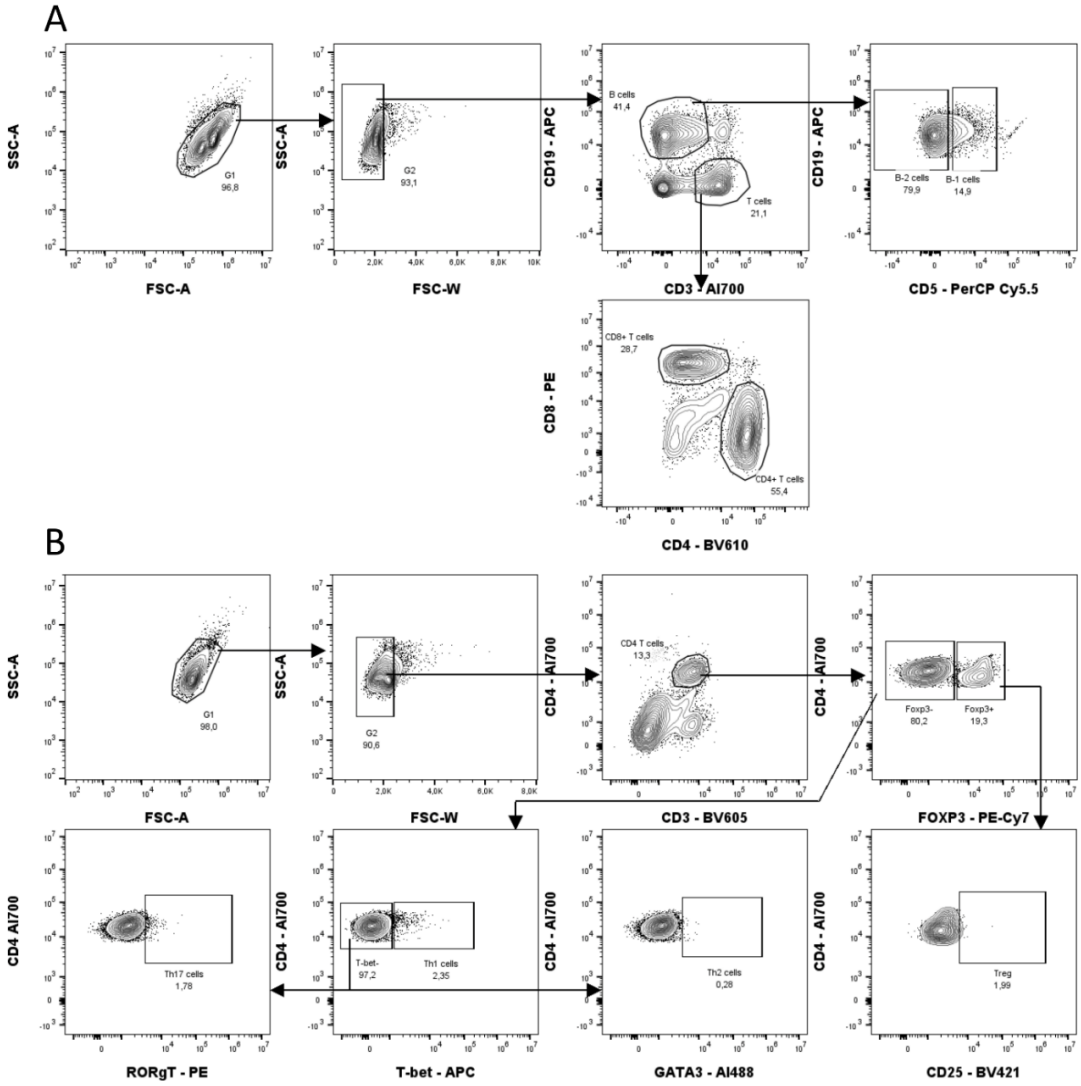


**Fig. 10: Gating strategy to identify lymphocytes**. Representative flow cytometry plots for the identification of **(A)** lymphocytes (CD4 T cells [$CD19^-$, $CD3^+$, $CD4^+$], CD8 T cells [$CD19^-$, $CD3^+$, $CD8^+$], B cells [$CD19^+$, $CD3^-$]) and **(B)** T helper subsets (Tregs [$CD3^+$, $CD4^+$, $Foxp3^+$, $CD25^+$], Th1 cells [$CD3^+$, $CD4^+$, $Foxp3^-$, T-bet$^+$], Th2 cells [$CD3^+$, $CD4^+$, $Foxp3^-$, T-bet$^-$, $GATA3^+$], Th17 cells [$CD3^+$, $CD4^+$, $Foxp3^-$, T-bet$^-$, RORγT$^+$]).

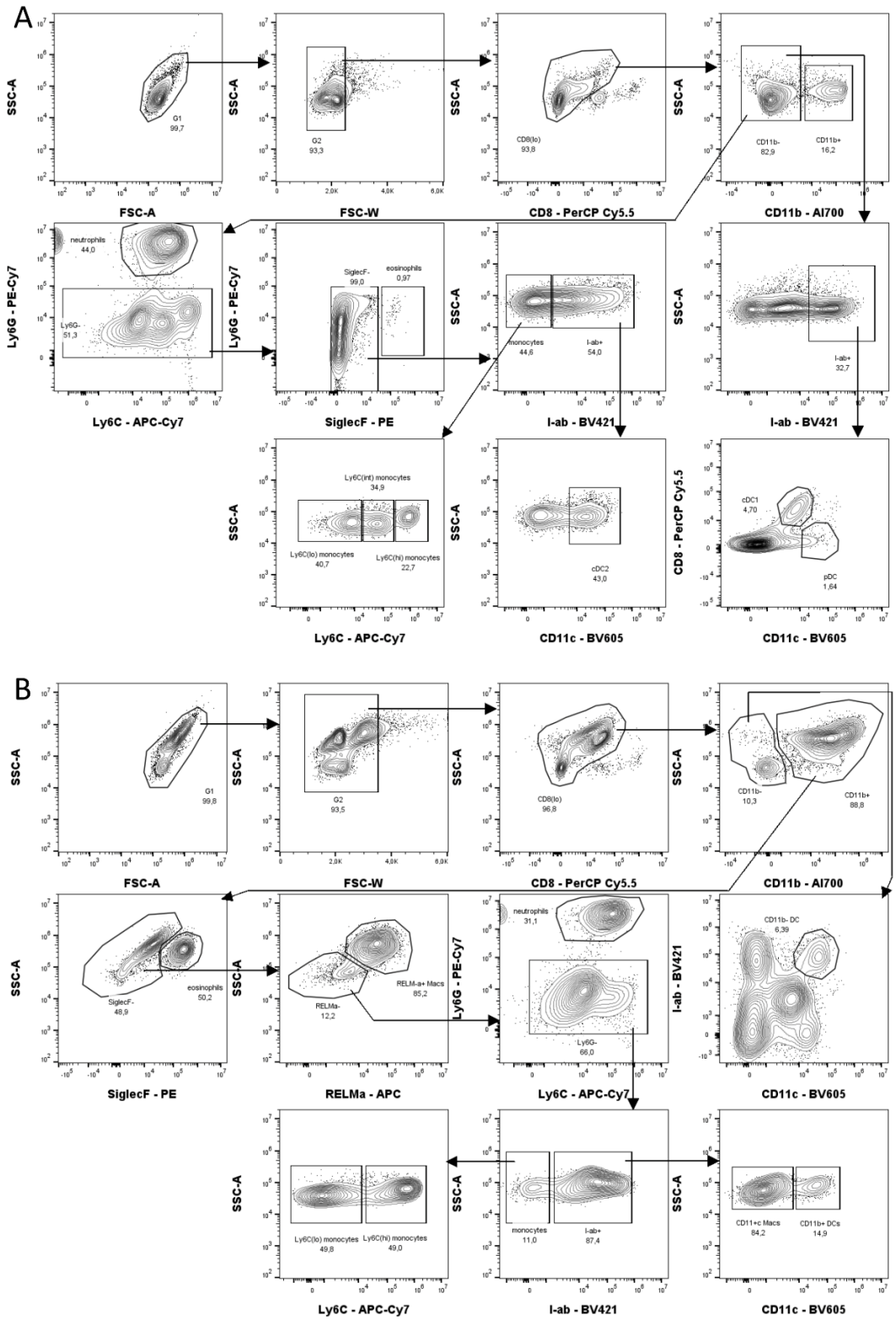


**Fig. 11: Gating strategy to identify myeloid cells**. Representative flow cytometry plots for the identification of myeloid cells in the **(A)** spleen (neutrophils [$CD8^{-/lo}$, $CD11b^{+}$, $Ly6C^{+}$, $Ly6G^{+}$], eosinophils [$CD8^{-/lo}$, $CD11b^{+}$, $Ly6G^{-}$, $Siglec\text{-}F^{+}$], monocytes [$CD8^{-/lo}$, $CD11b^{+}$, $Ly6G^{-}$, $Siglec\text{-}F^{-}$, $I\text{-}ab^{-}$], cDC1 [$CD8^{-/lo}$, $CD11b^{-}$, $I\text{-}ab^{+}$, $CD11c^{+}$, $CD8^{+}$], cDC2 [$CD8^{-/lo}$, $CD11b^{-}$, $I\text{-}ab^{+}$, $CD11c^{+}$, $CD8^{-}$],

pDC [CD8$^{-/lo}$, CD11b$^{+}$, Ly6G$^{-}$, Siglec-F$^{-}$, I-ab$^{+}$, CD11c$^{+}$]) and **(B)** thoracic cavity (neutrophils [CD8$^{-/lo}$, CD11b$^{+}$, Siglec-F$^{-}$, RELMα$^{-}$, Ly6G$^{+}$], eosinophils [CD8$^{-/lo}$, CD11b$^{+}$, Siglec-F$^{+}$], monocytes [CD8$^{-/lo}$, CD11b$^{+}$, Siglec-F$^{-}$, RELMα$^{-}$, Ly6G$^{-}$, I-ab$^{-}$], CD11c$^{+}$ Mϕ [CD8$^{-/lo}$, CD11b$^{+}$, Siglec-F$^{-}$, RELMα$^{-}$, Ly6G$^{-}$, I-ab$^{+}$, CD11c$^{lo/int}$], RELMα$^{+}$ MΦ [CD8$^{-/lo}$, CD11b$^{+}$, Siglec-F$^{-}$, RELMα$^{+}$], CD11b$^{+}$ DCs [CD8$^{-/lo}$, CD11b$^{+}$, Siglec-F$^{-}$, RELMα$^{-}$, Ly6G$^{-}$, I-ab$^{+}$, CD11c$^{hi}$], CD11b$^{-}$ DCs [CD8$^{-/lo}$, CD11b$^{-}$, CD11c$^{+}$, I-ab$^{+}$]).

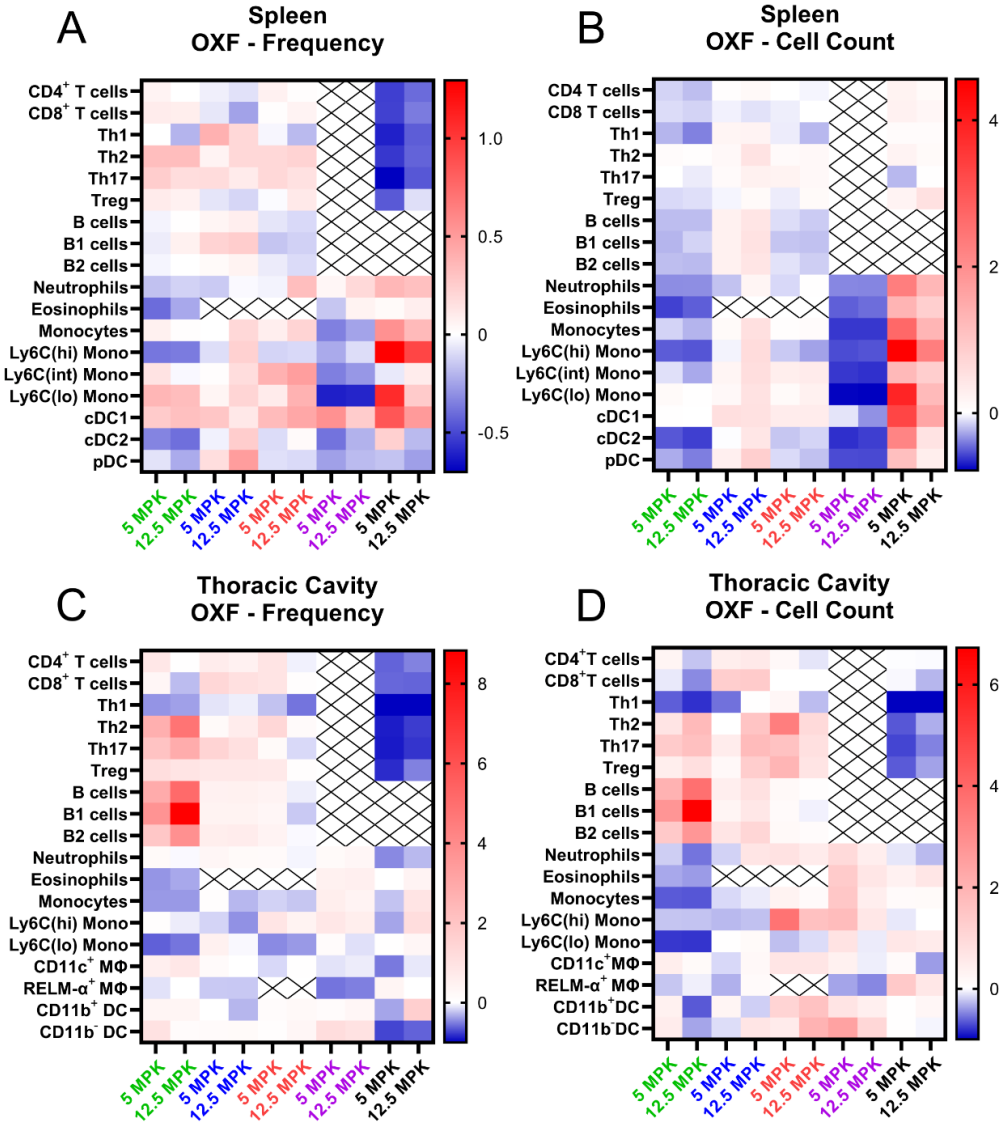


**Fig. 12: Distinct immunological changes in different immunodeficient strains after oxfendazole treatment**. Different mouse strains were naturally infected with *Litomosoides sigmodontis* and treated orally with 5 or 12.5 mg/kg oxfendazole twice per day for 5 days starting 35 days after infection. Necropsies were performed 70 days after the infection and immune cell populations in the **(A-B)** spleen and **(C-D)** thoracic cavity were analyzed via flow cytometry. Heat maps show fold change of the **(A, C)** mean of immune cell frequencies and **(B, D)** mean of total cell counts after treatment in comparison to corresponding vehicle controls. **(A-D)** Data for BALB/c pooled from 6 experiments (green, total n per group = 21-27 mice), *IL-4r/IL-5*$^{-/-}$ pooled from 3 experiments (red, n = 12-13 mice), Δ*dblGata1* (blue, n = 9-11 mice), *Rag2/IL-2rγ*$^{-/-}$ (purple, n = 3-6 mice) and µMT (black, n = 8-10 mice) pooled from 2 experiments; MPK = mg/kg

Unlike the Δ*dblGata1* and *IL-4R/IL-5*$^{-/-}$ mice, both *Rag2/IL-2rγ*$^{-/-}$ and µMT mice had strong changes in the immune cell composition of the spleen (Fig. 12A+B). Frequencies of myeloid cells in the T cell, B cell and ILC-deficient *Rag2/IL-2rγ*$^{-/-}$ mice with the exception of neutrophils and cDC1 were strongly downregulated (Fig. 12A, purple). For the total cell counts, all myeloid cell populations had lower numbers after treatment with no strong difference between both treatment conditions (Fig. 12B, purple). In contrast, the mature B cell-deficient µMT mice had mostly higher frequencies and total cell counts of myeloid cells (Fig. 12A+B, black). The only exception were pDCs (CD8$^{-/lo}$, CD11b$^{+}$, Ly6G$^{-}$, Siglec-F$^{-}$, I-ab$^{+}$, CD11c$^{+}$) with lower cell frequencies after both OXF dosages and cDC2s with lower frequencies after 12.5 mg/kg OXF (Fig. 12A, black). T cells, on the other hand, had significantly lower frequencies but mostly unchanged total cell counts (Fig. 12A+B, black).

Overall, fold changes in the thoracic cavity were significantly higher than in the spleen after treatment (Fig. 12). Breaking it down by strain, BALB/c WT mice had an increase in most lymphocyte frequencies and total cell counts with the exception of Th1 cells (CD3$^{+}$, CD4$^{+}$, Foxp3$^{-}$, T-bet$^{+}$) and CD4$^{+}$ and CD8$^{+}$ T cells after 12.5 mg/kg OXF (Fig. 12C+D, green). Myeloid cell numbers were mostly similar or decreased with the strongest changes for eosinophils (CD8$^{-/lo}$, CD11b$^{+}$, Siglec-F$^{+}$), monocytes overall (CD8$^{-/lo}$, CD11b$^{+}$, Siglec-F$^{-}$, RELMα$^{-}$, Ly6G$^{-}$, I-ab$^{-}$) and Ly6C$^{lo}$ monocytes (CD8$^{-/lo}$, CD11b$^{+}$, Siglec-F$^{-}$, RELMα$^{-}$, Ly6G$^{-}$, I-ab$^{-}$, Ly6C$^{lo}$) in particular (Fig. 12C+D, green). Both Δ*dblGata1* and *IL-4r/IL-5*$^{-/-}$ had comparatively only minor changes in frequencies and total cell counts similar to the observations in the spleen (Fig. 12C+D, blue and red). In contrast to the relatively large changes seen in the spleen of *Rag2/IL-2rγ*$^{-/-}$ mice after treatment, the numbers in the thoracic cavity were mostly similar to the vehicle control with the only exception being the significantly lower numbers of RELMα$^{+}$ macrophages (CD8$^{-/lo}$, CD11b$^{+}$, Siglec-F$^{-}$, RELMα$^{+}$) (Fig. 12C+D, purple). Intriguingly, treatment in µMT mice led to lower numbers of T cells after both OXF dosages while myeloid cell numbers were slightly downregulated after 5 mg/kg OXF but for the most part unchanged after 12.5 mg/kg OXF (Fig. 12C+D, black).

Next, the immunological changes after FBZ treatment were evaluated (Fig. 13). Differences in the immune cell composition of the spleen of BALB/c WT mice after FBZ

treatment were similar but not identical to the changes after OXF treatment (Fig. 13A, green). Most frequencies were comparable to the vehicle control numbers, however frequencies of Th1 cells as well cDC2s and pDCs were notably lower for both the 2- and 5-day FBZ treatment groups (Fig. 13A, green). In addition, the frequencies of Th17 ($CD3^+$, $CD4^+$, $Foxp3^-$, $T\text{-}bet^-$, $ROR\gamma T^+$), and Treg cells were reduced only in the 5 day FBZ group (Fig. 13A, green). Total cell counts in the spleen – as was the case for OXF – were reduced across the board (Fig. 13B, green). Treatment with FBZ in Δ*dblGata1* mice led to largely similar changes as in BALB/c WT mice with decreases in Th1, cDC2 and pDC frequencies and overall decreased total cell counts (Fig. 13A+B, blue). For the *IL-4r/IL-5*$^{-/-}$ mice, treatment with FBZ reduced both frequencies and total cell counts of most lymphocytes with the exception of Th2 ($CD3^+$, $CD4^+$, $Foxp3^-$, $T\text{-}bet^-$, $GATA\text{-}3^+$) and Th17 which had increased total cell counts (Fig. 13A+B, red). Myeloid cells on the other hand were mostly increased in comparison to the vehicle controls except for cDC2s and pDCs (Fig. 13A+B, red). *Rag2/IL-2rγ*$^{-/-}$ mice had overall decreased frequencies and total cell counts of lymphocytes after FBZ treatment (Fig. 13A+B, purple). µMT mice had increased T cell numbers after FBZ treatment whereas monocytes and neutrophils were increased while eosinophils and cDC numbers were decreased (Fig. 13A+B, black).

In a similar fashion to OXF, fold changes in the thoracic cavity were generally stronger than in the spleen after FBZ treatment (Fig. 13). In BALB/c WT mice, FBZ led to an increase of most lymphocyte frequencies, while for total cell counts B cells were increased and T cells were mostly decreased (Fig. 13C+D, green). Myeloid cells were largely unchanged with the exception of eosinophils which were strongly downregulated (Fig. 13C+D, green). For Δ*dblGata1* and *IL-4r/IL-5*$^{-/-}$ mice, myeloid numbers were generally slightly increased after treatment (with the exception of $CD11c^+$ macrophages [$CD8^{-/lo}$, $CD11b^+$, $Siglec\text{-}F^-$, $RELM\alpha^-$, $Ly6G^-$, $I\text{-}ab^+$, $CD11c^{lo/int}$] in *IL-4r/IL-5*$^{-/-}$ mice) while changes lymphocytes were different for each treatment regimen (Fig. 13C+D, blue and red). Interestingly, Δ*dblGata1* mice had decreased B ($CD3^-$, $CD19^+$), Th2 and Treg numbers only in the 2-day FBZ treatment group whereas *IL-4r/IL-5*$^{-/-}$ mice had decreased numbers of overall T cells as well as Th1 and Th2 cells in the 2-day FBZ but not 5-day FBZ group (Fig. 13C+D, blue and red). For *Rag2/IL-2rγ*$^{-/-}$ mice, treatment with FBZ led to a slight decrease in myeloid cell frequencies and significantly stronger decrease in total myeloid

cell numbers (Fig. 13C+D, purple). Lastly, µMT mice had mostly decreased or unchanged cell frequencies, however, total cell counts were unchanged or slightly elevated (Fig. 13C+D, black).

Overall, treatment with OXF and FBZ induced notably differences in the immune cell composition in both the spleen and thoracic cavity with distinct patterns in each strain.

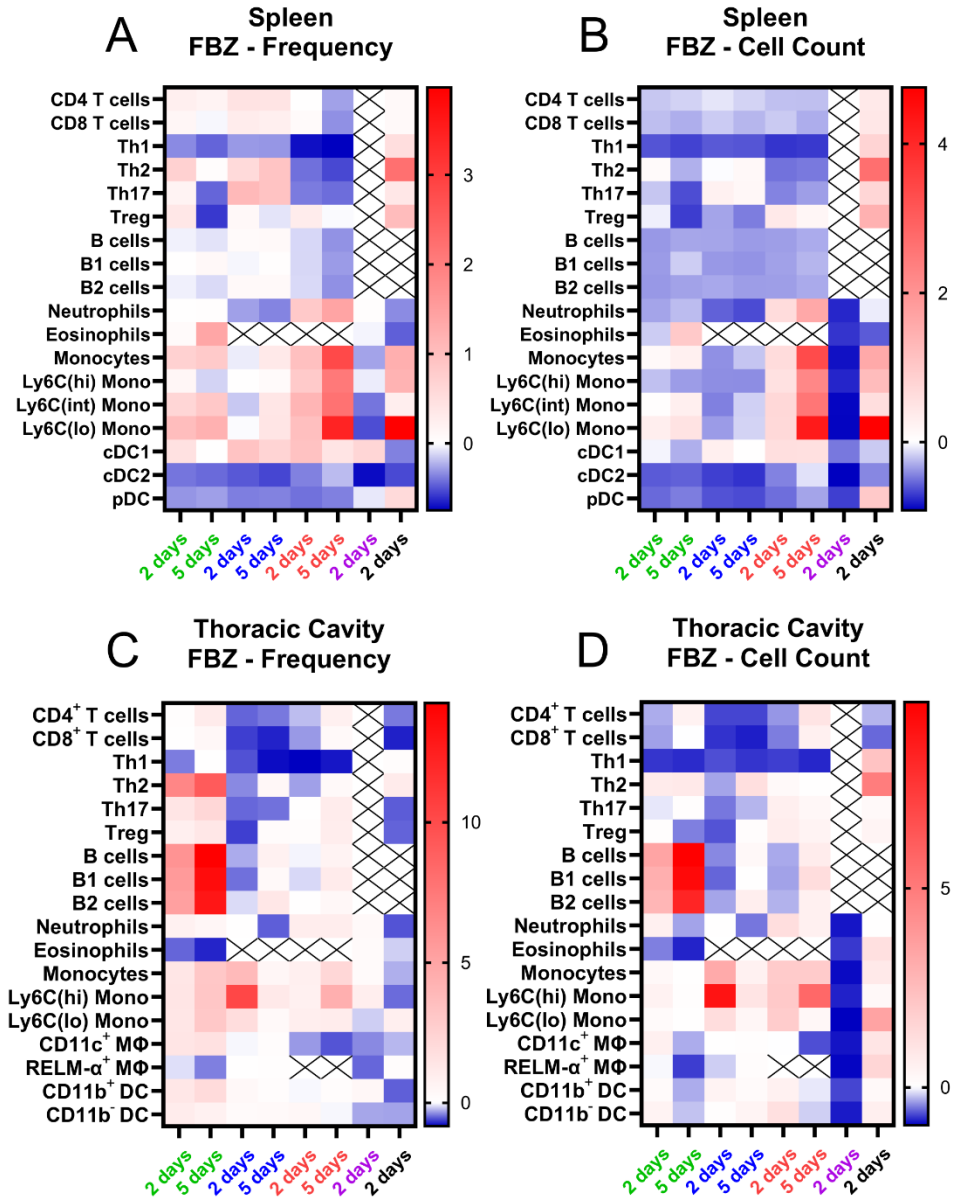


**Fig. 13: Distinct immunological changes in different immunodeficient strains after flubendazole treatment**. Different mouse strains were naturally infected with *Litomosoides sigmodontis* and treated orally with 5 or 12.5 mg/kg oxfendazole twice per day for 5 days starting 35 days after infection. Necropsies were performed 70 days after the infection and immune cell populations in **(A-B)** spleen and **(C-D)** thoracic cavity were analyzed via flow

cytometry. Heat maps show fold change of the **(A, C)** mean of immune cell frequencies and **(B, D)** mean of total cell counts after treatment in comparison to corresponding vehicle controls. **(A-D)** Data for BALB/c (green) pooled from 5 experiments (total n per group = 15-25 mice), Δ*dblGata1* (blue, n = 10-11 mice) and *IL-4r/IL-5*$^{-/-}$ (red, n = 9-10 mice) pooled from 2 experiments, *Rag2/IL-2rγ*$^{-/-}$ (purple, n = 5 mice) and µMT (black, n = 5 mice) from 1 experiment.

### 3.2 Treatment efficacy of anti-*Wolbachia* compounds against *Litomosoides sigmodontis* in immunodeficient mice

Apart from directly acting compounds like benzimidazoles, it is also possible to treat filarial nematodes with antibiotics which are then classified as indirectly acting drugs. These compounds target the previously discussed *Wolbachia*, bacteria of the order Rickettsiales which live as obligate endobacteria in a symbiotic relationship in the cells of a number of filarial nematodes including *L. sigmodontis*. Depleting *Wolbachia* with antibiotics can lead to sterility, growth retardation and eventual death of the worms [12,68,119].

In this part of the project, the efficacy of anti-*Wolbachia* treatment was evaluated in immunodeficient mice similar to the previous experiments with OXF and FBZ. BALB/c WT as well as Δ*dblGata1* and *IL-4r/IL-5*$^{-/-}$ mice were naturally infected with *L. sigmodontis* and treated with the antibiotic corallopyronin A (CorA) for 14 days once (QD) or twice (BID) per day with 18 mg/kg per intraperitoneal injection starting 35 dpi. Mice were again sacrificed 70 dpi to evaluate parasitological and immunological changes (Fig. 14A).

Treatment for 14 days with CorA did not have a statistically significant impact on the adult worm burden in BALB/c WT mice (Fig. 14B). Similarly, neither Δ*dblGata1* nor *IL-4r/IL-5*$^{-/-}$ mice had significant differences in the number of adult worms after treatment with either dose of CorA (Fig. 14B). Next, the impact on MF numbers was evaluated (Fig. 14C). However, while all treated BALB/c and Δ*dblGata1* mice were negative for MF in their peripheral blood, it is impossible to calculate a reduction as the vehicle controls were also negative in this experiment (Fig. 14C). In case of the *IL-4r/IL-5*$^{-/-}$ mice, all mice developed microfilaremia. While there was a reduction in MF numbers after the BID CorA treatment of 67% in *IL-4r/IL-5*$^{-/-}$ mice, the difference was not statistically significant (Fig. 14C).

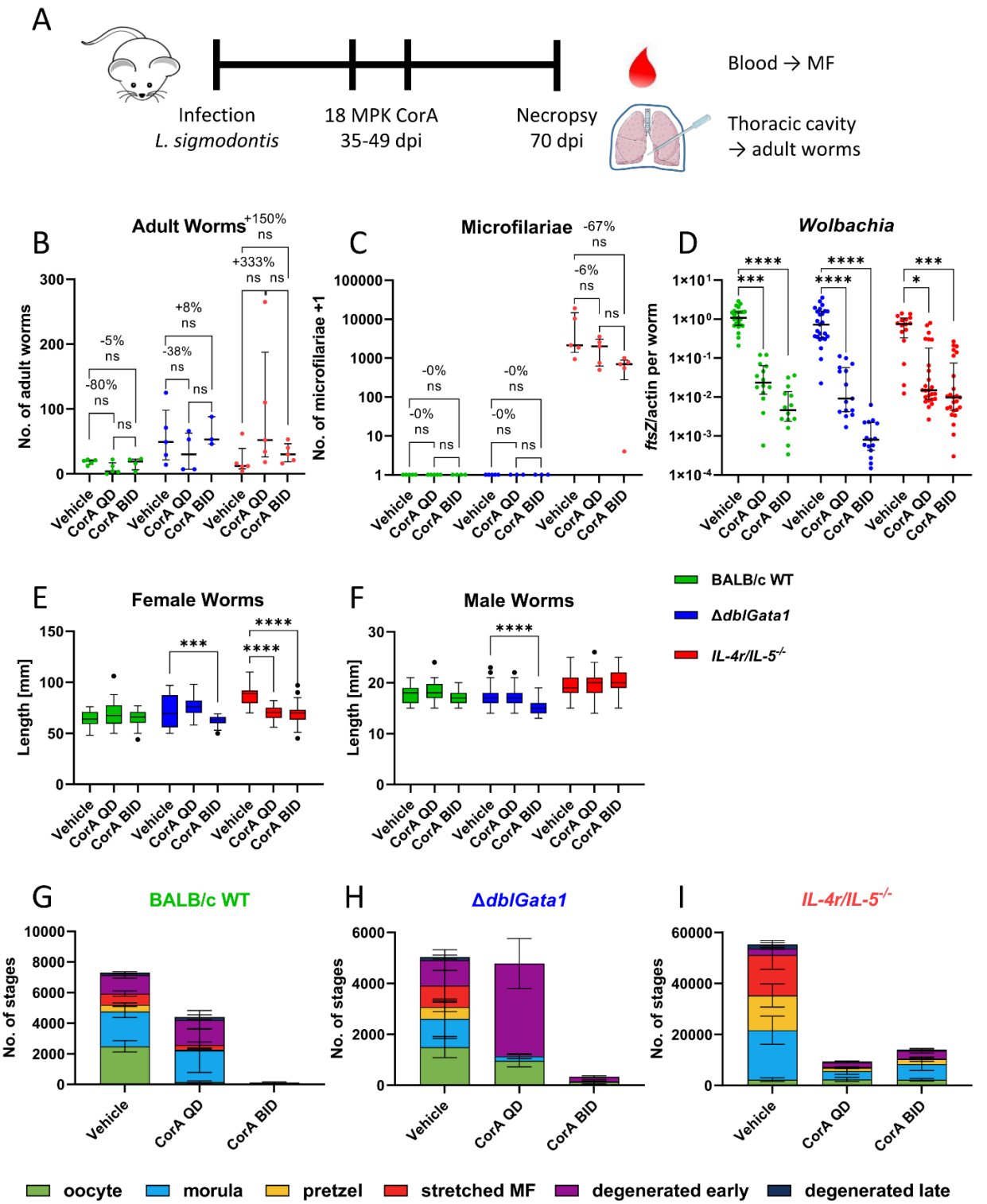


**Fig. 14: Anti-*Wolbachia* effect of corallopyronin A is not reduced in immunodeficient strains**. Different mouse strains were naturally infected with *Litomosoides sigmodontis* and treated orally with 18 mg/kg corallopyronin A (CorA) once (QD) or twice (BID) per day for 14 days 35 days after infection. Necropsies were performed 70 days after infection. **(A)** Experimental setup. **(B)** Adult worm burden (total n per group = 3-5 mice). **(C)** Microfilariae per 50 µl peripheral blood (n = 3-5 mice). **(D)** *Wolbachia ftsZ*/filarial actin per female worm (n = 14-25 worms). **(E)**

Length of adult female worms (n = 20-48 worms). **(F)** Length of adult male worms (n = 12-47 worms). **(G-I)** Average number of embryonal stages per female worm (n = 6-15 worms) in **(G)** BALB/c, **(H)** Δ*dblGata1* and **(I)** *IL-4r/IL-5*$^{-/-}$ mice. **(A-D)** Data shown as median with interquartile range. **(A-B)** Numbers show reduction of median in comparison to corresponding vehicle control. **(E-F)** Data shown as Tukey box plot. **(G-I)** Data shown as mean ± SEM. **(A-I)** Data from 1 experiment except for the BALB/c vehicle numbers in **(G)** which are pooled from 12 experiments (n = 162). **(B-D)** Statistical analysis using Kruskal-Wallis with Dunn's post-hoc test, **(E-F)** statistical analysis using one-way ANOVA with Holm-Šídák post-hoc test, * p<0.05, *** p<0.001, **** p<0.0001.

Next, *Wolbachia* numbers were quantified in female adult worms via qPCR (Fig. 14D). Importantly, all female worms were positive for *Wolbachia* and treatment with CorA led to a 1.5 to 3 $\log_{10}$ reduction with an overall stronger reduction in the BID CorA groups which was independent of the immune status of the mice (Fig. 14D). Interestingly, while the length of female worms was reduced significantly in *IL-4r/IL-5*$^{-/-}$ mice after both QD CorA ($p < 0.0001$) and BID CorA ($p < 0.0001$) treatment, only the BID CorA group had shorter worms in Δ*dblGata1* mice ($p = 0.0009$) (Fig. 14E). The length of female worms in BALB/c WT mice was unaffected by either CorA dosage (Fig. 14E). In the case of male worms, the length was not reduced in BALB/c WT and *IL-4r/IL-5*$^{-/-}$ mice after treatment while male worms from Δ*dblGata1* were reduced in the BID CorA group ($p < 0.0001$) (Fig. 14F). Further, the effect of CorA on the embryonal development was quantified (Fig. 14G-I). There were significant differences between the effect of QD and BID CorA treatment in BALB/c WT and Δ*dblGata1* mice (Fig. 14G+H). The QD treatment led to a strong decrease in viable embryonal stages in both strains while the BID treatment led to a near complete elimination of all stages (Fig. 14G+H). By contrast, in the *IL-4r/IL-5*$^{-/-}$ mice, both the QD and BID treatment led to overall significantly decreased numbers of embryonal stages in comparison to the vehicle control with only negligible differences between both treatment conditions (Fig. 14I). Furthermore, both QD and BID treatment did not lead to an elimination of late stages with an average 1260.0 ± 334.0 (QD, mean ± SEM) to 1966.6 ± 831.4 (BID) pretzel stages and 306.6 ± 149.7 (QD) to 341.6 ± 255.3 (BID) stretched MF per female worm remaining (Fig. 14I).

Overall, CorA did not affect the adult worm burden in any of the tested strains. While the effect on MF numbers remains unclear, the efficacy against *Wolbachia* was unaffected by the lack of eosinophils or IL-4 receptor and IL-5. The quantification of embryonal stages

and presence of MF in the *IL-4r/IL-5*$^{-/-}$ suggests that remaining female worms may remain fertile in immunodeficient mice using this CorA regimen.

### 3.3 Effect of anti-filarial compounds on eosinophils

The previous results have shown an impaired treatment efficacy against *L. sigmodontis* in immunocompromised mice. In addition, flow cytometric analysis revealed significant changes in eosinophils numbers, particularly in the thoracic cavity, after treatment. Based on these observations, it became clear that a more detailed characterization of the involved immune cells might improve our understanding of their role during anti-filarial treatment. As a first step, the impact of both OXF and CorA on eosinophils during anti-filarial treatment was examined (Fig. 15). 6-week old female BALB/c WT mice were naturally infected with *L. sigmodontis* and treated with OXF or CorA for 5 and 14 days starting at 35 dpi, respectively. Treated mice as well as corresponding vehicle controls (n=6 per group) were sacrificed one day after the treatment was concluded, i.e., 40 (OXF) and 50 (CorA) dpi, and eosinophils from the thoracic cavity were isolated, their RNA was extracted and analyzed further via NGS (Fig. 15A).

As expected, treatment with OXF did not affect the adult worm burden under these conditions yet (Fig. 15B), as clearance of the adult worms after treatment with OXF requires multiple days (unpublished observations, Coralie Martin). Similarly, for mice treated with CorA, no change in the adult worm numbers was observed (Fig. 15C), while the *Wolbachia* numbers were already reduced by >99% (Fig. 15D).

Starting with eosinophils isolated from mice treated with OXF, analysis of the NGS data showed that there were only a handful of genes up- or downregulated after OXF treatment in comparison to the eosinophils from the associated vehicle control mice (Fig. 15E). Downregulated genes encode for the proteins Collagen alpha-1(I) chain (P11087) and Collagen alpha-6(VI) chain (Q8C6K9), respectively, and they are involved in integrin signaling pathways and inflammation mediated by chemokine or cytokine signaling (Fig. 15E). Additional downregulated genes encode for the eosinophil cationic protein 2 and the granulocyte colony-stimulating factor receptor, respectively.

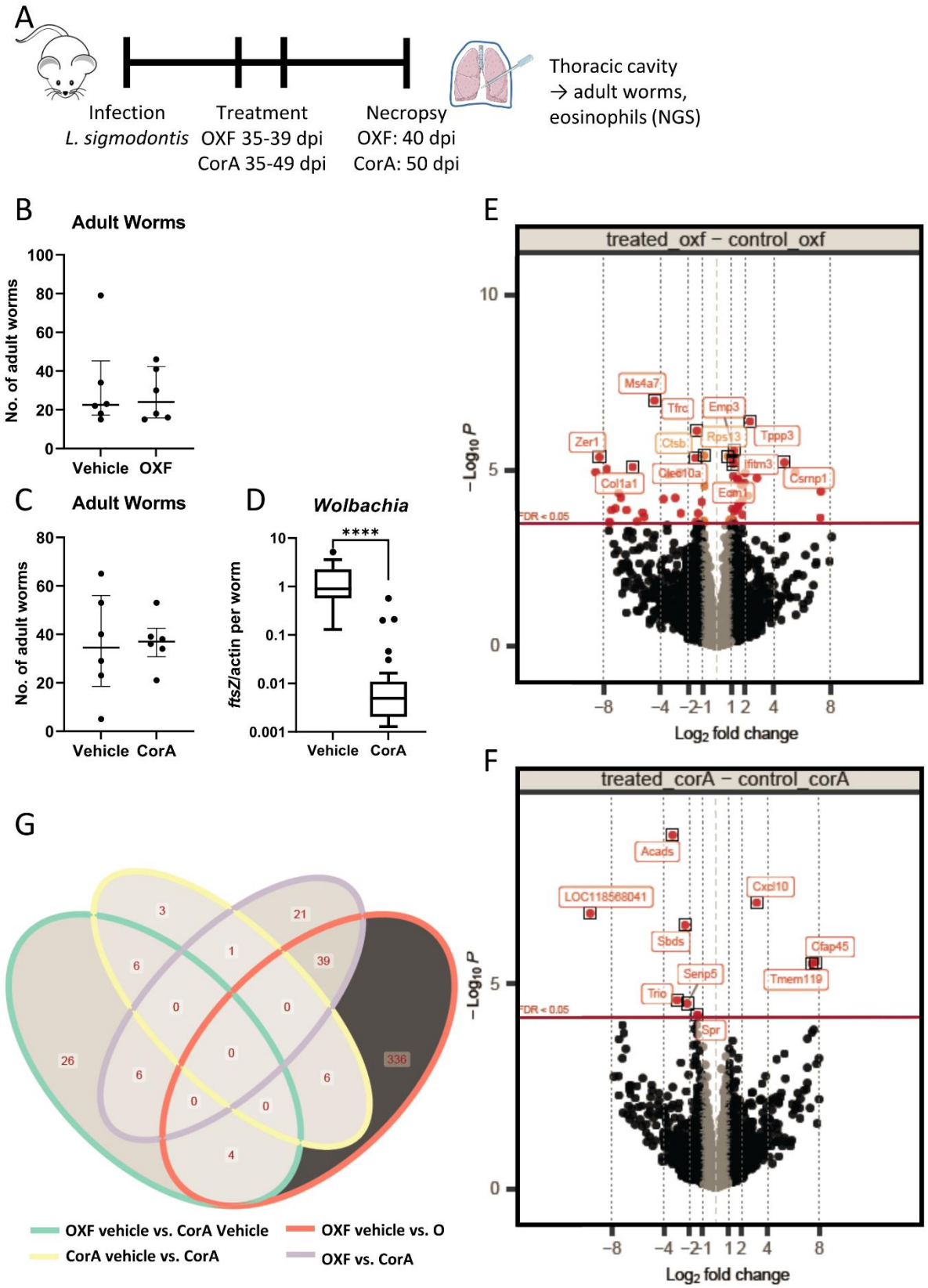


**Fig. 15: Impact of anti-filarial treatment on eosinophils**. 6-week old female BALB/c mice were naturally infected with *Litomosoides sigmodontis* and treated orally with 12.5 mg/kg oxfendazole

twice per day for 5 days or 30 mg/kg corallopyronin A twice per day for 14 days starting from day 35 after infection. Necropsies of treated mice and vehicle controls were performed 1 day after treatment, i.e., 40 days post infection (oxfendazole) and 50 days post infection (corallopyronin A). Eosinophils were then isolated from the thoracic cavity, RNA was extracted and changes in gene expression were analyzed via NGS. **(A)** Experimental setup. **(B)** Adult worm burden for oxfendazole treatment. **(C)** Adult worm burden for corallopyronin A treatment. **(D)** *Wolbachia ftsZ*/filarial *actin* per female worm. **(E)** Volcano plot showing up- and down regulated genes in eosinophils after treatment with oxfendazole in comparison to vehicle controls. **(F)** Volcano plot showing up- and down regulated genes in eosinophils after treatment with corallopyronin A in comparison to vehicle controls. **(G)** Venn-diagram showing shared gene profile of oxfendazole and corallopyronin A treatment. **(B-C)** Data shown as median with interquartile range. **(D)** Data shown as Tukey box plot. Data from 1 experiment, n = 6 per group. **(B-D)** Statistical analysis using Kruskal-Wallis with Dunn's post hoc test, **** $p<0.0001$.

Furthermore, upregulated genes that were identified encode for the PtdIns(3,4,5)P3 binding protein, which is a phosphatidylinositol 3,4,5-triphosphate-dependent GTPase-activating protein and interacts with the actin cytoskeleton.

Similarly to the eosinophils from OXF-treated mice, eosinophils from CorA-treated mice had only a small number of up- or downregulated genes in comparison to the vehicle control. Downregulated genes encode for the Triple functional domain protein, short-chain specific acyl-CoA dehydrogenase and Sentrin-specific protease 5 (Fig. 15F). Interestingly, eosinophils from CorA-treated mice upregulated a gene, which encodes for the C-X-C motif chemokine 10 suggesting an effect on cell migration due to treatment with CorA (Fig. 15F). Of note, the up- and downregulated genes showed very little overlap (Fig. 15G). However, the comparison of eosinophils from OXF and CorA-treated mice had the highest intersection of up- and downregulated genes (Fig. 15G).

Overall, analysis of the NGS data revealed that treatment with OXF or CorA only had a limited impact on eosinophils. However, the analysis did highlight an effect on some noteworthy genes, in particular the downregulation of eosinophilic cationic protein 2 and the granulocyte colony-stimulating factor receptor in OXF-treated mice and upregulation of CXCL-10 after CorA treatment. As such, the analysis is a useful starting point for further and more detailed examinations of how these and other anti-filarial compounds affect not only the parasite but also the host.

## 3.4 Combination therapy

### 3.4.1 Three-day combination therapy improves macrofilaricidal efficacy of OXF

Experiments in the first part of this project were conducted to characterize the role of the immune system during anti-filarial treatment. It was established that the state of the innate and adaptive immune system affects the treatment efficacy of both directly acting compounds, e.g., OXF and FBZ, as well as indirectly acting drugs, e.g., CorA. Thus, the following question arose: If the treatment efficacy is reduced in immunocompromised hosts, can the treatment outcome be improved via targeted stimulations of the immune system during anti-filarial treatments?

In order to investigate this question, certain type 2 cytokines, i.e., Interleukin-4 (IL-4), IL-5 and IL-33 were selected as potential immunostimulants based on the impaired treatment outcomes observed in mice lacking eosinophils (Δ*dblGata1*) or eosinophils and RELMα$^{+}$ macrophages (*IL-4r/IL-5*$^{-/-}$) to strengthen the type 2 immune response. IL-33 is an alarmin released by a variety of cells upon cell damage and leads to the recruitment and activation of ILC2s (among other cells) in the initial phase of a type 2 immune response [195]. OXF was chosen as the drug candidate for these experiments as OXF is currently in preparation for phase II clinical trials in humans as a pan-nematode drug and the most promising drug candidate. In addition, as the previously described treatment regimen with OXF for 5 days already led to a reduction of the adult worm burden of up to 94%, the aim of these experiments was to shorten the treatment duration needed for clearance (Fig. 16). As such, 6-8 week old female BALB/c WT mice were again naturally infected with *L. sigmodontis* and treated orally with 12.5 mg/kg OXF twice per day for only 3 days with or without additional application of 2 µg IL-4, IL-5 or IL-33 intranasally once per day starting at 35 dpi. Animals were also treated with only the vehicle, only OXF for 5 days as well as the cytokines by themselves as controls. Mice were sacrificed 70 dpi (Fig. 16A).

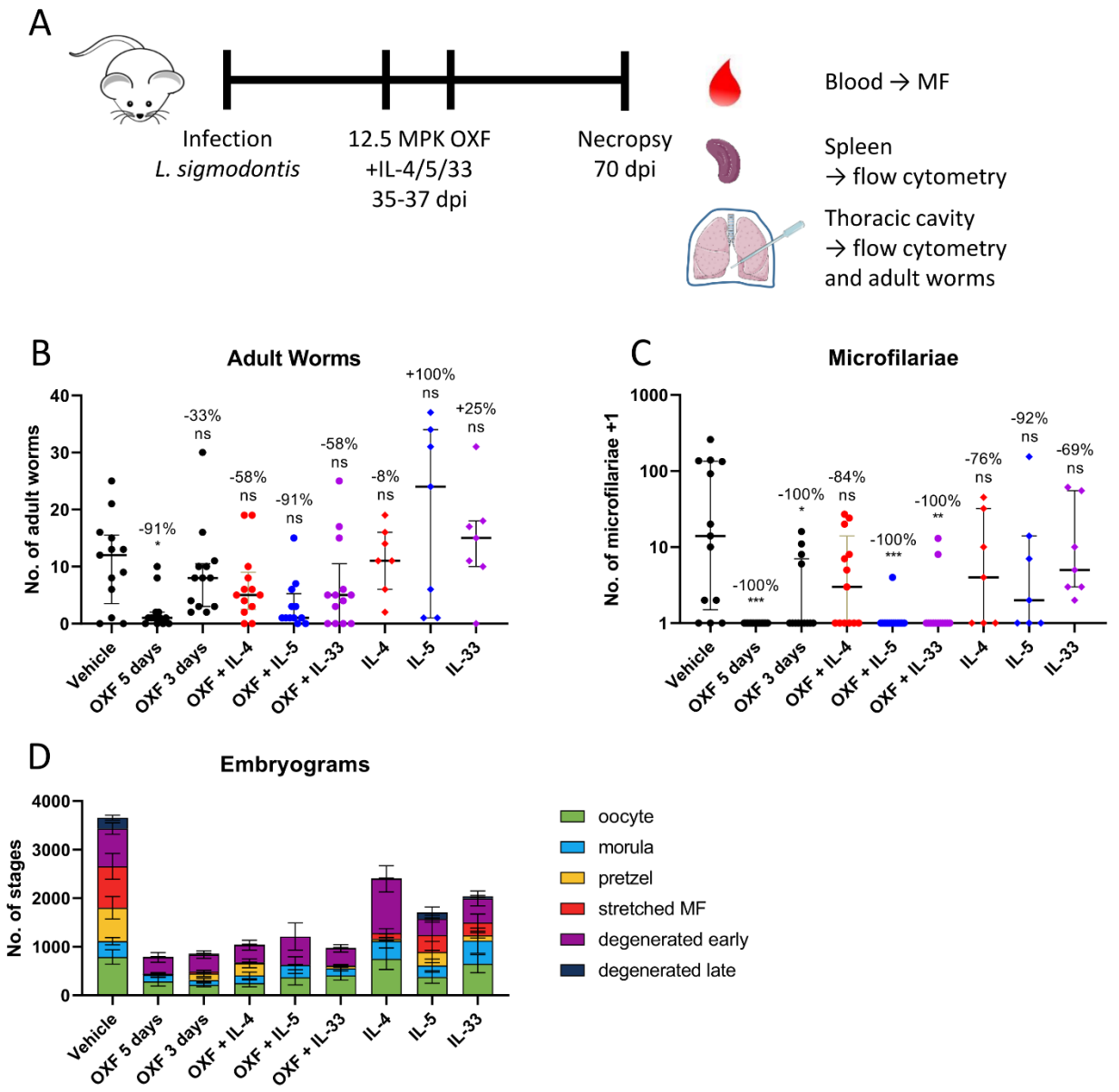


**Fig. 16: Combination of oxfendazole with interleukin-5 improves macrofilaricidal treatment efficacy in shortened treatment regimen.** 6-week old female BALB/c mice were naturally infected with *Litomosoides sigmodontis* and treated with 12.5 mg/kg oxfendazole twice per day for 5 days (positive control) or 3 days (shortened treatment) with or without intranasal addition of 2 µg IL-4, IL-5 or IL-33 once per day starting at 35 days post infection. Necropsies were performed 70 days after the infection. **(A)** Experimental setup. **(B)** Adult worm burden. **(C)** Microfilariae per 50 µl peripheral blood. **(D)** Average number of embryonal stages per female worm. **(B-C)** Data shown as median with interquartile range. Numbers show reduction of median in comparison to vehicle control. **(D)** Data shown as mean ± SEM. Data for IL-4, IL-5, IL-33 from 1 experiment (total n per group = 7 mice, 4-18 worms), data for other groups (n = 13 mice, 12-35 worms) pooled from 2 experiments. **(B-C)** Statistical analysis using Kruskal-Wallis with Dunn's post hoc test, * p<0.05, ** p<0.01, *** p<0.001.

Quantification of the adult worm burden showed that the treatment with OXF for 5 days by itself led to a significant median reduction of 91% ($p = 0.0158$) compared to the vehicle control treated mice (Fig. 16B). Treatment with only OXF for 3 days by contrast led to a median reduction of 33% ($p > 0.05$) (Fig. 16B). Interestingly all combinations of OXF with the chosen cytokines led to an improved efficacy and the combination with IL-4 and IL-33 reached reductions of 58% ($p > 0.05$) while the combination with IL-5 achieved the same efficacy as the 5-day OXF treatment (91%, $p > 0.05$) (Fig. 16B). Of note, the combinations did not lead to a statistically significant difference compared to the vehicle control with the available sample size as assessed via the Dunn's post hoc test. However, a direct comparison of the 3-day OXF+IL-5 treatment via the Mann-Whitney U test indicated a statistically significant difference compared to both the vehicle control ($p = 0.0253$) as well as the 3-day OXF treatment ($p = 0.004$) (Fig. 16B). Treatment with the cytokines alone did not lead to significant reductions of the adult worm burden (Fig. 16B). Next, the effect on MF was assessed (Fig. 16C). Treatment with OXF for 5 days led to a 100% median reduction of MF numbers in the peripheral blood ($p = 0.0002$) with all mice free of MF (Fig. 16C). While the 3-day OXF also reduced the median numbers by 100% ($p = 0.0445$), 4/13 mice remained MF positive (Fig. 16C). The combinations with both IL-5 ($p = 0.0006$) and IL-33 ($p = 0.0036$) similarly led to median reductions of 100% and further reduced the number of MF positive mice to 1/13 (IL-5) and 2/13 (IL-33) (Fig. 16C).

Quantification of the embryonal stages supported the MF data (Fig. 16D). OXF for 3 days alone led to a significant reduction of overall stages from 3654 (vehicle) to 855 (3-day OXF), however, each worm still harbored a large number of late stages, i.e., 137.1 ± 61.8 (mean ± SEM) pretzel and 36.7 ± 24.9 MF stages per female worm (Tab. 10). By comparison, worms isolated from mice that received both OXF and IL-5 for 3 days had only 5.8 ± 4.3 pretzel stages and 0.0 ± 0.0 stretched MF on average (Tab. 10). Similar to the effect on peripheral MF numbers, the other two combination therapies were unable to prevent or eliminate late stages after treatment. Worms from mice that received OXF and IL-4 had on average 250.9 ± 91.8 pretzel and 17.1 ± 8.2 stretched MF stages per worm, while the OXF + IL-33 group had 48.3 ± 29.4 pretzel and 4.1 ± 4.1 stretched MF stages (Tab. 10).

Overall, the combination of OXF with cytokines, in particular the combination with IL-5, improved the macrofilaricidal treatment efficacy of OXF and allowed a >90% of the adult worm burden after only 3 days of treatment. In addition, the combination therapy with IL-5 had a stronger impact on the fertility of the female adult worms and reduced the number of MF-positive mice.

**Tab. 10: Combination of oxfendazole with interleukin-5 leads to absence of late embryonal stages**. 6-week old female BALB/c mice were naturally infected with *Litomosoides sigmodontis* and treated with 12.5 mg/kg oxfendazole twice per day for 5 days (positive control) or 3 days (shortened treatment) with or without addition of intranasal application of 2 µg IL-4, IL-5 or IL-33 once per day starting at 35 days post infection. Necropsies were performed 70 days after the infection. Embryonal development was analyzed in up to 5 intact female worms per mouse. Data for IL-4, IL-5, IL-33 from 1 experiment (total n per group = 4-18 worms), data for other groups pooled from 2 experiments (n = 12-35 worms). Statistical analysis using Kruskal-Wallis with Dunn's post hoc test, * p<0.05, ** p<0.01, *** p<0.001.

| | | Oocyte | | Morula | | Pretzel | | Stretched MF | | Degenerated early | | Degenerated late | |
|---|---|---|---|---|---|---|---|---|---|---|---|---|---|
| | | Mean ± SEM, statistical significance | | | | | | | | | | | |
| Wildtype BALB/c | **Veh** | 789.7 ± 149.6 | | 323.4 ± 75.8 | | 688.2 ± 230.6 | | 854.5 ± 265.3 | | 779.1 ± 116.3 | | 221.4 ± 50.3 | |
| | **5d OXF** | 284.2 ± 94.3 | ns | 135.7 ± 49.3 | ns | 22.1 ± 15.4 | * | 0.7 ± 0.7 | ** | 337.1 ± 98.9 | ns | 10.7 ± 7.7 | * |
| | **3d OXF** | 213.5 ± 38.0 | * | 98.3 ± 37.6 | ns | 137.1 ± 61.8 | ns | 36.7 ± 24.9 | * | 350.9 ± 76.4 | * | 21.9 ± 7.6 | ns |
| | **OXF + IL-4** | 246.6 ± 72.9 | * | 161.4 ± 65.8 | ns | 250.9 ± 91.8 | ns | 17.1 ± 8.2 | ns | 353.8 ± 101.4 | * | 14.7 ± 7.9 | ns |
| | **OXF + IL-5** | 370.0 ± 156.8 | ns | 250.0 ± 171.2 | ns | 5.8 ± 4.3 | ** | 0.0 ± 0.0 | ** | 583.3 ± 278.1 | ns | 0.0 ± 0.0 | ** |
| | **OXF + IL-33** | 408.7 ± 98.3 | ns | 146.6 ± 51.2 | ns | 48.3 ± 29.4 | ** | 4.1 ± 4.1 | *** | 359.1 ± 76.0 | ns | 9.5 ± 5.7 | ** |
| | **IL-4** | 751.1 ± 220.3 | ns | 367.7 ± 143.7 | ns | 42.2 ± 26.8 | * | 122.2 ± 89.8 | ** | 1113.3 ± 268.7 | ns | 11.1 ± 7.6 | ** |
| | **IL-5** | 376.6 ± 129.5 | ns | 234.0 ± 136.5 | ns | 280.0 ± 220.8 | * | 346.6 ± 312.7 | * | 339.3 ± 73.5 | ns | 127.3 ± 112.6 | ns |
| | **IL-33** | 648.6 ± 185.1 | ns | 475.3 ± 260.0 | ns | 111.3 ± 55.8 | ns | 262.0 ± 177.5 | ns | 496.0 ± 153.5 | ns | 42.0 ± 23.3 | ns |

### 3.4.2 Immunological changes after three-day combination therapy

In order to better understand how the combination therapy improved the treatment outcome, flow cytometry was performed to quantify changes in the spleen (Fig. 17+18) and thoracic cavity (Fig. 19+20).

Overall, there were a number of differences in the immune cell frequencies of splenocytes between the different treatment regimens, in particular in comparison to the vehicle controls (Fig. 17). In the case of lymphocytes, $CD4^+$ T cell frequencies were elevated in the 5-day OXF group compared to the vehicle control, but for the remaining groups frequencies of $CD4^+$ and $CD8^+$ T cells were generally similar (Fig. 17A+B). Frequencies of all B cells as well as $CD5^-$ B cells were lower in mice treated with the combination of OXF + IL-5 while $CD5^+$ B cells were only reduced in mice that received OXF + IL-4 when compared to the vehicle control animals (Fig. 17C-E). In terms of myeloid cells, frequencies of neutrophils as well as $Ly6C^{hi}$ and $Ly6C^{lo}$ monocytes were similar across all treatment groups (Fig. 17F, H-I). Interestingly, eosinophil frequencies were significantly lower in all treated mice compared to the vehicle control, while numbers of cDC1s were significantly increased in all treated mice (Fig. 17G, 17J). Numbers of cDC2s were only increased in mice that were treated with IL-5 or IL-33 alone while pDC frequencies remained unchanged by the treatment (Fig. 17K-L).

The changes in total cell counts were generally similar with some minor differences when compared to the trends observed for cell frequencies (Fig. 18). Total cell counts of $CD4^+$ T cells were not reduced in 5-day OXF-treated mice and similar across all groups while $CD8^+$ T cells numbers were only elevated in mice that received IL-33 (Fig. 18A+B). In contrast to the cell frequencies, total cell counts of B cells as well as the $CD5^+$/$CD5^-$ subtypes were reduced only in the 5-day OXF treatment group in comparison to the vehicle controls (Fig. 18C-E). In terms of myeloid cells, similar to the changes in frequencies, numbers of eosinophils were decreased in treated mice, while cDC1 and cDC2 cells were elevated compared to the vehicle controls (Fig. 18G, J-K). Further, numbers of neutrophils, monocytes and pDCs were similar to the vehicle controls in mice that were treated with OXF and cytokines while neutrophils and $Ly6C^{hi}$ monocytes were reduced in animals that were treated with OXF for 5 days (Fig. 18F, H-I, L).

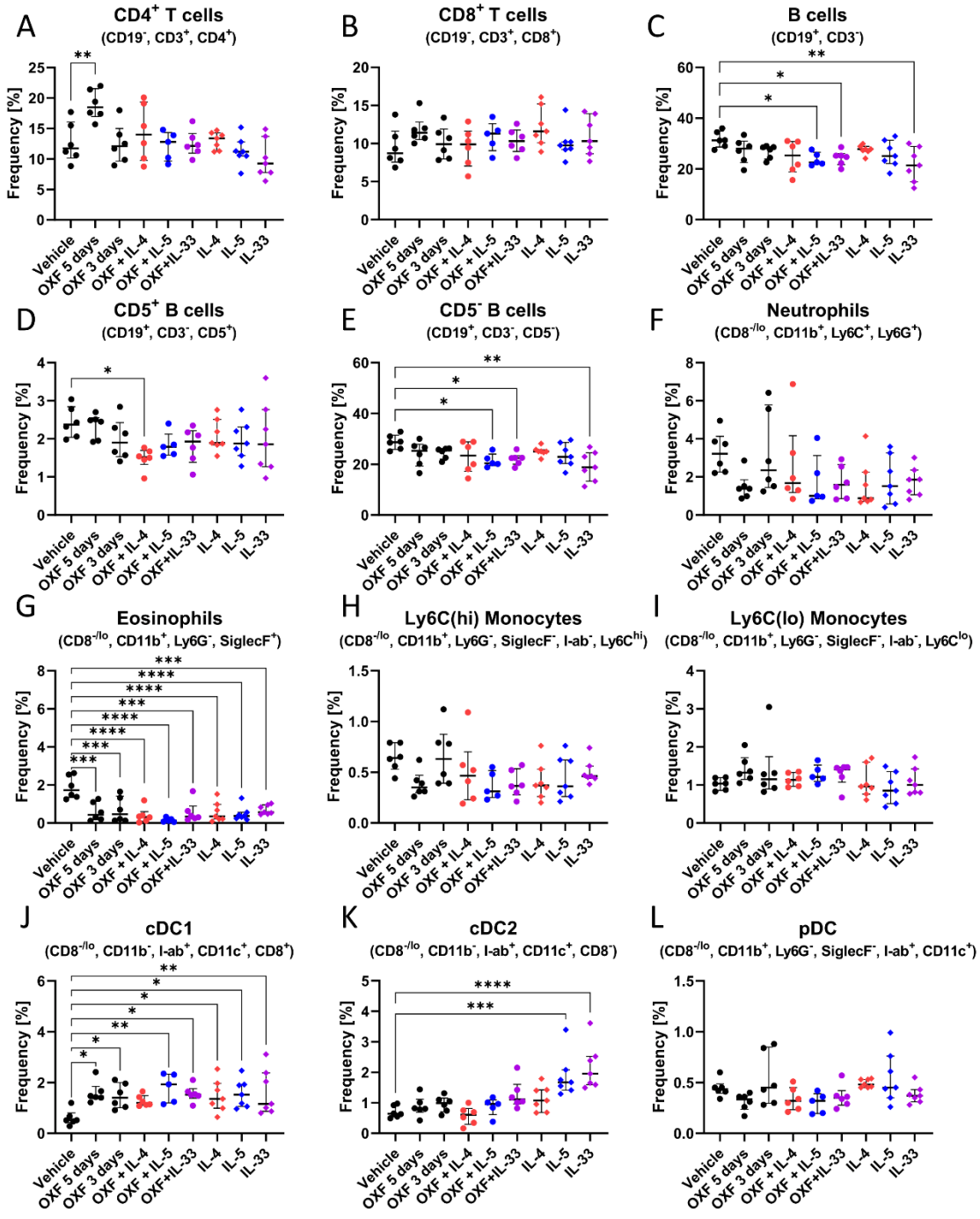


**Fig. 17: Changes in immune cell frequencies in the spleen after combination therapy.** 6-week old female BALB/c mice were naturally infected with *Litomosoides sigmodontis* and treated with 12.5 mg/kg oxfendazole twice per day for 3-5 days with or without addition of 2 µg IL-4, IL-5 or IL-33 once per day starting 35 dpi. Necropsies were performed 70 dpi and splenocytes were analyzed via flow cytometry. Frequencies of **(A)** $CD4^+$ T cells, **(B)** $CD8^+$ T cells, **(C)** B cells, **(D)** $CD5^+$ B cells, **(E)** $CD5^-$ B cells, **(F)** neutrophils, **(G)** eosinophils, **(H)** Ly6C(hi) monocytes, **(I)** Ly6C(lo) monocytes, **(J)** cDC1, **(K)** cDC2, **(L)** pDC. **(A-L)** Data shown as median with interquartile range. Data from 1 representative experiment out of 2 (n = 6-7 per group). Statistical analysis using Kruskal-Wallis with Dunn's post hoc test, * p<0.05, ** p<0.01, *** p<0.001, **** p<0.0001.

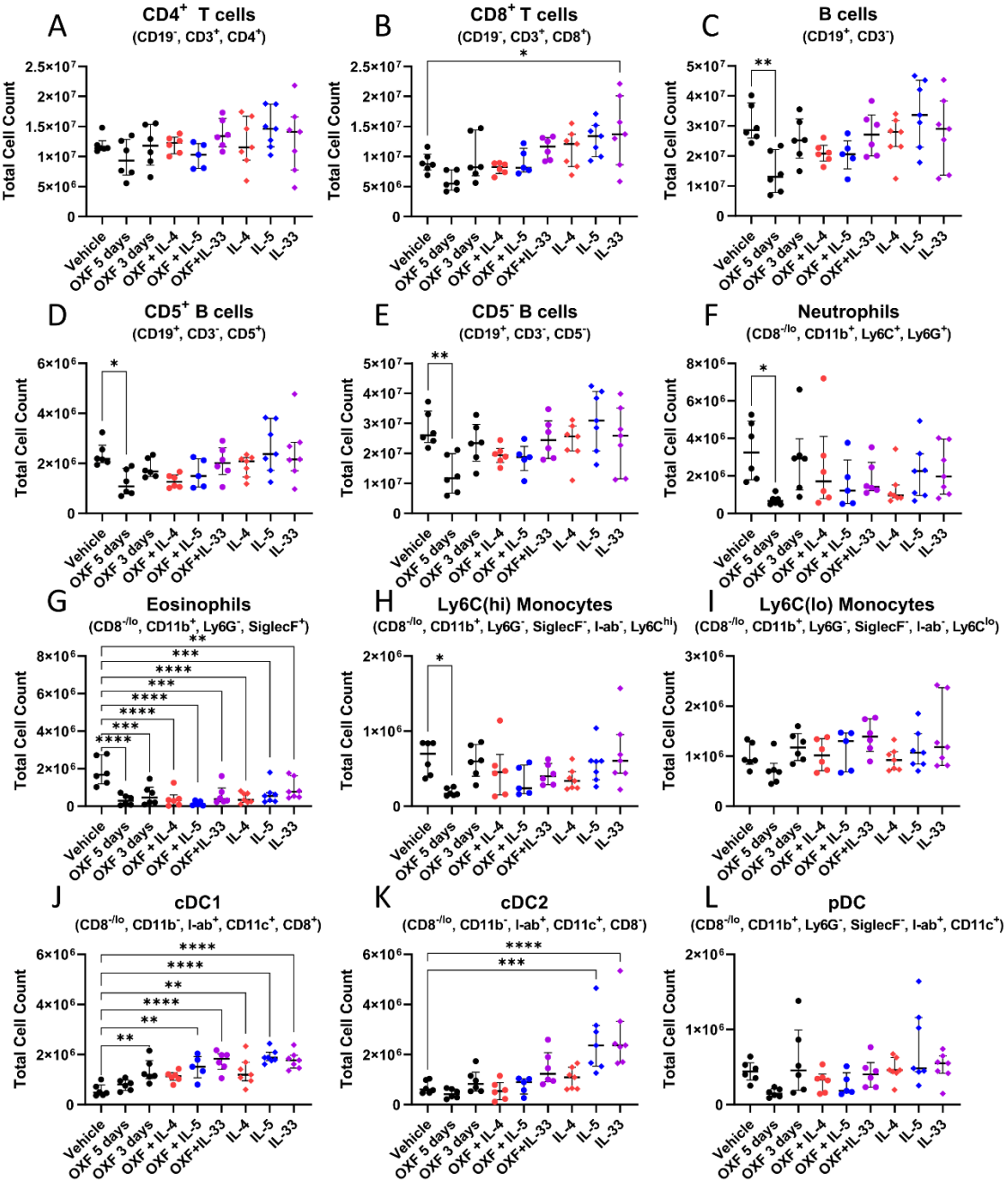


**Fig. 18: Changes in immune cell counts in the spleen after combination therapy.** 6-week old female BALB/c mice were naturally infected with *Litomosoides sigmodontis* and treated with 12.5 mg/kg oxfendazole twice per day for 3-5 days with or without addition of 2 µg IL-4, IL-5 or IL-33 once per day starting 35 dpi. Necropsies were performed 70 dpi and splenocytes were analyzed via flow cytometry. Total cell counts of **(A)** $CD4^+$ T cells, **(B)** $CD8^+$ T cells, **(C)** B cells, **(D)** $CD5^+$ B cells, **(E)** $CD5^-$ B cells, **(F)** neutrophils, **(G)** eosinophils, **(H)** Ly6C(hi) monocytes, **(I)** Ly6C(lo) monocytes, **(J)** cDC1, **(K)** cDC2, **(L)** pDC. **(A-L)** Data shown as median with interquartile range. Data from 1 representative experiment out of 2 (n = 6-7 per group). Statistical analysis using Kruskal-Wallis with Dunn's post hoc test, * p<0.05, ** p<0.01, *** p<0.001, **** p<0.0001.

Next, immunological changes in the thoracic cavity were evaluated (Fig. 19). Frequencies of T cells were reduced in mice that received OXF + IL-33 as well as IL-4 compared to vehicle controls (Fig. 19A+B). Interestingly, B cells overall as well as the $CD5^+/CD5^-$ subtypes were elevated in the 5-day OXF treatment group but unaffected in the other groups (Fig. 19C-E). Myeloid cells were mostly unchanged after treatment with only slight increases in neutrophil, monocyte and $CD11b^+$ DC frequencies in mice that were treated with OXF alone (Fig. 19F-L). In terms of total cell counts, the numbers of T cells were similar across all treatment groups, while B cells were only increased in mice that were treated with OXF for 3 days (Fig. 20A-E). For the myeloid cell populations, eosinophil and macrophage numbers displayed no significant differences (Fig. 20F-H). Numbers of neutrophils, monocytes and $CD11b^+$ DCs by contrast were increased in mice that were treated with OXF alone for 3 days, while the combinations with cytokines had little to no effect (Fig. 20I-L).

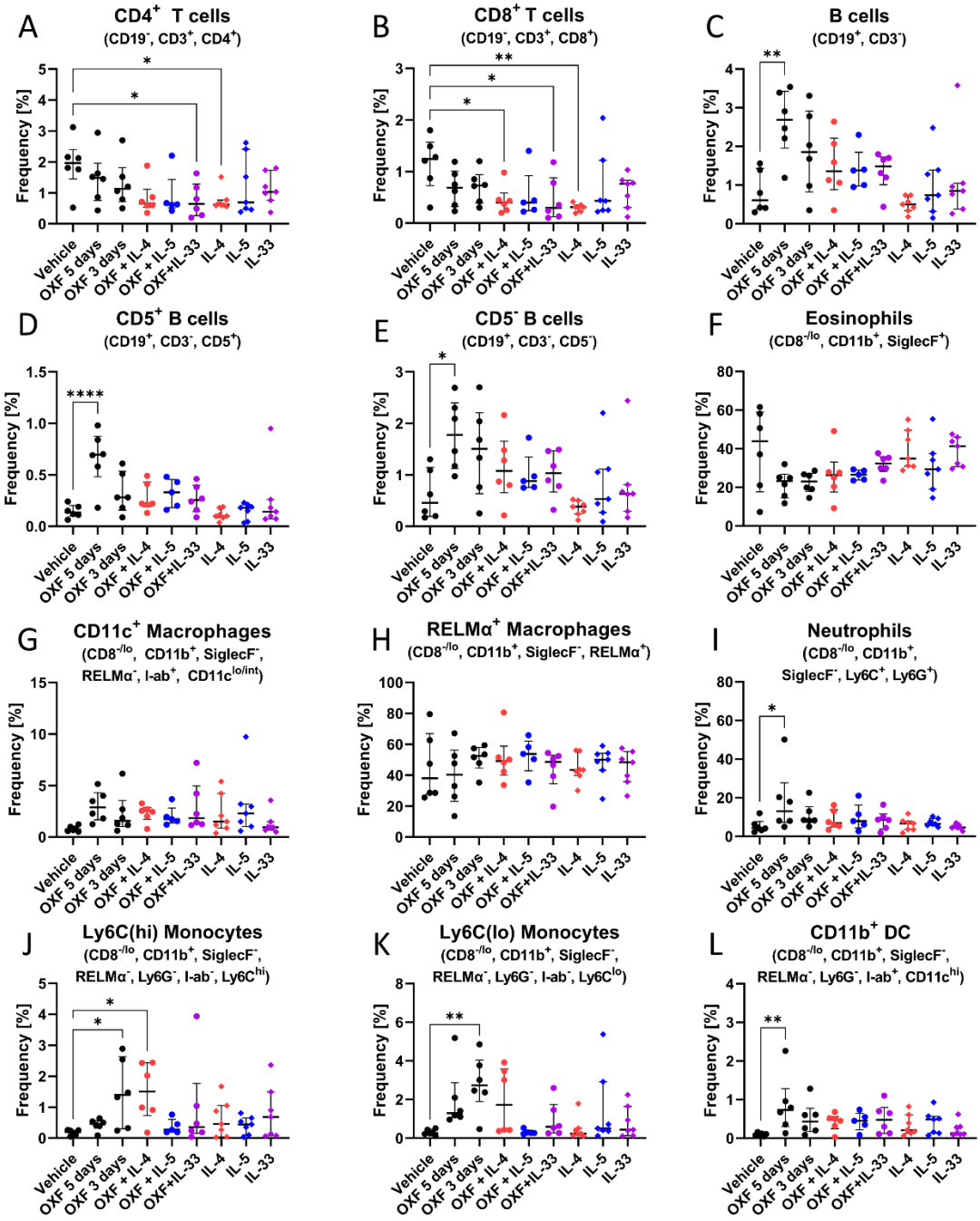


**Fig. 19: Changes in immune cell frequencies in the thoracic cavity after combination therapy.** 6-week old female BALB/c mice were naturally infected with *Litomosoides sigmodontis* and treated with 12.5 mg/kg oxfendazole twice per day for 3-5 days with or without addition of 2 µg IL-4, IL-5 or IL-33 once per day starting 35 dpi. Necropsies were performed 70 dpi and cells were analyzed via flow cytometry. Frequencies of **(A)** $CD4^+$ T cells, **(B)** $CD8^+$ T cells, **(C)** B cells, **(D)** $CD5^+$ B cells, **(E)** $CD5^-$ B cells, **(F)** eosinophils, **(G)** $CD11c^+$ macrophages, **(G)** $RELM\alpha^+$ macrophages, **(I)** neutrophils, **(J)** Ly6C(hi) monocytes, **(K)** Ly6C(lo) monocytes, **(L)** $CD11c^+$ macrophages. **(A-L)** Data shown as median with interquartile range. Data from 1 representative experiment out of 2 (n = 6-7 per group). Statistical analysis using Kruskal-Wallis with Dunn's post hoc test, * $p<0.05$, ** $p<0.01$, *** $p<0.001$, **** $p<0.0001$.

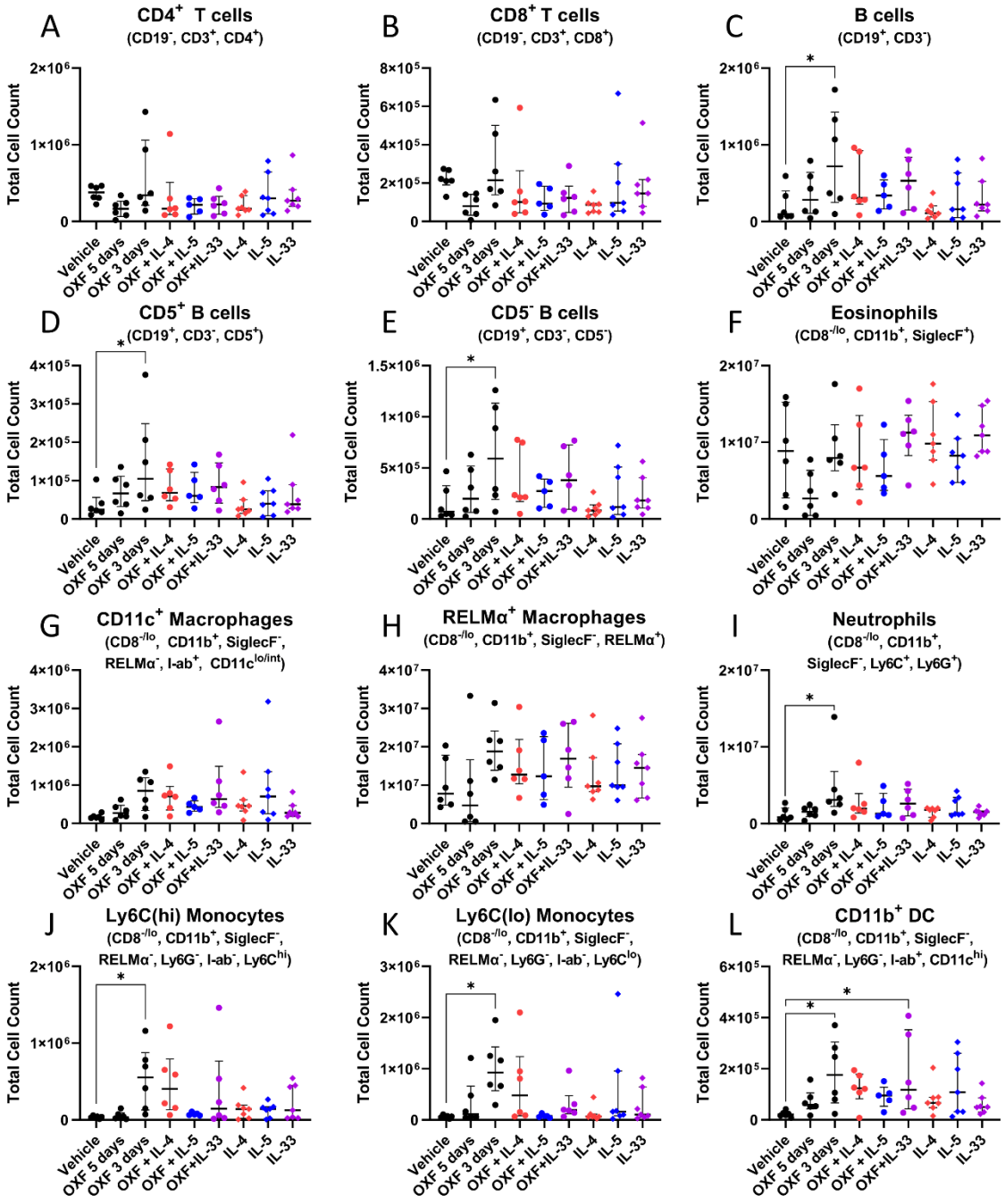


**Fig. 20: Changes in immune cell counts in the thoracic cavity after combination therapy.** 6-week old female BALB/c mice were naturally infected with *Litomosoides sigmodontis* and treated with 12.5 mg/kg oxfendazole twice per day for 3-5 days with or without addition of 2 µg IL-4, IL-5 or IL-33 once per day starting 35 dpi. Necropsies were performed 70 dpi and cells were analyzed via flow cytometry. Total cell counts of **(A)** $CD4^+$ T cells, **(B)** $CD8^+$ T cells, **(C)** B cells, **(D)** $CD5^+$ B cells, **(E)** $CD5^-$ B cells, **(F)** eosinophils, **(G)** $CD11c^+$ macrophages, **(G)** $RELM\alpha^+$ macrophages, **(I)** neutrophils, **(J)** Ly6C(hi) monocytes, **(K)** Ly6C(lo) monocytes, **(L)** $CD11c^+$ macrophages. **(A-L)** Data shown as median with interquartile range. Data from 1 representative experiment out of 2 (n = 6-7 per group). Statistical analysis using Kruskal-Wallis with Dunn's post hoc test, * $p<0.05$, ** $p<0.01$, *** $p<0.001$, **** $p<0.0001$.

### 3.4.3 Histological changes after three-day combination therapy

Next, histological changes in the lung were analyzed to evaluate potential pathological changes associated with the combination therapy (Fig. 21+22). In brief, lungs were filled and fixed with formaldehyde, dehydrated and then embedded in paraffin. Afterward, 7 µm thick sections were stained with hematoxylin and eosin (Fig. 21), Alcian blue (Fig. 22A) or Luxol blue (Fig. 22B).

Interestingly, treatment with IL-33 alone and in combination with OXF led to a significant infiltration of cells into the pulmonary vascular stroma (Fig. 21A+B). Further, treatment with OXF led to a slight decrease in the thickness of bronchial arteries, while treatment with IL-33 alone led to a significant increase in the average arterial thickness (Fig. 21C+D).

Next, lung sections were stained with Alcian blue to quantify the production of mucus in the bronchial epithelium (Fig. 22A). In lungs from vehicle controls, 14% of the bronchiole surfaces were covered with mucus (Fig. 22B). By contrast, treatment with OXF, cytokines or a combination thereof led to a significant reduction of mucus coverage in all groups and this reduction of mucus coverage was lowest in mice that were treated with IL-4 or IL-33 alone or IL-33 in combination with OXF (Fig. 22B). In addition, Luxol blue stainings of the lung sections highlighted an infiltration of eosinophils into lung in mice treated with IL-5 alone or the combination of OXF with IL-5 (Fig. 22C+D).

Overall, analysis of the lung histology revealed that treatment with IL-33 both alone and in combination with OXF caused an inflammatory response in treated mice. Importantly, the combination of OXF with IL-5 led to an infiltration of eosinophils into the lung but did not cause any noticeable pathology.

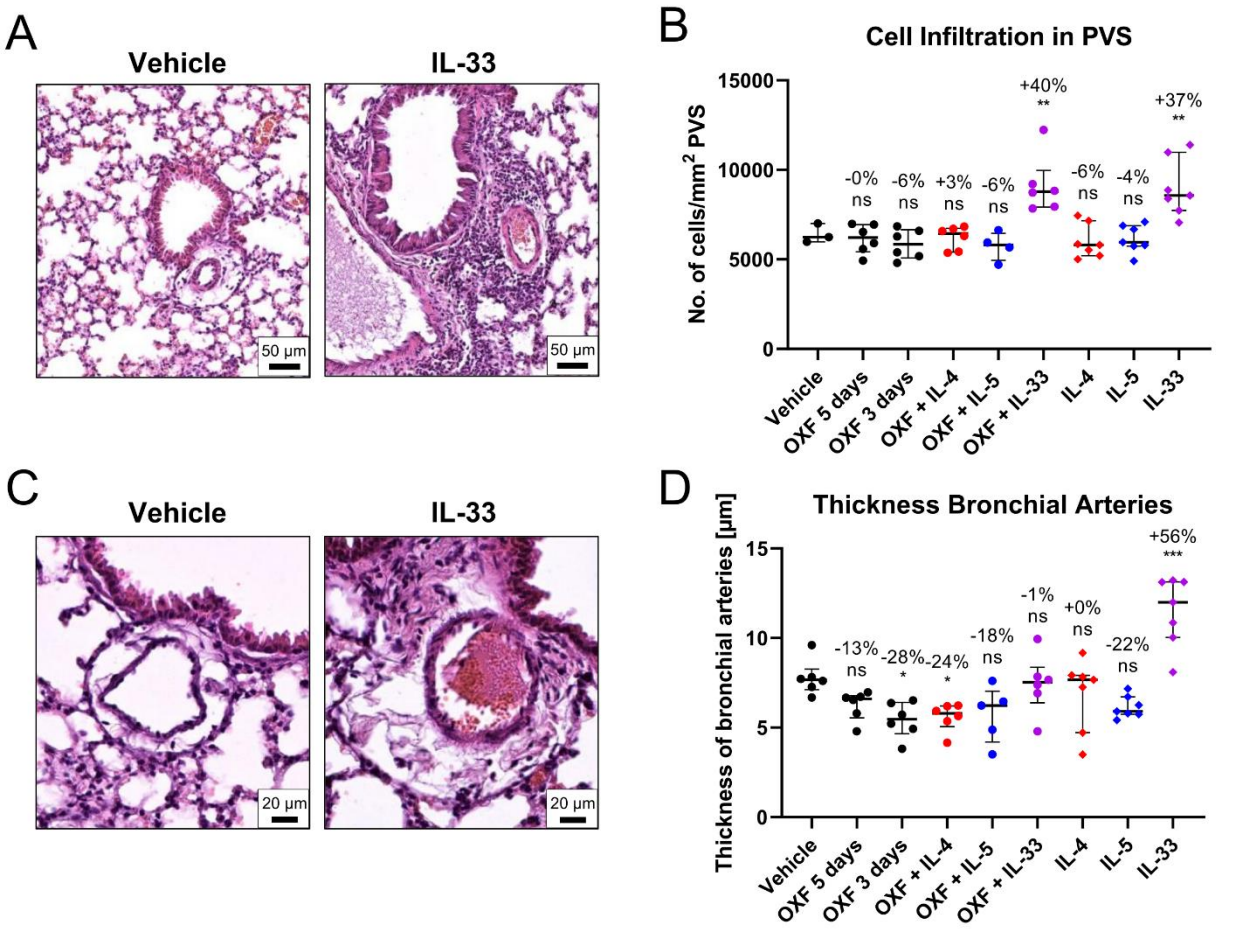


**Fig. 21: Pathological changes in the lung after combination therapy**. 6-week-old female BALB/c mice were naturally infected with *Litomosoides sigmodontis* and treated with 12.5 mg/kg oxfendazole (OXF) twice per day for 5 days (positive control) or 3 days (shortened treatment) with or without addition of intranasal application of 2 µg IL-4, IL-5 or IL-33 once per day starting 35 days post infection. Necropsies were performed 70 days after the infection and lungs were processed for histological analysis. **(A)** H&E staining of perivascular spaces (PVS). **(B)** Quantification of Hematoxylin positive nuclei per $mm^2$ in the PVS. **(C)** H&E staining of bronchial arteries. Arrows indicate the artery boundaries. **(D)** Quantification of bronchial vein thickness. **(B, D)** Results are expressed as median with interquartile range of n = 3-7 mice per group (1 experiment). Numbers show reduction of median in comparison to vehicle control. Statistical analysis using one-way ANOVA followed by Dunnett's multiple comparison tests, * $p<0.05$. ** $p<0.01$, *** $p<0.001$

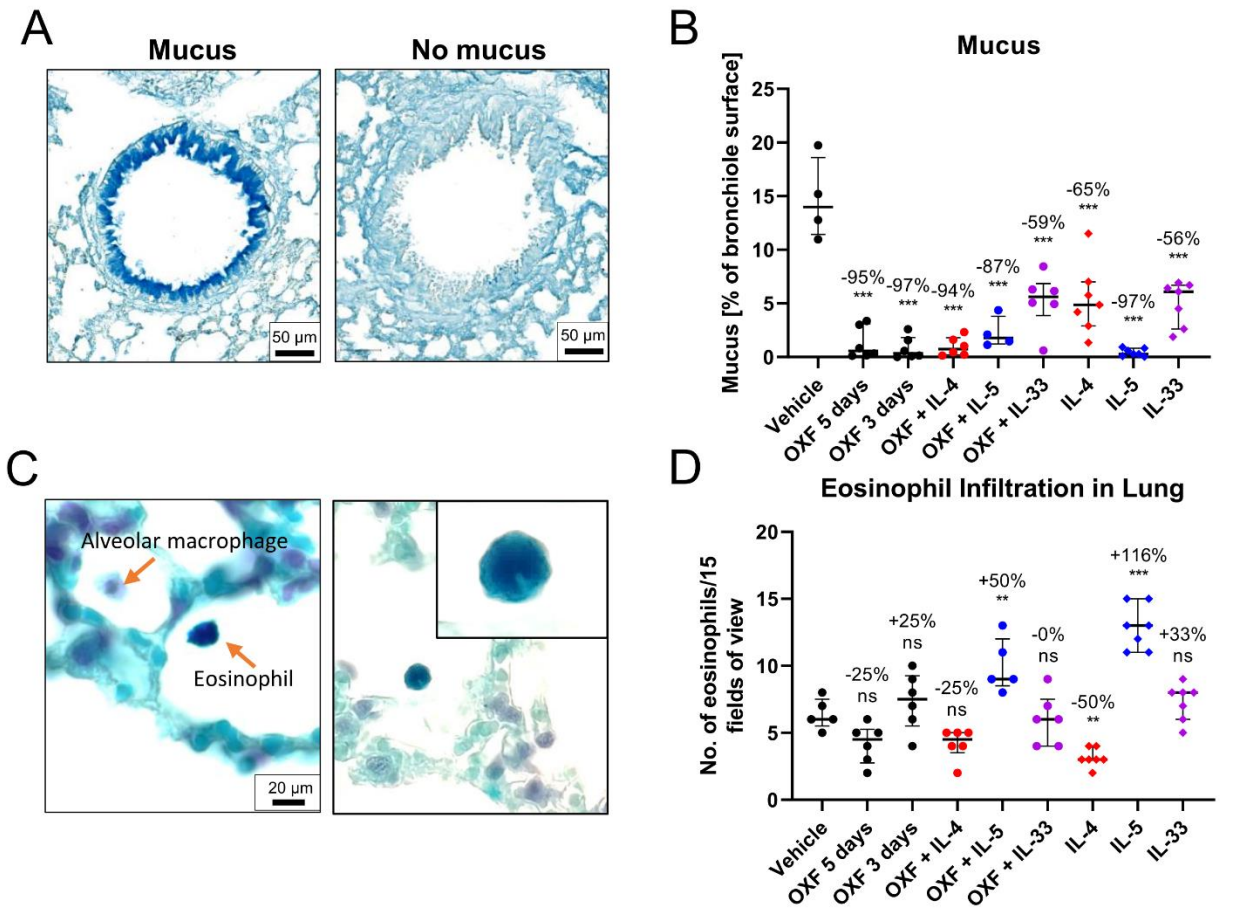


**Fig. 22: Histological changes in the lung after combination therapy**. 6-week-old female BALB /c mice were naturally infected with *Litomosoides sigmodontis* and treated with 12.5 mg/kg oxfendazole (OXF) twice per day for 5 days (positive control) or 3 days (shortened treatment) with or without addition of intranasal application of 2 µg IL-4, IL-5 or IL-33 once per day starting 35 days post infection. Necropsies were performed 70 days after the infection and lungs were processed for histological analysis. **(A)** Alcian blue staining of mucus in bronchial epithelium. **(B)** Quantification of mucus on bronchiole surface. **(C)** Luxol fast blue staining of eosinophils. Left image displays a Luxol blue positive eosinophil and an alveolar macrophage. The corner zoom on the right image highlights the eosinophil lobed nucleus. **(D)** Quantification of eosinophil infiltration in the lung. **(B, D)** Results are expressed as median with interquartile range of n = 3-7 mice per group (1 experiment). Numbers show reduction of median in comparison to vehicle control. Statistical analysis using one-way ANOVA followed by Dunnett's multiple comparison tests, * p<0.05. ** p<0.01, *** p<0.001

### 3.4.4 Combination therapy every second day has no effect on adult worm burden

Based on the successful anti-filarial activity of the 3-day combination therapy, an alternative treatment regimen was explored to identify any potential further improvements. *L. sigmodontis* infected mice were treated every second day, i.e., 35, 37 and 39 dpi, rather than every day for 3 continuous days (Fig. 23A). Similar as before, mice were sacrificed 70 dpi. However, neither the treatment with OXF alone nor the combination with cytokines led to a noticeable reduction of the adult worm burden (Fig. 23B). MF numbers were not quantified as the primary readout was not successful.

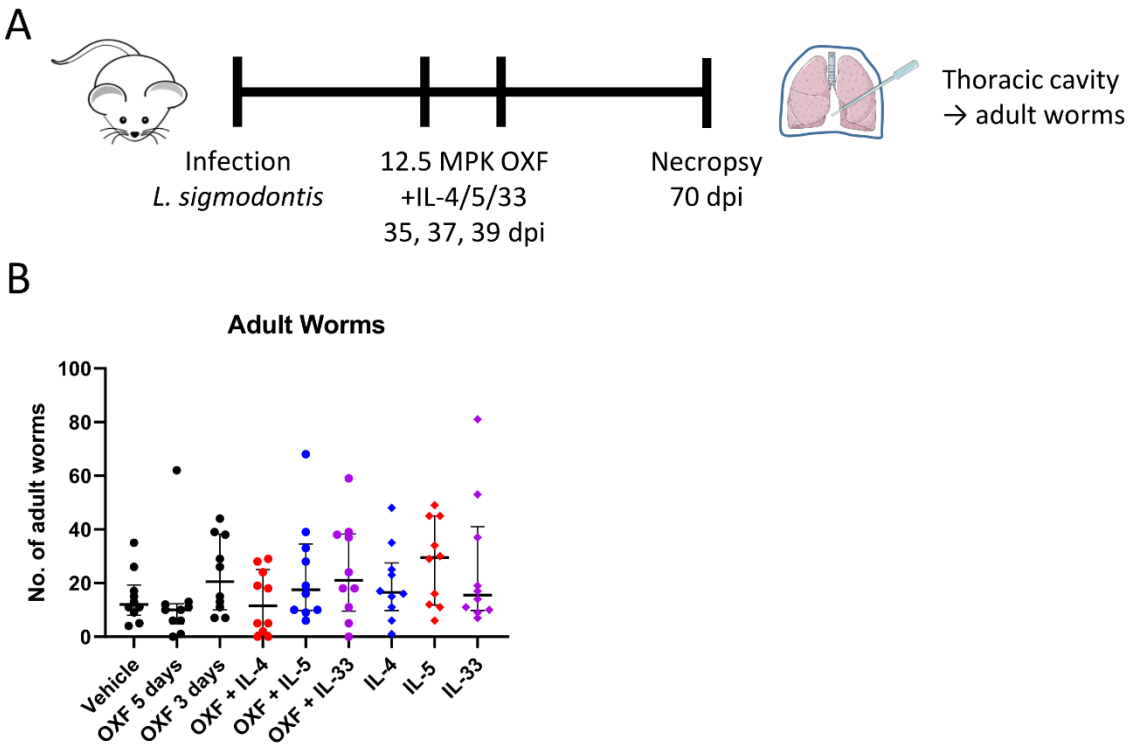


**Fig. 23: Combination therapy every second day has no effect on adult worm burden.** 6-week old female BALB/c mice were naturally infected with *Litomosoides sigmodontis* and treated with 12.5 mg/kg oxfendazole twice per day for 5 days (positive control) or three times every second day (shortened treatment) with or without intranasal addition of 2 µg IL-4, IL-5 or IL-33 once per day starting 35 days post infection. Necropsies were performed 70 days after the infection. **(A)** Experimental setup. **(B)** Adult worm burden**. (B)** Data shown as median with interquartile range. Data pooled from 2 experiments (total n per group = 10 mice). Statistical analysis using one-way ANOVA followed by Dunnett's multiple comparison tests.

### 3.4.5 Two-day combination therapy has no macrofilaricidal effect on *Litomosoides sigmodontis*

Since the continuous 3-day combination of OXF with IL-5 achieved a similar reduction as the full 5-day treatment, a follow-up experiment was designed to test a 2-day regimen. BALB/c mice were again naturally infected with *L. sigmodontis* and treated with either 12.5 mg/kg OXF per treatment as before or an increased dose of 25 mg/kg OXF per treatment with or without the addition of IL-5 (Fig. 24A). However, neither the 12.5 nor 25 mg/kg OXF dose alone or in combination with IL-5 led to a statistically significant reduction of the adult worm burden 70 dpi (Fig. 24B). Nevertheless, all treatments led to a reduced number of MF positive animals (Fig. 24C).

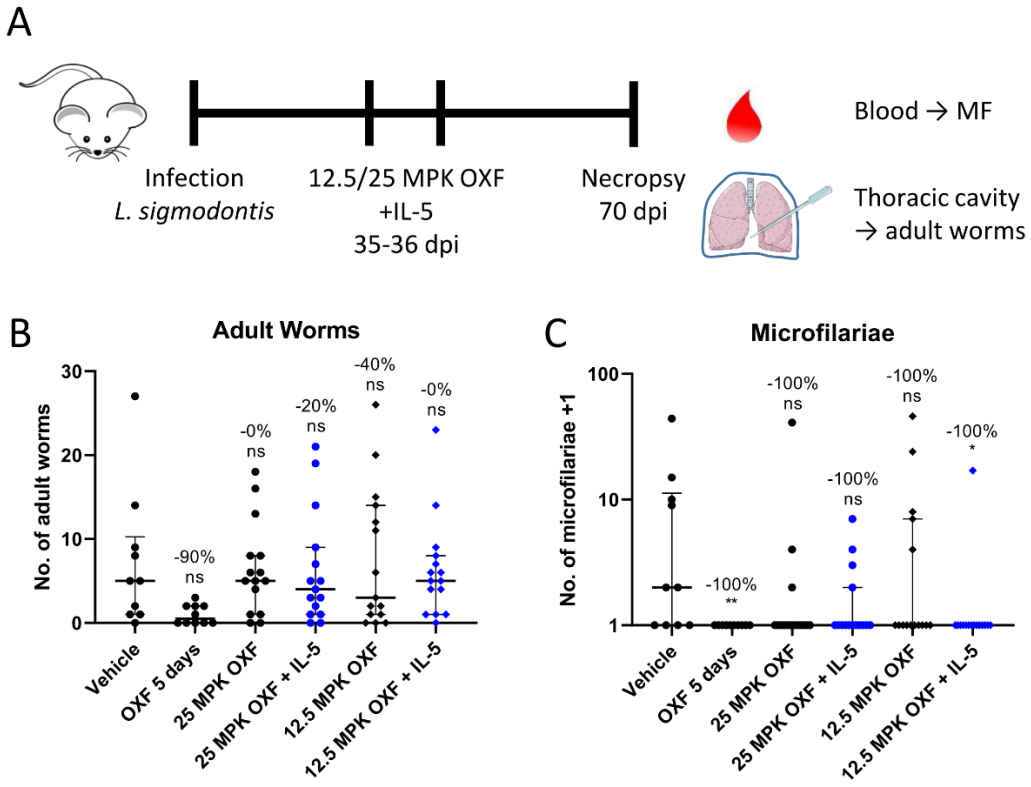


**Fig. 24: Two-day combination therapy has no macrofilaricidal effect on *Litomosoides sigmodontis***. 6-week old female BALB/c mice were naturally infected with *Litomosoides sigmodontis* and treated with 12.5 or 25 mg/kg oxfendazole twice per day for 5 days (positive control) or 2 days (shortened treatment) with or without intranasal application of 2 µg IL-5 once per day for a total of 2 days starting at 35 days post infection. Necropsies were performed 70 days after the infection. **(A)** Experimental setup. **(B)** Adult worm burden. **(C)** Microfilariae per 50 µl peripheral blood. **(B-C)** Data shown as median with interquartile range. Numbers show reduction of median in comparison to vehicle control. Data pooled from 2 experiments (total n per group = 10-15). Statistical analysis using Kruskal-Wallis with Dunn's post hoc test, * $p<0.05$, ** $p<0.01$.

### 3.5 Oxfendazole isomers display comparable macrofilaricidal activity and pharmacokinetic profile

Isomers can have vastly different effects and pharmacokinetic profiles [196]. Whether this is the case for OXF in the context of anti-filarial treatments has not been investigated before. As such, the efficacy and pharmacodynamics of two oxfendazole isomers were characterized in mice and dogs in a side project (Fig. 25).

To investigate the efficacy, female BALB/c WT mice (n=8) were naturally infected with *L. sigmodontis* and treated with a racemic mixture of OXF (Dolthene®) or one of two isomers (in the following OXF (+) and OXF (-)) for either 5 or 10 days starting at 35 dpi. Mice were sacrificed 70 dpi to quantify parasitological changes (Fig. 25A+B). The racemic mixture led to a reduction of the adult worm burden by 91.1% or 97.1% after 5 and 10 days of treatment respectively (Fig. 25A). Further, both regimens led to a complete absence of MF in the peripheral blood (Fig. 25B). In case of the isomers, there were some minor differences in the mice treated for 5 days as OXF (+) led to a reduction of 85.1% whereas OXF (-) led to a reduction of only 71.8% (Fig. 25A). The 10-day regimens, however, achieved comparable reductions as the racemic mixture with 97.5% for OXF (+) and 93.9 for OXF (-) (Fig. 25A). In addition, treatment with either isomer prevented the presence of MF in the peripheral blood 70 dpi (Fig. 25B).

Next, the pharmacokinetic profile of OXF in mice naturally infected with *L. sigmodontis* was evaluated. Female BALB/c WT mice (n=8) were treated with OXF for 5 days twice per day with either the racemic mixture (Dolthene®) or one of the two isomers starting 35 dpi. Blood was taken 2 h after the first treatment (35 dpi) and the second to last treatment (39 dpi) and the concentrations of the OXF isomers as well as the reduced (=fenbendazole) and oxidized form (=fenbendazole sulfone) of OXF were measured via HPLC-MS/MS (Fig. 25C). Of note, the plasma levels were higher after treatment with either isomer compared to the mice that received the racemic mixture (Fig. 25C). Further, plasma levels overall were similar at both time points indicating that there was no accumulation over time and that OXF was metabolized relatively quickly (Fig. 25C). In addition, the data showed that the OXF isomers were a) not metabolized into the alternative isomer form and b) either not metabolized at all or oxidized into fenbendazole

sulfone (Fig. 25C). Levels of fenbendazole were below or near the quantification limit (Fig. 25C). Interestingly, levels of fenbendazole sulfone were higher in mice treated with OXF (-) than in mice treated with OXF (+) at both time points (Fig. 25C). In mice treated with OXF (-), fenbendazole sulfone made up 52.8% - 59.8% of oxfendazole metabolites compared to 30.6% - 34.3% in mice treated with OXF (+) on the first and last day of treatment respectively (Fig. 25C). Accordingly, the levels of fenbendazole sulfone were significantly higher in mice treated with OXF (-) compared to mice treated with OXF (+) at the first time point (OXF (-): 10544 ng/ml vs. OXF (+): 5255 ng/ml, $p = 0.0023$) and second time point (OXF (-): 13100 ng/ml vs. OXF (+): 7148 ng/ml, $p = 0.0214$) (Fig. 25C).

The results from the pharmacokinetic study in dogs done by WuXi AppTec Co., Ltd supported the observations from the murine study (Fig. 25D+E). Male beagles (n=3) were treated with 10 mg/kg of either OXF (-) (Fig. 25D) or OXF (+) (Fig. 25E) and blood was taken at 8 time points in the following 24 hours. Similar to the situation in mice, OXF was metabolized quickly and was mostly eliminated from the system after 24 hours (Fig. 25D+E). In addition, both OXF (-) and OXF (+) were neither metabolized into the alternative isomer form nor reduced into fenbendazole (Fig. 25D+E). Lastly, plasma levels of fenbendazole sulfone were higher in dogs treated with OXF (-) (AUC: 3657 ± 1571 ng*h/ml, mean ± SD) than OXF (+) (799 ± 314 ng*h/ml) group (Fig. 25D+E).

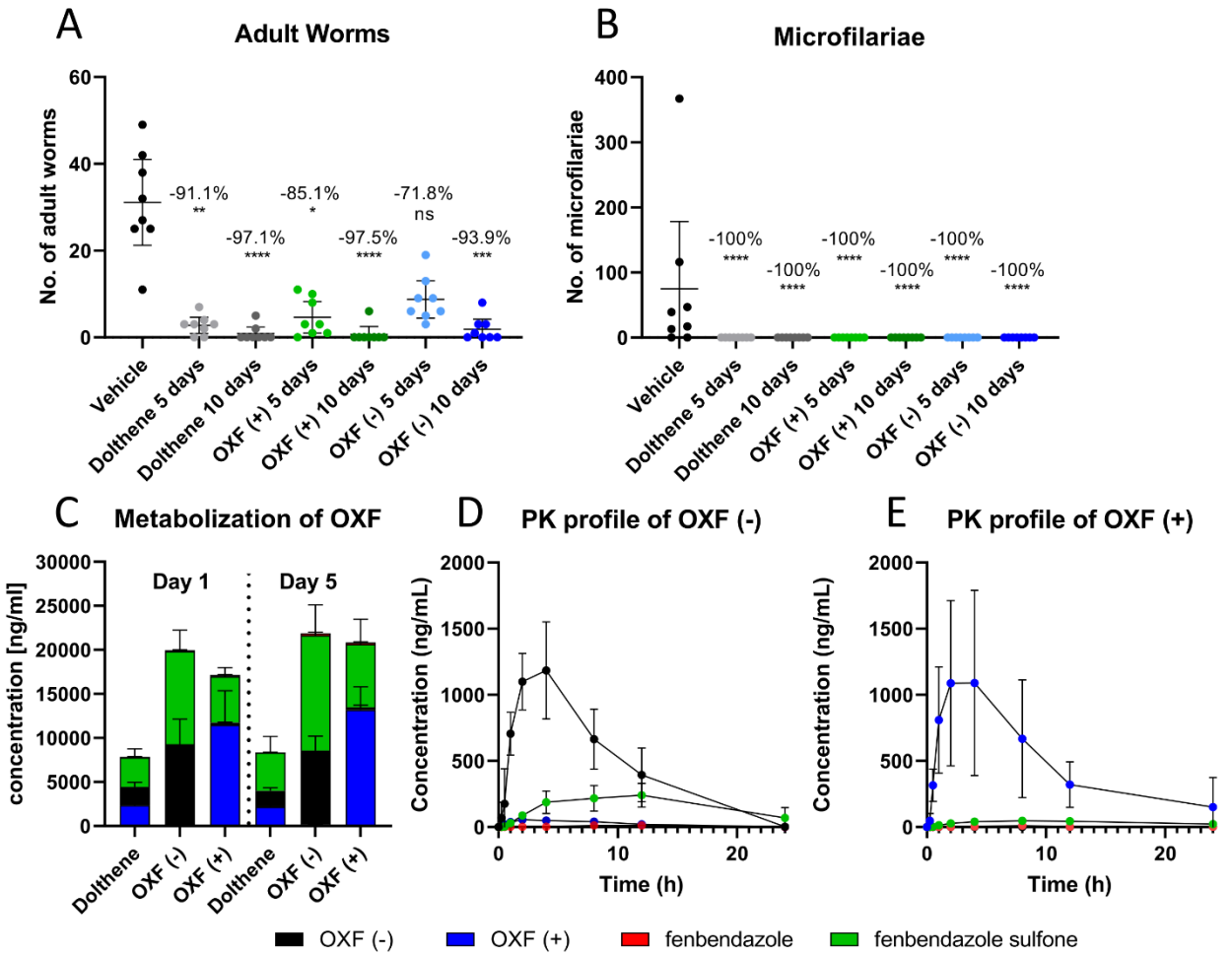


**Fig. 25: Oxfendazole isomers display comparable macrofilaricidal activity and pharmacokinetic profile. (A-B)** 6-8 week old female BALB/c mice (n=8) were naturally infected with *L. sigmodontis* and treated orally with 25 mg/kg of a racemic mixture of oxfendazole (Dolthene) or one of its isomers twice per day for 5 or 10 days starting 35 dpi. Necropsies were performed 70 dpi. **(A)** Adult worm burden. **(B)** Microfilariae per 50 µl peripheral blood. **(C)** 6-8 week old female BALB/c mice (n=8) were treated orally with 12.5 mg/kg of a racemic mixture of oxfendazole (Dolthene) or one of two isomers twice per day for 5 days starting 35 dpi. Shown is the plasma level of both oxfendazole isomers as well as its metabolites fenbendazole and fenbendazole sulfone in peripheral blood 2 h after the first and second to last treatment. **(D-E)** Male beagles (n=3) were treated orally with 10 mg/kg of each isomer. Concentration of oxfendazole (+) [blue], oxfendazole (-) [black], fenbendazole sulfone [green] and fenbendazole [red] were assessed via HPLC-MS/MS at indicated time points after treatment. **(D)** Plasma level of oxfendazole metabolites after treatment with 10 mg/kg oxfendazole (+). **(E)** Plasma level of oxfendazole metabolites after treatment with 10 mg/kg oxfendazole (-). **(A-B)** Data shown as arithmetic mean with 95% CI from a single experiment. Numbers show reduction of mean in comparison to vehicle control. **(C)** Data shown as mean with standard deviation from a single experiment. **(D-E)** Data shown as mean with standard deviation from a single experiment. Error bars that are not visible are smaller than the size of the symbol. **(A-B)** Statistical analysis using Kruskal-Wallis with Dunn's post hoc test, * $p<0.05$, ** $p<0.01$.

### 3.6 Further side projects and scientific contributions

The results described in the previous sections are either unpublished or published in Risch et al. 2022 (section 3.5) and Risch et al. 2023 (sections 3.1 and 3.4). In addition, I have contributed to various other related projects during my PhD and the resulting publications are summarized here with a complete list at the end of this thesis.

I contributed to a project led by Dr. Janina Kuehlwein and Dr. Max Borsche concerning the role of cross-presenting DCs during the development of experimental cerebral malaria [197]. In this model, C57BL/6 mice are infected with *Plasmodium berghei* ANKA and the mice develop neurological symptoms with certain similarities to human cerebral malaria after ~6 days. The mice die due to the infiltration of immune cells (particularly CD8 T cells which are primed by cross-presenting DCs) and parasites into the brain within 6-9 days after the infection. We were able to show that a lack of cross-presenting DCs (*Batf3*$^{-/-}$) protected mice from developing experimental cerebral malaria. This was associated with attenuated cytotoxic T cell responses and a shift towards a regulatory milieu in the spleen. For this project, I established flow cytometric analysis via t-distributed stochastic neighbor embedding (t-SNE) at our institute, validated previously done flow cytometric analysis and identified cell populations that were not seen with classical gating strategies.

In a second project, the role of ILCs in the *L. sigmodontis* mouse model was investigated by Dr. Julia Reichwald [198]. The paper established a kinetic profile of ILCs, particularly ILC2s in susceptible BALB/c and semi-resistant C57BL/6 mice and identified ILC2s as dominant producers of IL-5 during the course of infection. It could be demonstrated that ILC2s are key immune cells in the development of microfilaremia in this model as depletion of ILC2s resulted in significantly higher MF numbers in T and B cell deficient *Rag2*$^{-/-}$ mice. I assisted with the planning of experiments, the infections with *L. sigmodontis* as well as various *ex vivo* analyses. In addition, Benjamin Lenz and I performed additional immunological analyses (flow cytometry, ELISA) that were requested during the peer-review process.

In a third project, the potential of nucleic acid receptors agonists as adjuvants for an experimental vaccine with irradiated L3 larvae of *L. sigmodontis* was investigated by Dr. Johanna Scheunemann [199]. In a first step, it was shown that the nucleic acid receptor

agonists induced strong local immune responses after subcutaneous injections. It could then be demonstrated that the use of nucleic acid receptor agonists as adjuvants supported the development of a protective immune response and significantly improved the protective effect of the vaccine. The vaccine together with poly(I:C), an agonist of the RNA sensors TLR3, MDA5 and RIG-I, led to a significantly stronger reduction of the adult worm burden and reduced the number of MF-positive animals in comparison to the vaccination with L3 larvae alone. I assisted during the experiments, particularly all work concerning animals (vaccinations, injections, infections) and the various *ex vivo* analyses. In addition, I contributed to the re-writing and editing of the manuscript during the submission and review process.

Lastly, a novel mouse model for tropical pulmonary eosinophilia was established by Benjamin Lenz (publication submitted and under peer review). Tropical pulmonary eosinophilia is a syndrome that may occur during lymphatic filariasis and it is characterized by the trapping of MF in the lung which causes a variety of respiratory symptoms. To recapitulate this phenotype, BALB/c mice were sensitized with subcutaneous injections of dead MF from *L. sigmodontis* three times and then challenged with live MF via an intravenous injection. This model is an adaptation of an existing model for tropical pulmonary eosinophilia that uses larvae from *B. malayi*, which has certain limitations as larvae of *B. malayi* are difficult to obtain or maintain. In this new model, MF of *L. sigmodontis* were trapped in the lung and animals developed a dysregulated immune response which damaged the lung architecture similar to the pathology observed in humans. For this project, I assisted with the various *ex vivo* analyses as well as writing & editing of the original paper draft.

# 4. Discussion

Public health campaigns to combat and eliminate tropical diseases have a long history and concerted efforts coordinated by the WHO and others have had significant impact on infections such as malaria, tuberculosis, and HIV. However, numerous diseases have historically been neglected and not received the amount of funding and research needed to develop appropriate diagnostics, drugs or control measures. The concept of neglected tropical diseases (NTDs) emerged in the early 2000s [200]. Originally, the list of NTDs was comprised of 13 diseases, including lymphatic filariasis and onchocerciasis, but this was extended to 17 in 2010 and 20 in 2020 [43,200,201]. Despite all efforts to the contrary, filarial diseases remain prevalent in the Global South and are the cause of significant amounts of morbidity among some of the world's poorest regions [42]. In addition, it is far from certain that the WHO's goals of eliminating the transmission of onchocerciasis or elimination of lymphatic filariasis as a public health problem can be achieved by 2030 [43,56]. As a result, the development and deployment of a macrofilaricidal treatment option for onchocerciasis is one of the critical actions outlined in the current WHO NTD 2030 roadmap [43].

In this thesis, contributions of the immune system during anti-filarial treatment were evaluated in the *L. sigmodontis* rodent model. It was shown that the macrofilaricidal efficacy of two benzimidazole compounds, OXF and FBZ, was severely reduced in immunodeficient mice (Fig. 6B, 8B). The effect on MF numbers was similarly impaired in mice treated with OXF while injections of FBZ led to a complete absence of MF in the peripheral blood regardless of immune status (Fig. 6C, 8C). Quantification of the embryonal development supported these observations (Fig. 7, 9). In addition, immunological analysis via flow cytometry revealed significant strain- and drug-specific changes in both the thoracic cavity and spleen (Fig. 12, 13). Experiments with the anti-*Wolbachia* drug CorA showed that the host's immune status appears to have no effect on the depletion of *Wolbachia* though the elimination of MF was dependent on the host's immune system (Fig. 14).

Based on these observations, a combination therapy was developed using both OXF and different cytokines. It was demonstrated that a treatment for only three days with a

combination of OXF and IL-5 achieved a similar effect against adult worms, MF and worm fertility as a full five day treatment regimen (Fig. 16). Overall, this thesis helped to elucidate the role of the immune system during anti-filarial treatment and demonstrate the proof-of-concept for a new therapeutic approach for filarial diseases based on OXF.

### 4.1 Clearance of adult worms after benzimidazole treatment

In this thesis, BALB/c WT, eosinophil-deficient Δ*dblGata1*, eosinophil and RELMα$^{+}$ macrophage-deficient *IL-4r/IL-5*$^{-/-}$, T cell, B cell and ILC-deficient *Rag2/IL-2rγ*$^{-/-}$ and lastly mature B cell and antibody-deficient µMT mice were infected with *L. sigmodontis* and treated with OXF or FBZ. The treatment efficacy measured as the reduction of the adult worm burden was impaired in all immunodeficient strains with a similar pattern for OXF and FBZ (Fig. 6, 8). Of note, a comparison of the treatment efficacy in Δ*dblGata1* and *IL-4r/IL-5*$^{-/-}$ mice demonstrates a stronger impairment in the more severe knock out lines (Fig. 6, 8). In addition, treatment in *Rag2/IL-2rγ*$^{-/-}$ mice had no discernable effect on the number of adult worms even though the worm length was significantly reduced (Fig. 6, 8).

The role of immune cells during benzimidazole treatment of filarial infections has yet to be analyzed in detail. However, various reductionist studies utilizing knock out strains have demonstrated the contributions of both the innate and adaptive immune system to influence filarial development and clearance [7]. Studies by Le Goff et al. demonstrated that mature B cell-deficient µMT mice on a C57BL/6 background are – similar to C57BL/6 WT – resistant to infection with *L. sigmodontis*, i.e., they do not develop microfilaremia and clear the parasite by ~50-60 dpi, indicating that B cells are not crucial in worm clearance [202]. Martin et al. reported that µMT mice on a BALB/c background also develop comparable quantities of adult worms as BALB/c WT mice [203]. Intriguingly, they also observed that female worms isolated from BALB/c µMT mice lacked MF in their uterus and, consequently, the infected mice did not develop microfilaremia [203]. Results obtained in this thesis could confirm that BALB/c µMT mice develop comparable adult worm burdens as BALB/c WT mice (BALB/c WT (n=14): 30.4 ± 17.4 vs. BALB/c µMT (n=15): 31.8 ± 21.2; mean ± SD, vehicle controls from three pooled experiments).

However, the lack of MF in BALB/c µMT mice could not be replicated. This discrepancy might be caused by the small sample size (n=6) used in the previous study as BALB/c µMT mice appear to not always develop patent infections. In this thesis, 5/15 BALB/c µMT mice were negative for MF 70 dpi (Tab. 6, 8). Studies with other B cell knock outs ('B-less' or BKO mice) have also demonstrated that the lack of B cells does not affect the quantity of adult worms during infections with *L. sigmodontis* [204]. Of note, infection with *L. sigmodontis* in BALB.Xid mice that have reduced numbers of the innate-like B1a subset leads to significantly higher numbers of both adult worms and MF compared to BALB/c WT controls [205].

Similarly, weekly depletion of $CD4^+$ T cells in BALB/c WT mice leads to significantly higher numbers of both adult worms and MF in the peripheral blood compared to isotype controls [206]. There are no published reports that show how a T cell specific knock out would affect the course of *L. sigmodontis* infection. However, studies in *Rag2*$^{-/-}$ C57BL/6 mice, which are deficient for B and T cells, reported significantly increased numbers of adult worms compared to WT controls [198]. As the lack of B cells generally does not reduce the adult worm burden in infections with *L. sigmodontis*, these results indicate a significant role for T cells in controlling adult worm numbers. Furthermore, deletion of *rag2* leads to the development of MF in otherwise microfilaremic C57BL/6 mice [198].

The role of innate lymphoid cells (ILCs) during *L. sigmodontis* infections is still unclear. The most common definition of ILCs includes natural killer cells (NK), ILC1s, ILC2s and ILC3s [207,208]. Recently, Ziegler-Heitbrock et al. posited that plasmacytoid dendritic cells (pDCs) should also be included in the family of ILCs based on ontogenic similarities with lymphoid cells, but this is not yet widely accepted [209,210]. Regarding their contribution to protective immune responses against *L. sigmodontis*, Boyd et al. showed that ILC2s expanded only locally at the site of infection in the thoracic cavity and preceded the expansion of Th2 cells [211]. Subsequently, it was shown that ILC2s were expanded as early as 9 dpi, peak at ~30 dpi and decrease again (though numbers were still higher than in naïve mice) by 70 dpi corresponding to the molting of L3 to L4 larvae inside the thoracic cavity, development of adult worms and peak of microfilaremia in BALB/c mice, respectively [198]. However, a depletion of ILC2s did not affect the adult worm burden

[198]. In addition, ILCs were shown to be strong inducers of IL-5 and IL-5 was found to be highly present in the thoracic cavity of BALB/c mice 70 dpi [198]. IL-5 is relevant for the recruitment, expansion and activity of eosinophils [97]. By contrast, NK cells appear to be more directly involved in killing of *L. sigmodontis* adult worms [7]. It has been reported, that depletion of NK cells every five days over the course of infection leads to significantly higher quantities of adult worms and MF in BALB/c WT mice [212].

In addition to lymphocytes, granulocytes are key effector cells during *L. sigmodontis* infections [7,97,98]. Granulocytes include four types of immune cells: basophils, mast cells, eosinophils and neutrophils. Basophils are innate effector cells that mainly circulate in the blood stream, migrate to the tissue in response to specific stimuli and they have long been implicated in various helminth infections [213]. For *L. sigmodontis*, Torrero et al. were able to show that basophils amplify type 2 immune responses but do not serve in a protective role [214]. Specifically, depletion of basophils led to a significant decrease of eosinophilia, parasite specific IgE levels, $CD4^+$ T cell proliferation and production of IL-4 by $CD4^+$ T cells in response to stimulation with parasite antigen, however the number of adult worms recovered from the thoracic cavity was unaffected 56 dpi [214]. Hartmann et al. were later able to confirm that lack of basophils does not affect the adult worm burden or MF numbers in the peripheral blood using basophil-deficient *Mcpt8-cre* mice [215]. Similarly, mast cells, which are predominantly associated with the development of acute allergic reactions, appear to have a limited role during infection with *L. sigmodontis* [216,217]. Mast cell-deficient *Cpa3*$^{cre}$ BALB/c mice displayed a similar rate of migration of infective L3 larvae and comparable adult worm burden in the thoracic cavity as BALB/c WT controls after infection with *L. sigmodontis* [217].

While basophils and mast cells are relatively rare in the thoracic cavity, eosinophils, macrophages and neutrophils make up the majority of immune cells at the site of infection during later stages with *L. sigmodontis* and they are believed to play key roles in controlling and limiting the infection in mice [7,97,98]. A deficiency in eosinophils (*IL-5*$^{-/-}$ mice) or complete lack thereof (Δ*dblGata1*) is associated with an increased worm burden after infection with *L. sigmodontis* and higher rate of patent infections in BALB/c mice [91]. Similarly, the absence of IL-4 and IL-5 signaling as well as RELM$\alpha^+$ macrophages in *IL-*

*4r/IL-5*$^{-/-}$ mice has been linked to significantly higher parasite numbers in the *L. sigmodontis* model [91]. Results from this thesis have confirmed that eosinophils and macrophages make up the majority of immune cells in the thoracic cavity during late stage infections. In BALB/c WT mice, these macrophages are mostly RELM$\alpha^+$ and are also known as M2, alternatively activated or IL-4/IL-13 activated macrophages, while both the *IL-4r/IL-5*$^{-/-}$ and *Rag2/IL-2Rγ*$^{-/-}$ mice mostly developed CD11c$^+$ or M1/classically activated macrophages in line with previous publications [91,95,218].

How these immune cells mediate the clearance of adult worms in untreated or treated mice is still not clear, though the formation of granulomatous nodules encasing the adult worms appears to be of critical importance [7]. Granulomas are – generally speaking – aggregates of immune cells and a variety of structural or matrix components that encase and isolate a foreign substance that cannot be simply phagocytosed or otherwise destroyed. Macrophages are the primary cell associated with granuloma formations though other immune cells, e.g., eosinophils, neutrophils, monocytes, lymphocytes, and fibroblasts can also contribute to the formation of granulomas and the exact composition is target-specific [59,219,220]. As previously mentioned, BALB/c mice are permissible hosts for *L. sigmodontis* and develop patent infections (~50% in female mice) while C57BL/6 are semi-resistant and do not develop patent infections [198]. Further, BALB/c mice clear the infection within ~120 days while C57BL/6 mice eliminate the adult worms around 45 days post infection [7,198]. This early clearance in C57BL/6 mice is associated with an IL-4-dependent encasement of adult worms in granulomas [204]. In BALB/c mice, the formation of granulomas around adult worms seems to be unaffected by a lack of IL-4, however deletion of interferon (IFN)-γ as well as depletion of IL-5 have been shown to prevent encapsulation during the later stages of infection [204,221]. In terms of cell composition, granulomas encasing adult worms in C57BL/6 mice are mainly composed of eosinophils and then neutrophils while granulomas in BALB/c mice show the opposite order in terms of frequency [222]. The accumulation of neutrophils appears to be dependent on various host factors, including IL-5, IFN-γ and granulocyte-colony stimulating factor (G-CSF) [221,223]. Attout et al. reported that neutrophils were the major part of an inner circle of leukocytes binding to adult worms in BALB/c mice and were able to correlate this presence with an upregulation of the adhesion molecule CD11b on

neutrophils which might explain the ability of neutrophils to bind to the adult worms [222]. In addition, they demonstrated the presence of *Wolbachia* surface protein (WSP) in granulomas around late stage adult worms in BALB/c mice [222]. Neutrophils are known to recognize and target the *Wolbachia* endosymbiont and the presence of WSP would be a likely reason for the presence of neutrophils in these granulomas [49,70,98].

It is important to note that granulomas are generally not formed around healthy and motile worms but rather around already damaged or altered specimens [7,222]. These alterations include folded membranes in the syncytium, loosening of the hypodermis, altered cuticle surface, shrinking of muscle fibers and thickening of the syncytium [222]. These changes, a reduction in motility and damage to the cuticle are believed to make the worm susceptible to be recognized and eventually encased in granulomatous nodules by the immune system [7]. It is most likely that the treatment with benzimidazoles becomes relevant at this point. *In vitro* experiments with *Onchocerca gutturosa* have demonstrated that OXF does not kill the adult worms but rather only impairs the motility [105]. Similarly, *in vitro* experiments with *L. sigmodontis* adult worms could only show very limited reductions in motility after treatment with OXF (master theses by Sara Dörken 2022 & Hannah Wegner 2022). Potential other effects against the adult worms caused by the treatment with oxfendazole such as damage to the cuticle or muscle fibers have not been investigated so far.

Taken together, it is likely that treatment with OXF *in vivo* also reduces the motility of the adult worms and may damage or alter the worms. A reduction in motility reduces the amount of shear forces and makes it easier for immune cells to adhere to the parasite. In a similar vein, it is plausible that damage to the parasite caused by the OXF treatment may release worm antigen or parts of the cuticle which can be taken up by the host's immune system and thus recruit immune cells leading to the formation of granulomas [222]. In either case, the most plausible scenario is that the treatment with OXF or FBZ damages the adult worms of *L. sigmodontis in vivo* which leads to the eventual clearance by the immune system as is the case in the immunocompetent BALB/c WT mice (Fig. 6B, 8B).

From this follows the logical research question: Which parts of the immune system are actually involved and relevant? The impaired treatment efficacy in the immunodeficient strains gives some indications as to how different immune cells or host factors influence the drug-mediated worm clearance. Starting with the innate immune system, eosinophils, while one of the hallmarks of filarial and helminth infections [97], appear to play a limited role during benzimidazole-mediated worm clearance. Particularly after OXF treatment, the eosinophil-deficient Δ*dblGata1* mice still presented with an 80-90% reduction of the median adult worm burden compared to 88-94% in immunocompetent BALB/c WT mice. Interestingly, the difference was significantly greater after FBZ treatment (0-75% in Δ*dblGata1* vs 100% in BALB/c WT mice) indicating that the contribution of eosinophils might differ between both drugs. This discrepancy could be due to differences in immune cell recruitment or activation, which may be mediated by differences in the type of damage to the parasite or length of time that the worm is damaged after treatment. As will be discussed in more detail in the following section concerning the clearance of MF, subcutaneously injected FBZ has a significantly longer half-life in mice than orally given OXF and it is plausible that this affects the nature of the damage inflicted upon the adult worms. As mentioned before, eosinophils are one of the key components in natural granuloma formation of *L. sigmodontis* adult worms in BALB/c mice and it is therefore likely that granuloma formation was impaired in the Δ*dblGata1* mice following treatment with either OXF or FBZ [222]. Granuloma formation was not quantified in this study since the mice were opened up to five weeks after the treatment at which point the granulomas were oftentimes already gone. In particular BALB/c WT mice that were treated with FBZ had in almost all cases completely clear thoracic cavities with no indication of worms and granulomas. As such, a comparison of the granuloma formation between the different strains would have been impossible at this time point. This gap in our understanding should be tackled in a future study by analyzing different (earlier) time points after the treatment to create a kinetic overview over which cells are recruited at which time point.

Despite the limited effect on treatment efficacy due the lack of eosinophils that was seen in the Δ*dblGata1* mice, the additional absence of RELMα$^{+}$ macrophages as well as the overall IL-4R and IL-5 mediated signaling (including eosinophils) in the *IL-4r/IL-5*$^{-/-}$ mice led to a significantly reduced impact on the adult worm burden after treatment with either

OXF or FBZ. In the case of OXF, the adult worm burden was reduced by only 20-50% and only 1/25 treated mice were free of adult worms 70 dpi (Fig. 6B, Tab. 6). For FBZ, the median treatment efficacy was still relatively high at up to 92%, however, only 1/20 treated mice cleared the infection (Fig. 8B, Tab. 8). The precise phenotype of the *IL-4r/IL-5*$^{-/-}$ mice and the impact of this double knock out on the immune system in general and during infection with *L. sigmodontis* in particular is still unclear and evolving. Remion et al. recently showed that the maturation of macrophages in this strain was altered beyond the lack of the cytokine RELMα as macrophages isolated from the thoracic cavity were shown to have an altered balance of the arginine metabolic pathway [224]. In addition, they could show that monocyte-derived macrophages failed to mature into F4/80$^{high}$ resident macrophages [224]. As such, the significantly lower treatment efficacy observed in the *IL-4r/IL-5*$^{-/-}$ mice in comparison to the Δ*dblGata1* mice cannot only be attributed to the additional lack of RELMα$^{+}$ or alternatively activated macrophages. As discussed previously, though the precise mechanisms of worm clearance remain elusive and only incompletely understood, it is clear that it is not a single immune cell working in isolation but rather a synergistic combination of various cellular and humoral components mediating worm clearance [225]. Results obtained in this thesis support this idea and the combination of eosinophils with mature and RELMα$^{+}$ macrophages appears to play an important role in the benzimidazole-mediated worm clearance. In the case of the other innate immune cells, e.g. neutrophils or basophils, it remains to be seen how their absence would impact treatment efficacy.

Moving on to the lymphoid cells and the adaptive immune system, the experiments with the µMT and *Rag2/IL-2rγ*$^{-/-}$ mice show that the adaptive immune system also has a key role in the benzimidazole-mediated clearance of adult worms. The treatment efficacy in the mature B cell and antibody-deficient µMT mice was lowered to 35-64% for OXF and 78% for FBZ with only 1/21 mice cleared of adult worms after treatment (Fig 6B, 8B, Tab. 6, Tab. 8). As discussed previously, while the role of B cells and antibodies in controlling adult worm numbers during natural infections appears to be limited, these results highlight their importance during drug-mediated worm clearance. Under normal circumstances, filariae are able to aptly regulate the activity of B cells and prevent recognition and targeting with antibodies through immune evasion strategies [7]. In addition, this

modulation extends to co-infections. A recent study by Hartmann et al. showed that infection with *L. sigmodontis* impairs the development of a protective immune response, including lower virus-specific antibody titers after vaccination with an influenza vaccine in mice [226]. Thus, if the adult worms are damaged by the treatment and their capacity to influence and modulate the host's immune response is diminished, it may be plausible that recognition by B cells is more readily achieved. Treatment with IVM, for example, has been shown to specifically target glutamate-gated chloride channels in muscle structures surrounding the excretory-secretory vesicles of *Brugia malayi* [108]. As a result, treatment with IVM blocked the release of excretory-secretory vesicles *in vitro* and may therefore limit the ability of the parasite to module and evade the host's immune response *in vivo* [109]. Whether OXF may have similar effects on *L. sigmodontis* or other filariae is currently unknown and should be explored in future studies.

The lowest treatment efficacy was observed in the *Rag2/IL-2rγ*$^{-/-}$ mice. Neither OXF nor FBZ treatment reduced the number of adult worms (Fig. 6B, 8B). As this strain is severely immunodeficient and lacks B cells, T cells and ILCs, it is impossible to ascribe this phenotype to one specific immune cell type. As outlined previously, ILC2s have been shown to expand in the thoracic cavity during infection with *L. sigmodontis* and they have been implicated as strong producers of IL-5 [198]. Since IL-5 is required for eosinophil proliferation and expansion, the lack of ILC2s might hamper the presence of eosinophils at the site of infection [97]. In line with this, frequencies of eosinophils in the thoracic cavity of *Rag2/IL-2rγ*$^{-/-}$ mice ranged from 1.8 to 2.6% in OXF treated or untreated mice, while frequencies in BALB/c mice were 10x higher at 18.4 to 31.5%. In addition to the absence of IL-5 producing ILC2s, the lack of T cells may also impact the presence of a number of other important cytokines. Next to IL-5, both IL-4 and IFN-γ are produced by T cells and have been shown to play key roles in the formation of granulomas and recruitment of other immune cells including neutrophils around adult worms as outlined before [204,221]. As a result, granuloma formation in *Rag2/IL-2rγ*$^{-/-}$ mice is severely impaired during natural infections [218].

Overall, results from the four different immunodeficient strains have highlighted that the clearance of adult worms after benzimidazole treatment is not dependent on any single

immune cell or host factor but rather mediated by a complex combination of both the innate and adaptive immune system. Whether treatment with either OXF or FBZ causes a reduction in motility, overall damage to the worm or impairs immune evasion strategies, it is clear that the clearance of adult worms is a two-pronged attack: Firstly, weakening of the parasite by the drug and secondly, recognition, encasement and gradual phagocytosis by the immune system. However, various open questions remain: In what way is the parasite damaged exactly? Which immune cells are recruited at what time point? What targets do the immune cells recognize? Which mediators or humoral components are important?

### 4.2 Microfilaremia and embryogenesis after benzimidazole treatment

In addition to the clearance of adult worms, the impact of anti-filarial treatment on MF development and presence in the host can be equally important. As touched upon in the introduction, current treatment strategies for human filarial diseases are mainly based on drugs that predominantly target the MF stage of the various parasites. Thus, transmission may be interrupted but the diseases cannot be cured. Despite these shortcomings, MDA campaigns with these drugs have significantly reduced the prevalence of several human filarial diseases over the course of the last few decades [43]. However, the clearance of MF may impact the safety of any anti-filarial treatment. The rapid death of MF is associated with the release of large amounts of filarial and bacterial (*Wolbachia*) antigen, and this may lead to potentially dangerous inflammatory responses by the host [49,76].

In this thesis, treatment with OXF and FBZ presented with significantly different effects on the development and presence of MF. Treatment with OXF prevented microfilaremia in BALB/c WT and µMT mice 70 dpi while the other immunodeficient strains were MF-positive albeit to a lesser extent than the corresponding vehicle controls (Fig. 6C). Treatment with FBZ, on the other hand, led to a complete absence of MF in all treated mice (Fig. 8C). Quantification of the embryonal stages supported these observations (Fig. 7, 9). While treatment with either compound significantly reduced the number of developmental stages, i.e., oocytes, morulae, pretzel and stretched MF, and increased

the number of altered or degenerated forms, treatment with FBZ was notably more effective at preventing later embryonic stages.

The first question that arises is whether OXF or FBZ has a direct impact on MFs. Here, it is important to note that OXF was given orally to the mice while FBZ was injected subcutaneously. Further, treatment with either drug was conducted between 35-39 dpi, roughly 10-15 days before the first MF can be detected in the bloodstream [89]. Previous pharmacokinetic studies have shown that orally given OXF (5 mg/kg) has a $T_{1/2}$ of 2.8 hours in mice [105]. On the other hand, Mongolian jirds (*Meriones unguiculatus*) that were subcutaneously injected with FBZ had stable levels of FBZ in the plasma for at least two months [104]. Similarly, mice that received subcutaneous injections of FBZ had stable levels of FBZ in the plasma for at least one month [156]. As such, while OXF would have been cleared from the system before the onset of microfilaremia, FBZ was presumably still present at relevant concentrations in the treated mice of the current study, though this would need to be confirmed in a future project. Nevertheless, OXF and FBZ have been reported to be largely ineffective against the MF stage of various filariae and previous studies have already postulated that the damage to adult worms and negative impact on fertility are the main cause of lower MF numbers after treatment with either drug [104,156]. The efficacy of a compound is largely dependent on the amount of time that the bioavailable concentration remains above the minimal efficacious dose. Since the plasma level of FBZ remains stable and, importantly, above the minimal efficacious dose for at least one month after subcutaneous injections, it is likely that this difference in pharmacokinetic profile explains the stronger impact of FBZ on the embryonal development of *L. sigmodontis*.

Precisely how the adult worms were damaged and how this may translate to impaired development of MF as a result of the benzimidazole (particularly OXF) treatment, however, remains to be seen. In the current thesis, OXF and FBZ led to a reduction of female worm length regardless of the host's immune status. Previous work has highlighted that treatment of *L. sigmodontis* in gerbils with subcutaneous injections of FBZ causes extensive damage to the body wall, intestine and reproductive organs of adult female worms [104]. This damage included vacuolation, membrane disruption,

breakdown of anatomical structures, and calcification in the uterus, indicating the severe impact of FBZ on the fertility of adult female worms [104]. An analogous histological analysis for OXF has not been performed so far.

In regards to the impact of the immune system, results obtained in this thesis have highlighted that the FBZ-mediated damage appears to be independent of the immune system, whereas the efficacy of OXF was dependent on components of the innate and adaptive immune system but independent of B cells and antibodies. A plethora of studies have highlighted the impact of immune deficiencies on MF numbers and development (summarized in [7]). A lack of lymphocytes in general (*Rag2*$^{-/-}$ mice), but also B cells ('Xid', 'BKO' mice), CD4$^{+}$ T cells or NK cells in particular has been associated with increased MF numbers [198,204-206,227]. For myeloid cells, a deficiency in eosinophils and RELM$\alpha^{+}$ macrophages has been shown to lead to higher numbers of MF as well as an increase in the percentage of patent infections in BALB/c mice [91]. In terms of mechanisms, the release of extracellular DNA traps (ETosis), in particular by eosinophils (EETosis), has recently been shown to be produced *in vitro* in response to MF of different filariae and has been implicated in the clearance of MF from *L. sigmodontis in vivo* [228]. Results obtained during this thesis could confirm most of the published observations regarding MF numbers except for the previously mentioned discrepancy for µMT mice.

Apart from the MF present in the peripheral blood, adult female worms isolated from immunodeficient mice may also carry higher numbers of embryonal stages per worm as was shown in this thesis (Fig. 7, 9) and also previously published in [91]. One reason for the increased number of embryonal stages may be the length of adult female worms. In the case of vehicle controls for the OXF treatment, adult female worms from BALB/c WT mice had a mean length of 63.8 mm ± 11.2 mm (mean ± SD), while worms from *IL-4r/IL-5*$^{-/-}$ mice were 79.8 mm ± 11.1 mm and worms from *Rag2/IL-2rγ*$^{-/-}$ were 93.1 mm ± 13.9 mm. This corresponds to an increased length of +25.0% and +45.9% for the *IL-4r/IL-5*$^{-/-}$ and *Rag2/IL-2rγ*$^{-/-}$ mice, respectively. At the same time, adult female worms from BALB/c WT mice had on average 6578 embryonal stages in contrast to 43187 stages in worms isolated from *IL-4r/IL-5*$^{-/-}$ mice (increase of +557%) and 37300 stages in

worms isolated from *Rag2/IL-2rγ*$^{-/-}$ mice (increase of +467%). It is therefore unlikely that the increase in worm length alone is enough to explain the increase in fertility.

A second explanation is a difference in the available nutrition that may facilitate filarial development. However, the nutritional requirements of *L. sigmodontis* are poorly understood. It has been reported that *L. sigmodontis* is hematophagous for a short period after the final molt into adult worms (~27-34 dpi) which corresponds with a phase of extensive cell division, maturation of sexual organs, and growth [229]. How adult filariae feed beyond this point is unclear and may be explored in the future. There is a growing appreciation and understanding of how nutrition and metabolic changes affect and steer the immune response (and vice versa) in both humans and animal models [230-233]. It is likely that metabolic changes in the host, as well as changes to the feeding habits of filarial parasites, may also have a significant impact on filarial development. However, this question has so far not been investigated in any detail and thus remains unclear.

A third likely reason for the heightened fertility of worms from immunodeficient mice is the impaired immune response of the host. As previously discussed, damaged or otherwise altered adult worms are cleared via the formation of granulomatous nodules consisting of neutrophils, eosinophils and various other components [222]. In immunodeficient mice, this process is – depending on the severity of the immunodeficiency – impaired or completely abrogated, and thus the parasite can likely invest more energy into the production of oocytes which eventually mature into MF.

Taken together, both OXF and FBZ had a direct effect on adult worms and reduced the worm length and fertility of adult female worms regardless of the host's immune status. It is likely that OXF-mediated damage has a similar pattern as the already published effect of FBZ, though this remains to be seen. Due to the difference in pharmacokinetics, OXF is certain to have only affected the adult worms while FBZ may have also had a minor effect on MF directly. Overall, the role of the immune system was most likely limited to the clearance of and damage to adult worms. The presence of MF in OXF treated immunodeficient mice was most likely due to the incomplete clearance of and insufficient damage to adult worms.

### 4.3 Effect of CorA on *Litomosoides sigmodontis* in immunodeficient mice

In the next part of the thesis, contributions of the immune system to treatment strategies that target filariae indirectly were assessed (Fig. 14). Several filariae harbor obligate intracellular bacteria of the genus *Wolbachia* and the presence of *Wolbachia* is essential for the development, fertility and viability of filariae that harbor these bacteria [11,69]. As such, depletion of *Wolbachia* via the treatment with antibiotics such as doxycycline or CorA is a viable alternative treatment strategy for various filarial diseases in animal models, humans as well as companion animals [10-12,136,234].

In this thesis, BALB/c WT, Δ*dblGata1* and *IL-4r/IL-5*$^{-/-}$ mice were treated with CorA after infection with *L. sigmodontis*. Treatment with CorA had no effect on the adult worm burden (Fig. 14B). In addition, the worm length was unaffected in treated BALB/c WT mice while worms isolated from immunodeficient mice (particularly adult female worms) were reduced in length after treatment (Fig. 14E+F). While experiments in Mongolian jirds showed that a 14-day treatment with CorA is sufficient to significantly reduce the adult worm burden in animals infected with *L. sigmodontis*, it is important to note that the elimination of adult worms takes a significant amount of time after anti-*Wolbachia* treatment [139]. In the case of the jird experiment, the adult worm burden was quantified 16 weeks after treatment [139]. Since the infection with *L. sigmodontis* is cleared within ~110 days in mice, it is difficult to assess the macrofilaricidal efficacy of CorA in the mouse model [7].

Nevertheless, treatment with CorA led to a reduction of *Wolbachia* numbers of 1.5 to 3 $\log_{10}$ stages in both immunocompetent and immunocompromised mouse strains (Fig. 14D). Thus, the depletion of *Wolbachia* appears to be independent of the immune response. However, the experiment was only conducted with Δ*dblGata1* and *IL-4r/IL-5*$^{-/-}$ mice and it is therefore possible that the results would be different in *Rag2/IL-2rγ*$^{-/-}$ or µMT mice. In addition, since the *Rag2/IL-2rγ*$^{-/-}$ mice do not clear the infection within 110 days, it might be possible to perform necropsies 12-16 weeks after treatment similar to the abovementioned jird experiments and thus also analyze the impact of the immune system on the macrofilaricidal efficacy in mice.

Interestingly, while worms isolated from BALB/c WT and Δ*dblGata1* were devoid of late embryonal stages after the BID CorA treatment, worms isolated from *IL-4r/IL-5*$^{-/-}$ mice retained the development of all embryonal stages, indicating that worms were still fertile and capable of releasing MF (Fig. 14C, G-I). This is corroborated by the numbers of MF in the peripheral blood, as BALB/c WT and Δ*dblGata1* had no detectable MF, whereas *IL-4r/IL-5*$^{-/-}$ mice still had >1000 MF per 50 µl blood. This indicates that the CorA-mediated effect against embryonal development is at least partly dependent on the immune system. In line with the previous sections, it seems likely that the lack eosinophils, mature F4/80$^{high}$ and RELM$\alpha^{+}$ macrophages as well as the overall lack of IL-4 receptor and IL-5-mediated signaling hinders the development of an effective response by the host against the parasite and, thus, the adult worms would receive less damage than in immunocompetent mice after CorA treatment. Future studies could further investigate this point by characterizing and comparing how the adult worms are altered after treatment in BALB/c WT, Δ*dblGata1* and *IL-4r/IL-5*$^{-/-}$ mice with a histological approach.

Of note, treatment with CorA was found to downregulate the expression of CXCL10 in eosinophils immediately after treatment (Fig. 15). CXCL10 is considered a pro-inflammatory chemokine that is produced in response to IFN-γ stimulation and binds to CXCR3 as its receptor. CXCR3 is expressed on a variety of cells, including Th1 cells, NK cells, inflammatory DCs, macrophages and B cells and plays an integral role in leukocyte recruitment [235]. The effect of CXCL10 downregulation on cell migration in this context could not be analyzed due to technical issues with the flow cytometry and may be explored in the future.

Overall, depletion of *Wolbachia* after treatment with antibiotics appears to be immune system independent. By contrast, the effect against the embryogenesis and development of MF is at least partly dependent on the immune system as sterility was not achieved in *IL-4r/IL-5*$^{-/-}$ mice. The clearance of adult worms could not be analyzed in this study and remains unclear. However, it is likely, that the removal of adult worms would be similarly impaired as in mice that were treated with OXF or FBZ.

### 4.4 Combination therapy

In this study, a combination of OXF with three different cytokines (IL-4, IL-5, IL-33) was tested in the *L. sigmodontis* mouse model (Fig. 16). All three cytokines can be classified as type 2/Th2 cytokines and are often associated with helminth infections [7]. IL-4 is involved in a variety of immunological processes, including the differentiation of naïve T helper cells into Th2 cells, differentiation of B cells into plasma cells, B cell class switching to IgE and differentiation of macrophages into what is traditionally called M2/alternatively activated macrophages [236-238]. IL-5 is associated with mucosal immunity via an increased secretion of IgA by IL-5 stimulated B cells and the maturation, activation and proliferation of eosinophils [239]. Last but not least, IL-33 is an alarmin and released by damaged or necrotic endo- and epithelial cells [240]. IL-33 is involved in the stimulation and activation of Th2 cells, ILC2s and mast cells among others and plays a pivotal role in the establishment of type 2 immune responses [240]. The cytokines in question were chosen based on preliminary results from the treatments in immunodeficient mice. The combination therapy was planned between the experiments with OXF and FBZ in the eosinophil-deficient Δ*dblGata1* and *IL-4r/IL-5*$^{-/-}$ mice and the experiments in the µMT and *Rag2/IL-2rγ*$^{-/-}$ mice. As such, the cytokines were selected to selectively strengthen eosinophils (IL-5), M2 macrophages (IL-4) and type 2 immune responses in general (IL-33) in an attempt to reverse or invert the immunodeficiency.

Overall, the combination therapy of OXF with IL-5 for three consecutive days in BALB/c WT mice led to a significantly improved treatment outcome compared to OXF alone (Fig. 16). In addition to the stronger reduction in adult worm numbers 70 dpi, the combination with IL-5 increased the number of MF-negative mice and reduced the amount of late embryonal stages indicating significant damage to the remaining adult female worms (Fig. 16). Further, the treatment induced an infiltration of eosinophils into the lung but was not associated with any significant damage as assessed by histological analysis (Fig. 21, 22). While the combination therapy of OXF with IL-4 and IL-33 also led to reduced adult worm numbers in comparison to OXF alone, the difference was notably lower than for IL-5 and not statistically significant with the tested sample size (Fig. 16B). The control treatments with the cytokines alone did not reduce the adult worm burden (Fig. 16B).

As shown by the histological analysis, eosinophils were recruited into the lung and still present in elevated numbers more than one month after the treatment was concluded. It is likely that this presence is an indication of left-over eosinophils rather than a peak in numbers. Studies in mice and other rodents in which these animals were treated intranasally with IL-5 have shown significant infiltrations of eosinophils into the lung and bronchoalveolar space within 24 hours [241-243]. Van Oosterhout et al. reported that treatment with 1 µg IL-5 twice per day for three days led to a >4-fold increase of eosinophils in comparison to saline treated controls one day after the treatment [241]. In addition, they observed a significant increase in eosinophil peroxidase activity (EPO) in the supernatant of lung homogenates in the IL-5 treated group [241]. The effect on the thoracic cavity of intranasally applied IL-5 was not investigated. However, one can speculate that at least some migration of eosinophils from the lung into the thoracic cavity occurs, particularly in the context of the *L. sigmodontis* model. During the infection with *L. sigmodontis*, the parasite migrates through the lung twice [90]. The first occurrence is during the initial migration of L3 larvae 6-9 dpi when the larvae move into the thoracic cavity. The second movement happens from day ~50 onwards when MF that are released by the female adult worms in the thoracic cavity move out from the site of infection, migrate into and through the lung and are finally detectable in the peripheral blood system [90]. Both migratory periods are associated with lung pathology, e.g., hemorrhages [7,96]. It is quite possible that the migration of MF, which happens after the treatment with OXF and IL-5, would facilitate the movement of eosinophils from the lung in the context of the combination therapy. The eosinophils in this case might be recruited and activated due to the migration-associated damage to fulfill their homeostatic and tissue repair functions or due to the recognition of filarial antigen to fulfill their protective function and participate in the elimination of migrating MF or MF-producing adult worms [97,228].

Interestingly, the alternative treatment regimen in which mice were treated every second day for a total of three applications over five days had no noticeable effect on the adult worm numbers (Fig. 23). This is most likely caused by the relatively short half-life of orally given OXF and implies that the worms were able to recover in between each dose of OXF or at least were not damaged enough to be cleared by the immune system. Similarly, the even shorter treatment regimen of only 2 days did not achieve any noticeable reduction

in adult worm numbers even when the concentration of OXF was doubled (Fig. 24). Overall, this is in line with published observations that the treatment duration rather than dosage is key for the clearance of adult worms after OXF treatment [105].

Having established an improved treatment outcome by the use of the combination therapy, the question arises as to what extent the immune response was altered by the treatment. To that end, flow cytometric analysis was performed at the site of infection and in the spleen to analyze both local and systemic immune responses. The most striking result was the substantial reduction of eosinophil frequencies and numbers in the spleen of all treated mice in comparison to the vehicle controls (Fig. 17G+18G), which was not reflected by a comparable elevation in the thoracic cavity (Fig. 19F+20F). The drop in eosinophil numbers in the spleen did not correlate with a reduction in worm burden. It is possible that the eosinophils migrated from the spleen to other organs, as histological analysis revealed an infiltration of eosinophils into the lung after treatment with IL-5 (Fig. 22C+D). However, this would not explain the reduction seen in the other treatment conditions. As the flow cytometric analysis could only be performed *ex vivo*, i.e., 31 days after the treatment ended, the time course of eosinophil numbers in the spleen immediately after treatment remains unknown. In untreated *L. sigmodontis*-infected mice, the number of eosinophils in the spleen increases between 35 (time of treatment in this thesis) and 70 (time of necropsy in this thesis) dpi [193]. Future studies may further investigate how the treatment alters the immune response and supplement the existing flow cytometric data with characterizations of earlier time points as well as a description of the cytokine release via ELISA or Luminex® assays or RT-PCR to assess transcriptomic profiles.

Apart from an improved and more detailed immunological analysis of the combination therapy of OXF with IL-5, characterization of other immunostimulatory compounds, that may synergistically strengthen the effect of OXF and clear adult worms, may yield additional and better treatment regimens. “Better” in this context refers to multiple aspects that need to be considered in order to develop an alternative macrofilaricidal treatment strategy for use in human patients. These aspects include the efficacy, safety, cost and required regulatory approval.

While the efficacy and safety are obvious concerns and need to be evaluated in multiple models (both host and parasite species if possible), the inherent immunomodulation by helminth parasites may further complicate safety issues caused by targeted stimulations of the immune system. As of 2023, there are – despite numerous attempts – no vaccines available for human helminth infections [199]. While this may be discouraging, sometimes, more information may be gleaned from failure than success. In one phase I clinical trial, Diemert et al. reported numerous adverse events following vaccinations with a recombinant secreted protein from the hookworm *Necator americanus* (*Na*-ASP-2) [244]. Vaccination with *Na*-ASP-2 induced severe erythema at the injection site in two out of nine participants and urticaria, a type of skin rash, in three out of nine participants [244]. Interestingly, the authors could correlate the development of urticaria with the presence of *Na*-ASP-2-specific IgE antibodies in the prevaccination sera [244]. This study highlights the danger of immunostimulation in patients with a previous history of helminth infections. Based on this, it is possible that a combination therapy in patients with a history of helminth infections may cause unforeseen adverse events. As eosinophils are hallmarks of helminth infections, targeted stimulations of eosinophils via IL-5 may be particularly prone for adverse events of this nature and, therefore, a variety of immunostimulatory compounds should be considered for further research in this direction.

An informed choice of potential immunostimulatory compounds that may be more efficacious is quite difficult. The field of immunology has made tremendous progress in recent decades and identified, described and characterized a variety of immune mechanisms and immune responses. Despite this figurative mountain of research, it would still be difficult to answer one basic and simple question: What kind of immune response would be effective at clearing the adult worms? In the absence of a clear answer, it is challenging to select an appropriate immunostimulatory compound to support a chemotherapy with OXF or any other drug. Helminth infections in general and filarial infections in particular are often associated with type 2 immune responses [7,245-247]. However, from the simple fact that type 2 immune responses can be characteristic of chronic helminth infections that may last years, it is clear that this immune response (as induced by the parasite) is not by itself able to clear the infection. As such, it may be useful to employ immunostimulatory compounds that skew the immune system to a pro-

inflammatory type 1 immune response. Type 1 immune responses are generally associated with viruses, bacteria and protozoa, and characterized by the production of type I interferons, IL-1β, IL-6, IL-12, and an expansion of Th1/Th17 cells [248]. In the case of filariae, comparisons of the infection with *L. sigmodontis* in susceptible and resistant strains have demonstrated strong arguments for a protective role of type 1 immune responses against filarial infections [7]. C57BL/6 mice infected with *L. sigmodontis* do not develop microfilaremia and clear the infection within ~70 days, whereas BALB/c mice develop patent infections in 50% of cases and only clear the infection after ~110 days [7,198]. A recent comparison of the immune response in both strains was able to highlight that C57BL/6 mice develop a stronger type 2 immune response than BALB/c mice, e.g., increased numbers of Th2 cells and ILC2s as well as a higher production of IL-5 and IL-13 in the thoracic cavity [198]. However, the same study also found increased levels of the type 1 associated cytokine IFN-γ in the thoracic cavity, indicating that C57BL/6 develop a mixed type 1/type 2 immune response against *L. sigmodontis* [198]. Results obtained in this thesis, however, also present compelling evidence that a further strengthening of the type 2 immune response with cytokines like IL-4, IL-5 or IL-33 improves treatment outcomes. Taken together, there are plausible arguments to strengthen either a type 1 or type 2 immune response and it is likely that any disruption of the regulatory immune response that is under normal circumstances carefully modulated by the parasite may improve worm clearance. With our current understanding of immune responses against filariae, it seems that any selection will have to be mostly empirical and carefully validated for both efficacy and safety.

The third aspect, the cost of any potential treatment, is of particular concern for the development of anti-filarial treatments. As outlined in the beginning, filarial infections are mainly present in the Global South, i.e., comparatively economically poor regions with limited monetary resources to obtain and distribute expensive therapies. Taking a somewhat recent example from the covid pandemic, the cost of a single treatment regimen with REGEN-COV (a combination of two monoclonal antibodies called Casirivimab and Imdevimab) was roughly 1820 € in late 2021 [249]. In contrast, the drugs currently used for filarial treatments IVM, DEC and ALB are far cheaper to manufacture and the production costs are estimated at 0.19 USD for one 400 mg ALB tablet, 0.0025

USD for one 50 mg DEC tablet and 0.50 USD for one 3 mg tablet of IVM [250]. In addition, IVM (marketed as Mectizan®), for example, is donated by Merck and the company has pledged to continue its donation program until the elimination of onchocerciasis is achieved [250]. As such, even if a hypothetical monoclonal treatment existed for filarial infections, it would be unlikely to be of use in any of the affected regions unless costs could be reduced by a factor of ~1000-10000.

A similar problem exists for potential combination therapies with immunostimulatory compounds. To illustrate the costs, it may be beneficial to look at the costs for the herein described mouse treatment. In the 3-day combination therapy, mice were treated with a commercially available formulation of OXF called Dolthene® and cytokines were sourced from BioLegend as recombinant, carrier free versions (see method section). For each treatment, mice received 2 µg of one of three cytokines and 12.5 mg/kg OXF, or for the whole 3-day treatment 6 µg of the respective cytokine and 75 mg/kg OXF. At an average weight of 25 g per mouse, this equates to 75 mg/kg * 0.025 kg = 1.875 mg per mouse for a 3-day treatment or 125 mg/kg * 0.025 kg = 3.125 mg for a 5-day treatment. 50 ml of Dolthene® (containing 22.65 mg/ml OXF) was purchased for 11.37 €. Therefore, one mouse on average received 1.875 mg / 22.65 mg/ml = 0.082 ml of Dolthene® during a 3-day treatment or 3.125 mg / 22.65 mg/ml = 0.165 ml of Dolthene® during a 5-day treatment in total. This equates to a price of (0.082 ml / 50 ml) * 11.37 € = 0.018 € for a 3-day treatment per mouse. Accordingly, the 5-day treatment would cost 0.037 € per mouse. 100 µg of recombinant IL-5 was purchased at a price of 460 € and therefore the cost of treatment per mouse was 460 € * 0.06 = 27.60 €. This illustrates that, while the combination therapy reduced the required treatment duration, it also substantially increased the costs. While the exact numbers would no doubt be different in the field, this example highlights potential draw backs in the development of new combination therapies.

The fourth aspect, the required regulatory approval can be another roadblock in the developmental pipeline. Identifying, testing, validating and developing new treatment options usually takes years or oftentimes decades. One way to reduce the necessary steps and shorten the timeframe is to repurpose existing compounds that have already

received regulatory approval by the American FDA or European counterpart (EMA). Potential immunostimulatory compounds include the various vaccine adjuvants such as aluminum-based adjuvants, CpG or Marix-M™ (a saponin compound used in the Novavax COVID-19 vaccine) [251,252]. Employing already approved immunostimulatory compounds in a combination therapy may significantly shorten the time needed for an eventual approval.

## 4.5 Conclusions and Outlook

In this thesis, the role of the immune system during anti-filarial treatment was characterized. It could be shown that both the innate and adaptive immune system contribute to the clearance of adult worms after treatment with benzimidazoles. In addition, treatment with OXF in immunodeficient mice did not prevent microfilaremia in most immunodeficient mice, while treatment with FBZ led to a complete abrogation of MF development in treated animals. Further, flow cytometry analysis revealed strain and treatment specific patterns of immunological changes. For anti-*Wolbachia* compounds, it could be shown that the depletion of *Wolbachia* after treatment with CorA was independent of the host's immune status, however the impact of CorA on MF development was reduced in immunodeficient mice.

In a second part, the potential of a combination therapy with OXF and three cytokines, IL-4, IL-5 and IL-33 was evaluated. The combination with IL-5 in particular led to a significant increase in the anti-filarial efficacy in a shortened treatment regimen. While a 3-day OXF treatment only reduced the adult worm burden by 33%, the combination with IL-5 achieved a reduction of 91%, comparable to a 5-day OXF treatment regimen. Overall, this presents the first proof of concept study to investigate combinations of immunostimulatory compounds with OXF against filariae and demonstrates the potential of a combination therapy to shorten the time needed for worm clearance.

Future studies may further characterize the role of the immune system during anti-filarial treatment and elucidate the involved mechanisms. In particular the clearance of adult worms via the formation of granulomas after chemotherapy is still largely unknown. In addition, there are still a lot of open questions regarding the combination therapy that may be investigated. It would be imperative to investigate other potential immunostimulatory compounds such as type 1 cytokines, vaccine adjuvants or natural plant extracts.

Taken together, results from this thesis and future investigations into combination therapies might contribute to the development of OXF-based therapies as a macrofilaricidal option and as such yield a macrofilaricidal treatment that could potentially be employed in MDA strategies.

# Scientific contributions

## Publications in peer-reviewed journals

Kuehlwein, J. M., Borsche, M., Korir, P. J., **Risch, F**., Mueller, A. K., Hübner, M. P., Hildner, K., Hoerauf, A., Dunay, I. R., & Schumak, B. (2020). Protection of Batf3-deficient mice from experimental cerebral malaria correlates with impaired cytotoxic T-cell responses and immune regulation. *Immunology*, *159*(2), 193–204. https://doi.org/10.1111/imm.13137

**Risch, F**.*, Ritter, M.*, Hoerauf, A., & Hübner, M. P. (2021). Human filariasis-contributions of the *Litomosoides sigmodontis* and *Acanthocheilonema viteae* animal model. *Parasitology research*, *120*(12), 4125–4143. https://doi.org/10.1007/s00436-020-07026-2

*joint first authorship

**Risch, F**., Koschel, M., Lenz, B., Specht, S., Hoerauf, A., Hübner, M. P. & Scandale, I. (2022). Comparison of the macrofilaricidal efficacy of oxfendazole and its isomers against the rodent filaria *Litomosoides sigmodontis*. *Frontiers in Tropical Diseases*, 3. https://doi.org/10.3389/fitd.2022.982421

Reichwald, J. J., **Risch, F**., Neumann, A. L., Frohberger, S. J., Scheunemann, J. F., Lenz, B., Ehrens, A., Strutz, W., Schumak, B., Hoerauf, A., & Hübner, M. P. (2022). ILC2s control microfilaremia during *Litomosoides sigmodontis* infection in *Rag2*$^{-/-}$ mice. *Frontiers in immunology, 13, 863663.* https://doi.org/10.3389/fimmu.2022.863663

Scheunemann, J. F.*, **Risch, F**.*, Reichwald, J. J., Lenz, B., Neumann, A. L., Garbe, S., Frohberger, S. J., Koschel, M., Ajendra, J., Rothe, M., Latz, E., Coch, C., Hartmann, G., Schumak, B., Hoerauf, A., & Hübner, M. P. (2023). Potential of Nucleic Acid Receptor Ligands to Improve Vaccination Efficacy against the Filarial Nematode *Litomosoides sigmodontis*. *Vaccines*, *11*(5), 966. https://doi.org/10.3390/vaccines11050966

*joint first authorship

**Risch, F.**, Scheunemann, J. F., Reichwald, J. J., Lenz, B., Ehrens, A., Gal, J., Fercoq, F., Koschel, M., Fendler, M., Hoerauf, A., Martin, C., Hübner, M. P. (2023). The efficacy

of the benzimidazoles oxfendazole and flubendazole against *Litomosoides sigmodontis* is dependent on the adaptive and innate immune system. *Frontiers in Microbiology,* 14. https://doi.org/10.3389/fmicb.2023.1213143

**Submitted publications**

Lenz, B., Ehrens, A., Ajendra, J., **Risch, F**., Gal, J., Neumann, A. L., Reichwald, J. J., Strutz, W., McSorley, H., Martin, C., Hoerauf, A., Hübner, M. P. (2023). Repeated sensitization of mice with microfilariae of *Litomosoides sigmodontis* induces pulmonary eosinophilia in an IL-33-dependent manner.

**Presentations at scientific conferences**

Poster presentation at the 29th biannual meeting of the German Society for Parasitology (DGP) in Bonn, Germany, 2021 (**title**: Treatment efficacy of oxfendazole and flubendazole against *Litomosoides sigmodontis* is reduced in immunocompromised mice)

Poster presentation at the 22nd biannual meeting of the Drug Design & Development Seminar (DDDS) of the German Society for Parasitology in Munich, Germany, 2022 (**title**: The benzimidazoles oxfendazole and flubendazole eliminate adult worms of *Litomosoides sigmodontis* in an immune system-dependent manner)

Oral presentation at the 15th International Congress of Parasitology in Copenhagen, Denmark, 2022 (**title**: Treatment efficacy of oxfendazole and flubendazole against the rodent filaria *Litomosoides sigmodontis* is dependent on the immune system)

Oral presentation at the 30th biannual meeting of the German Society for Parasitology (DGP) in Gießen, Germany, 2023 (**title**: Treatment efficacy of oxfendazole and flubendazole against the rodent filaria *Litomosoides sigmodontis* is dependent on the immune system)

**Acknowledgements**

First, I would like to thank Prof. Dr. Achim Hoerauf, the director of the Institute for Medical Microbiology, Immunology and Parasitology at the University Hospital Bonn, for giving me the opportunity to pursue my doctoral thesis at his institute.

Second, I would like to thank Prof. Dr. Oliver Gruß for being my second supervisor and Prof. Dr. Ulrike Endesfelder and Prof. Dr. Karl G. Wagner for completing my examination committee.

Third, I would like to thank my first supervisor, Prof. Dr. Marc P. Hübner. He has been a terrific group leader and supervisor and has supported me greatly during my time at the IMMIP.

In addition, I would like to thank my former group leader, Dr. Beatrix Schumak, for her help, advice and support during my transition from master thesis to doctoral studies. Further, I would like to thank our collaboration partners without whom the project would not have been possible. In particular, I would like to thank Prof. Dr. Coralie Martin and her group members Joséphine Gal and Dr. Frédéric Fercoq from the Muséum national d'Histoire naturelle in Paris for their help with histological analysis, Ivan Scandale and Lorenzo Bizzari from the Drugs for Neglected Disease initiative (DNDi) for their collaboration during the isomer and NGS study, the NGS and bioinformatics core facilities of the UKB for their assistance during the NGS study and Tim Becker from the pharmaceutical department of the University of Bonn for the preparation of CorA.

Special thanks go to Dr. Johanna Scheunemann, Dr. Julia Reichwald and Benjamin Lenz with whom I have worked together for many years and shared (many) offices. Thank you for your great support, friendship and fun times over the years. I would also like to thank all other current and former members of our group and the parasitology department, in particular Martina Fendler, Marianne Koschel and Tilman Aden for their invaluable help during many experiments and creating a wonderful and enjoyable work environment.

Lastly, I would like to thank my friends and family for all their support and help during these years.

# References


1. Cho, H.Y.; Lee, Y.J.; Shin, S.Y.; Song, H.O.; Ahn, M.H.; Ryu, J.S. Subconjuctival *Loa loa* with calabar swelling. *J Korean Med Sci* **2008**, *23*, 731-733.
2. Downes, B.L.; Jacobsen, K.H. A systematic review of the epidemiology of mansonelliasis. *Afr J Infect Dis* **2010**, *4*, 7-14.
3. Taylor, M.J.; Hoerauf, A.; Bockarie, M. Lymphatic filariasis and onchocerciasis. *Lancet* **2010**, *376*, 1175-1185.
4. Blaxter, M. Imagining sisyphus happy: DNA barcoding and the unnamed majority. *Philos Trans R Soc Lond B Biol Sci* **2016**, *371*, 20150329.
5. Lefoulon, E.; Bain, O.; Makepeace, B.L.; d'Haese, C.; Uni, S.; Martin, C.; Gavotte, L. Breakdown of coevolution between symbiotic bacteria *Wolbachia* and their filarial hosts. *Peerj* **2016**, *4*.
6. Fischer, P.; Hoerauf, A.; Weil, G. The filariases. In *Manson's tropical disease*, 24th ed. Elsevier: 2023.
7. Finlay, C.M.; Allen, J.E. The immune response of inbred laboratory mice to *Litomosoides sigmodontis*: A route to discovery in myeloid cell biology. *Parasite Immunol* **2020**, *42*, e12708.
8. Hawryluk, N.A. Macrofilaricides: An unmet medical need for filarial diseases. *ACS Infect Dis* **2020**, *6*, 662-671.
9. Geary, T.G.; Mackenzie, C.D.; Silber, S.A. Flubendazole as a macrofilaricide: History and background. *PLoS Negl Trop Dis* **2019**, *13*, e0006436.
10. Hoerauf, A.; Pfarr, K.; Mand, S.; Debrah, A.Y.; Specht, S. Filariasis in africa--treatment challenges and prospects. *Clin Microbiol Infect* **2011**, *17*, 977-985.
11. Ehrens, A.; Hoerauf, A.; Hubner, M.P. Current perspective of new anti-wolbachial and direct-acting macrofilaricidal drugs as treatment strategies for human filariasis. *GMS Infect Dis* **2022**, *10*, Doc02.
12. Hoerauf, A.; Mand, S.; Fischer, K.; Kruppa, T.; Marfo-Debrekyei, Y.; Debrah, A.Y.; Pfarr, K.M.; Adjei, O.; Buttner, D.W. Doxycycline as a novel strategy against bancroftian filariasis-depletion of *Wolbachia* endosymbionts from *Wuchereria bancrofti* and stop of microfilaria production. *Med Microbiol Immunol* **2003**, *192*, 211-216.
13. Mand, S.; Debrah, A.Y.; Klarmann, U.; Batsa, L.; Marfo-Debrekyei, Y.; Kwarteng, A.; Specht, S.; Belda-Domene, A.; Fimmers, R.; Taylor, M.*, et al.* Doxycycline improves filarial lymphedema independent of active filarial infection: A randomized controlled trial. *Clin Infect Dis* **2012**, *55*, 621-630.
14. Irvine, M.A.; Stolk, W.A.; Smith, M.E.; Subramanian, S.; Singh, B.K.; Weil, G.J.; Michael, E.; Hollingsworth, T.D. Effectiveness of a triple-drug regimen for global elimination of lymphatic filariasis: A modelling study. *Lancet Infect Dis* **2017**, *17*, 451-458.
15. Pineda, M.A.; Lumb, F.; Harnett, M.M.; Harnett, W. Es-62, a therapeutic anti-inflammatory agent evolved by the filarial nematode *Acanthocheilonema viteae*. *Mol Biochem Parasitol* **2014**, *194*, 1-8.
16. Cox, F.E. History of human parasitology. *Clin Microbiol Rev* **2002**, *15*, 595-612.
17. Small, S.T.; Tisch, D.J.; Zimmerman, P.A. Molecular epidemiology, phylogeny and evolution of the filarial nematode *Wuchereria bancrofti*. *Infect Genet Evol* **2014**, *28*, 33-43.
18. Bach, J.F. The hygiene hypothesis in autoimmunity: The role of pathogens and commensals. *Nat Rev Immunol* **2018**, *18*, 105-120.
19. Pfefferle, P.I.; Keber, C.U.; Cohen, R.M.; Garn, H. The hygiene hypothesis - learning from but not living in the past. *Front Immunol* **2021**, *12*, 635935.
20. Santiago, H.C.; Nutman, T.B. Human helminths and allergic disease: The hygiene hypothesis and beyond. *Am J Trop Med Hyg* **2016**, *95*, 746-753.

21. de Ruiter, K.; Tahapary, D.L.; Sartono, E.; Soewondo, P.; Supali, T.; Smit, J.W.A.; Yazdanbakhsh, M. Helminths, hygiene hypothesis and type 2 diabetes. *Parasite Immunol* **2017**, *39*, e12404.
22. Goncalves, M.L.; Araujo, A.; Ferreira, L.F. Human intestinal parasites in the past: New findings and a review. *Mem Inst Oswaldo Cruz* **2003**, *98 Suppl 1*, 103-118.
23. David, A.R. Natsef-amun, keeper of the bulls: A comparative study of the paleopathology and archaeology of an egyptian mummy. *Journal of Biological Research - Bollettino della Società Italiana di Biologia Sperimentale* **1970**, *80*.
24. Veiga, P. Studying mummies and human remains: Some current developments and issues. *Journal of the Washington Academy of Sciences* **2012**, *98*, 1-21.
25. Veiga, P. Oncology and infectious diseases in ancient egypt: The ebers papyrus' treatise on tumours 857-877 and the cases found in ancient egyptian human material. University of Manchester, 2009.
26. Sanchez, G.M.; Siuda, T. Ebers papyrus case #873: A probable case of neurofibromatosis 1. **2002**.
27. http://parasitology.kasralainy.edu.eg/draft-plan-status. (access: 11.05.2023)
28. Otsuji, Y. History, epidemiology and control of filariasis. *Trop Med Health* **2011**, *39*, 3-13.
29. Samuels, T. Undoing the hottentoting of "the queen of punt" a jamaican afronography on the kemetiu depiction of ati of punt. *Journal of Black Studies* **2020**, *52*, 3-23.
30. De-Jian, S.; Xu-Li, D.; Ji-Hui, D. The history of the elimination of lymphatic filariasis in China. *Infect Dis Poverty* **2013**, *2*, 30.
31. https://commons.wikimedia.org/wiki/File:By_ovedc_-_Egyptian_Museum_(Cairo)_-_087.jpg?uselang=de. (access: 11.05.2023),
32. Edwards, A.B. Pharaohs, fellahs and explorers. Harper: 1892.
33. Laurence, B.R. The curse of saint thomas. *Med Hist* **1970**, *14*, 352-363.
34. Farmer, D. *The oxford dictionary of saints, revised*. OUP Oxford: 2011.
35. Huber, H.G.; Gruntzig, J. [discovery of loa ophthalmia by the french ship's surgeon francois guyot (1742-1816)]. *Klin Monbl Augenheilkd* **1986**, *189*, 178-182.
36. Cox, F.E.G. The golden age of parasitology-1875-1925: The scottish contributions. *Parasitology* **2017**, *144*, 1567-1581.
37. Manson, P. On the nature and origin of calabar swellings. *Trans. R. Soc. Trop. Med. Hyg* **1910**, *3*, 244-251.
38. O'Neill, S. On the presence of a filaria in "craw-craw.". *The Lancet* **1875**, *105*, 265-266.
39. Manson, P.; Davidson, A. Diseases of the skin in tropical climates. *Hygiene and diseases of warm climates. Young J. Pentland, London, United Kingdom* **1893**, 928-995.
40. Chernin, E. Sir patrick manson's studies on the transmission and biology of filariasis. *Rev Infect Dis* **1983**, *5*, 148-166.
41. Manson, P. On the development of filaria sanguinis hominis, and on the mosquito considered as a nurse*. *Zoological Journal of the Linnean Society* **1878**, *14*, 304-311.
42. James, S.L.; Abate, D.; Abate, K.H.; Abay, S.M.; Abbafati, C.; Abbasi, N.; Abbastabar, H.; Abd-Allah, F.; Abdela, J.; Abdelalim, A.*, et al.* Global, regional, and national incidence, prevalence, and years lived with disability for 354 diseases and injuries for 195 countries and territories, 1990–2017: A systematic analysis for the global burden of disease study 2017. *The Lancet* **2018**, *392*, 1789-1858.
43. WHO. Ending the neglect to attain the sustainable development goals: A road map for neglected tropical diseases 2021–2030. Geneva: World health organization; **2020**.
44. Simonsen, P.E.; Onapa, A.W.; Asio, S.M. *Mansonella perstans* filariasis in africa. *Acta Trop* **2011**, *120 Suppl 1*, S109-120.
45. Meyrowitsch, D.W.; Simonsen, P.E.; Magesa, S.M. A 26-year follow-up of bancroftian filariasis in two communities in north-eastern tanzania. *Ann Trop Med Parasitol* **2004**, *98*, 155-169.

46. Local Burden of Disease Neglected Tropical Diseases, C. The global distribution of lymphatic filariasis, 2000-18: A geospatial analysis. *Lancet Glob Health* **2020**, *8*, e1186-e1194.
47. Lourens, G.B.; Ferrell, D.K. Lymphatic filariasis. *Nurs Clin North Am* **2019**, *54*, 181-192.
48. Dreyer, G.; Medeiros, Z.; Netto, M.J.; Leal, N.C.; de Castro, L.G.; Piessens, W.F. Acute attacks in the extremities of persons living in an area endemic for bancroftian filariasis: Differentiation of two syndromes. *Trans R Soc Trop Med Hyg* **1999**, *93*, 413-417.
49. Taylor, M.J. *Wolbachia* in the inflammatory pathogenesis of human filariasis. *Ann N Y Acad Sci* **2003**, *990*, 444-449.
50. Bennuru, S.; Nutman, T.B. Lymphangiogenesis and lymphatic remodeling induced by filarial parasites: Implications for pathogenesis. *PLoS Pathog* **2009**, *5*, e1000688.
51. Dreyer, G.; Addiss, D.; Gadelha, P.; Lapa, E.; Williamson, J.; Dreyer, A. Interdigital skin lesions of the lower limbs among patients with lymphoedema in an area endemic for bancroftian filariasis. *Tropical Medicine & International Health* **2006**, *11*, 1475-1481.
52. Noroes, J.; Addiss, D.; Cedenho, A.; Figueredo-Silvan, J.; Lima, G.; Dreyer, G. Pathogenesis of filarial hydrocele: Risk associated with intrascrotal nodulescaused by death of adult *Wuchereria bancrofti*. *Transactions of the Royal Society of Tropical Medicine and Hygiene* **2003**, *97*, 561-566.
53. Bernhard, P.; Makunde, R.W.; Magnussen, P.; Lemnge, M.M. Genital manifestations and reproductive health in female residents of a *Wuchereria bancrofti*-endemic area in tanzania. *Trans R Soc Trop Med Hyg* **2000**, *94*, 409-412.
54. Ottesen, E.A.; Nutman, T.B. Tropical pulmonary eosinophilia. *Annu Rev Med* **1992**, *43*, 417-424.
55. Gulati, S.; Gupta, N.; Singh, N.P.; Batra, S.; Garg, S.; Beniwal, P.; Kumar, S. Chyluria with proteinuria or filarial nephropathy? An enigma. *Parasitol Int* **2007**, *56*, 251-254.
56. Lakwo, T.; Oguttu, D.; Ukety, T.; Post, R.; Bakajika, D. Onchocerciasis elimination: Progress and challenges. *Res Rep Trop Med* **2020**, *11*, 81-95.
57. Specht, S.; Brattig, N.; Buttner, M.; Buttner, D.W. Criteria for the differentiation between young and old *Onchocerca volvulus* filariae. *Parasitol Res* **2009**, *105*, 1531-1538.
58. Plaisier, A.P.; van Oortmarssen, G.J.; Remme, J.; Habbema, J.D. The reproductive lifespan of *Onchocerca volvulus* in west african savanna. *Acta Trop* **1991**, *48*, 271-284.
59. Korten, S.; Wildenburg, G.; Darge, K.; Buttner, D.W. Mast cells in onchocercomas from patients with hyperreactive onchocerciasis (sowda). *Acta Trop* **1998**, *70*, 217-231.
60. Ottesen, E.A. Immune responsiveness and the pathogenesis of human onchocerciasis. *J Infect Dis* **1995**, *171*, 659-671.
61. Korten, S.; Hoerauf, A.; Kaifi, J.T.; Buttner, D.W. Low levels of transforming growth factor-beta (tgf-beta) and reduced suppression of th2-mediated inflammation in hyperreactive human onchocerciasis. *Parasitology* **2011**, *138*, 35-45.
62. Brattig, N.W.; Tenner-Racz, K.; Korten, S.; Hoerauf, A.; Buttner, D.W. Immunohistology of ectopic secondary lymph follicles in subcutaneous nodules from patients with hyperreactive onchocerciasis (sowda). *Parasitol Res* **2010**, *107*, 657-666.
63. Katawa, G.; Layland, L.E.; Debrah, A.Y.; von Horn, C.; Batsa, L.; Kwarteng, A.; Arriens, S.; D, W.T.; Specht, S.; Hoerauf, A*., et al.* Hyperreactive onchocerciasis is characterized by a combination of th17-th2 immune responses and reduced regulatory t cells. *PLoS Negl Trop Dis* **2015**, *9*, e3414.
64. Brattig, N.W.; Cheke, R.A.; Garms, R. Onchocerciasis (river blindness)-more than a century of research and control. *Acta Tropica* **2021**, *218*.
65. André, A.v.S.; Blackwell, N.M.; Hall, L.R.; Hoerauf, A.; Brattig, N.W.; Volkmann, L.; Taylor, M.J.; Ford, L.; Hise, A.G.; Lass, J.H*., et al.* The role of endosymbiotic *Wolbachia* bacteria in the pathogenesis of river blindness. *Science* **2002**, *295*, 1892-1895.

66. Bouchery, T.; Lefoulon, E.; Karadjian, G.; Nieguitsila, A.; Martin, C. The symbiotic role of *Wolbachia* in onchocercidae and its impact on filariasis. *Clinical Microbiology and Infection* **2013**, *19*, 131-140.
67. Kaur, R.; Shropshire, J.D.; Cross, K.L.; Leigh, B.; Mansueto, A.J.; Stewart, V.; Bordenstein, S.R.; Bordenstein, S.R. Living in the endosymbiotic world of *Wolbachia*: A centennial review. *Cell Host Microbe* **2021**, *29*, 879-893.
68. Hoerauf, A.; Nissen-Pahle, K.; Schmetz, C.; Henkle-Duhrsen, K.; Blaxter, M.L.; Buttner, D.W.; Gallin, M.Y.; Al-Qaoud, K.M.; Lucius, R.; Fleischer, B. Tetracycline therapy targets intracellular bacteria in the filarial nematode *Litomosoides sigmodontis* and results in filarial infertility. *J Clin Invest* **1999**, *103*, 11-18.
69. Taylor, M.J.; Hoerauf, A. A new approach to the treatment of filariasis. *Curr Opin Infect Dis* **2001**, *14*, 727-731.
70. Hise, A.G.; Gillette-Ferguson, I.; Pearlman, E. Immunopathogenesis of *Onchocerca volvulus* keratitis (river blindness): A novel role for tlr4 and endosymbiotic *Wolbachia* bacteria. *J Endotoxin Res* **2003**, *9*, 390-394.
71. Hise, A.G.; Daehnel, K.; Gillette-Ferguson, I.; Cho, E.; McGarry, H.F.; Taylor, M.J.; Golenbock, D.T.; Fitzgerald, K.A.; Kazura, J.W.; Pearlman, E. Innate immune responses to endosymbiotic *Wolbachia* bacteria in *Brugia malayi* and *Onchocerca volvulus* are dependent on tlr2, tlr6, myd88, and mal, but not tlr4, trif, or tram. *J Immunol* **2007**, *178*, 1068-1076.
72. Tamarozzi, F.; Halliday, A.; Gentil, K.; Hoerauf, A.; Pearlman, E.; Taylor, M.J. Onchocerciasis: The role of *Wolbachia* bacterial endosymbionts in parasite biology, disease pathogenesis, and treatment. *Clin Microbiol Rev* **2011**, *24*, 459-468.
73. Vieri, M.K.; Hendy, A.; Mokili, J.L.; Colebunders, R. Nodding syndrome research revisited. *Int J Infect Dis* **2021**, *104*, 739-741.
74. Abd-Elfarag, G.O.E.; Edridge, A.W.D.; Spijker, R.; Sebit, M.B.; van Hensbroek, M.B. Nodding syndrome: A scoping review. *Trop Med Infect Dis* **2021**, *6*, 211.
75. Whittaker, C.; Walker, M.; Pion, S.D.S.; Chesnais, C.B.; Boussinesq, M.; Basanez, M.G. The population biology and transmission dynamics of *Loa loa*. *Trends Parasitol* **2018**, *34*, 335-350.
76. Risch, F.; Ritter, M.; Hoerauf, A.; Hubner, M.P. Human filariasis-contributions of the *Litomosoides sigmodontis* and *Acanthocheilonema viteae* animal model. *Parasitol Res* **2021**, *120*, 4125-4143.
77. Ta-Tang, T.H.; Luz, S.L.B.; Crainey, J.L.; Rubio, J.M. An overview of the management of mansonellosis. *Res Rep Trop Med* **2021**, *12*, 93-105.
78. Ritter, M.; Ndongmo, W.P.C.; Njouendou, A.J.; Nghochuzie, N.N.; Nchang, L.C.; Tayong, D.B.; Arndts, K.; Nausch, N.; Jacobsen, M.; Wanji, S*., et al. Mansonella perstans* microfilaremic individuals are characterized by enhanced type 2 helper t and regulatory t and b cell subsets and dampened systemic innate and adaptive immune responses. *PLoS Negl Trop Dis* **2018**, *12*, e0006184.
79. Hoffmann, W.; Petit, G.; Schulz-Key, H.; Taylor, D.; Bain, O.; Le Goff, L. *Litomosoides sigmodontis* in mice: Reappraisal of an old model for filarial research. *Parasitol Today* **2000**, *16*, 387-389.
80. Scott, J.A.; Macdonald, E.M.; Terman, B. A description of the stages in the life cycle of the filarial worm *Litomosoides carinii*. *The Journal of Parasitology* **1951**, *37*, 425-432.
81. Williams, R.W.; Brown, H.W. The transmission of *Litomosoides carinii*, filariid parasite of the cotton rat, by the tropical rat mite, *Liponyssus bacoti*. *Science* **1946**, *103*, 224-224.
82. Bertram, D.S.; Unsworth, K.; Gordon, R.M. The biology and maintenance of *Liponyssus bacoti* hirst, 1913, and an investigation into its rôle as a vector of *Litomosoides carinii* to cotton rats and white rats, together with some observations on the infection in the white rats. *Annals of Tropical Medicine & Parasitology* **1946**, *40*, 228-254.

83. Vaz, Z. Ackertia gen. Nov. For *Litomosa burgosi* de la barrera, 1926, with notes on the synonymy and morphological variations of litomosoides carinii (travassos, 1919). *Annals of Tropical Medicine & Parasitology* **1934**, *28*, 143-149.
84. Bain, O.; Petit, G.; Diagne, M. [*Litomosoides*, parasites of rodents; taxonomic consequences]. *Ann Parasitol Hum Comp* **1989**, *64*, 268-289.
85. Schneider, C.R.; Blair, L.S.; Schardein, J.L.; Boche, L.K.; Thompson, P.E. Comparison of early *Litomosoides carinii* infections in cotton rats and gerbils. *J Parasitol* **1968**, *54*, 1099-+.
86. Ramakrishnan, S.; Dalip, S.; Bhatnagar, V.; Raghavan, N. Infection of the albino rat with the filarial parasite, *Litomosoides carinii*, of rats. *Indian journal of malariology* **1961**, *15*, 255-261.
87. Pringle, G.; King, D.F. Some developments in techniques for the study of the rodent filarial parasite *Litomosoides carinii.* I. A preliminary comparison of the host effciency of the multimammate rat, praomys (mastomys) natalensis, with that of the cotton rat, sigmodon hispidus. *Ann Trop Med Parasitol* **1968**, *62*, 462-468.
88. Hawking, F.; Sewell, P. The maintenance of a filarial infection (*Litomosoides carinii*) for chemotherapeutic investigations. *British Journal of Pharmacology and Chemotherapy* **1948**, *3*, 285-296.
89. Petit, G.; Diagne, M.; Marechal, P.; Owen, D.; Taylor, D.; Bain, O. Maturation of the filaria *Litomosoides sigmodontis* in BALB/c mice; comparative susceptibility of nine other inbred strains. *Ann Parasitol Hum Comp* **1992**, *67*, 144-150.
90. Hübner, M.P.; Torrero, M.N.; McCall, J.W.; Mitre, E. *Litomosoides sigmodontis*: A simple method to infect mice with l3 larvae obtained from the pleural space of recently infected jirds (*Meriones unguiculatus*). *Exp Parasitol* **2009**, *123*, 95-98.
91. Frohberger, S.J.; Ajendra, J.; Surendar, J.; Stamminger, W.; Ehrens, A.; Buerfent, B.C.; Gentil, K.; Hoerauf, A.; Hubner, M.P. Susceptibility to *L. sigmodontis* infection is highest in animals lacking il-4r/il-5 compared to single knockouts of il-4r, il-5 or eosinophils. *Parasit Vectors* **2019**, *12*, 248.
92. Karadjian, G.; Fercoq, F.; Pionnier, N.; Vallarino-Lhermitte, N.; Lefoulon, E.; Nieguitsila, A.; Specht, S.; Carlin, L.M.; Martin, C. Migratory phase of *Litomosoides sigmodontis* filarial infective larvae is associated with pathology and transient increase of s100a9 expressing neutrophils in the lung. *PLoS Negl Trop Dis* **2017**, *11*, e0005596.
93. Frohberger, S.J.; Fercoq, F.; Neumann, A.L.; Surendar, J.; Stamminger, W.; Ehrens, A.; Karunakaran, I.; Remion, E.; Vogl, T.; Hoerauf, A*., et al.* S100a8/s100a9 deficiency increases neutrophil activation and protective immune responses against invading infective l3 larvae of the filarial nematode *Litomosoides sigmodontis*. *PLoS Negl Trop Dis* **2020**, *14*, e0008119.
94. Fercoq, F.; Remion, E.; Frohberger, S.J.; Vallarino-Lhermitte, N.; Hoerauf, A.; Le Quesne, J.; Landmann, F.; Hubner, M.P.; Carlin, L.M.; Martin, C. Il-4 receptor dependent expansion of lung cd169+ macrophages in microfilaria-driven inflammation. *PLoS Negl Trop Dis* **2019**, *13*, e0007691.
95. Ritter, M.; Tamadaho, R.S.; Feid, J.; Vogel, W.; Wiszniewsky, K.; Perner, S.; Hoerauf, A.; Layland, L.E. Il-4/5 signalling plays an important role during *Litomosoides sigmodontis* infection, influencing both immune system regulation and tissue pathology in the thoracic cavity. *International Journal for Parasitology* **2017**, *47*, 951-960.
96. Fercoq, F.; Remion, E.; Vallarino-Lhermitte, N.; Alonso, J.; Raveendran, L.; Nixon, C.; Le Quesne, J.; Carlin, L.M.; Martin, C. Microfilaria-dependent thoracic pathology associated with eosinophilic and fibrotic polyps in filaria-infected rodents. *Parasit Vectors* **2020**, *13*, 551.
97. Ehrens, A.; Hoerauf, A.; Hubner, M.P. Eosinophils in filarial infections: Inducers of protection or pathology? *Front Immunol* **2022**, *13*, 983812.
98. Ajendra, J.; Allen, J.E. Neutrophils: Friend or foe in filariasis? *Parasite Immunology* **2022**, *44*.

99. Hewitt, R.; Kushner, S. Experimental chemotherapy of filariasis; effect of 1-diethyl-carbamyl-4-methylpiperazine hydrochloride against naturally acquired filarial infections in cotton rats and dogs. *The Journal of laboratory and clinical medicine* **1947**, *32 11*, 1314-1329.
100. Hawking, F.; Sewell, P.; Thurston, J.P. The mode of action of hetrazan on filarial worms. *Br J Pharmacol Chemother* **1950**, *5*, 217-238.
101. Schardein, J.L.; Lucas, J.A.; Dickerson, C.W. Ultrastructural changes in *Litomosoides carinii* microfilariae in gerbils treated with diethylcarbamazine. *J Parasitol* **1968**, *54*, 351-358.
102. Zahner, H.; Schares, G. Experimental chemotherapy of filariasis: Comparative evaluation of the efficacy of filaricidal compounds in *Mastomys coucha* infected with *Litomosoides carinii*, acanthocheilonema viteae, brugia malayi and b. Pahangi. *Acta Tropica* **1993**, *52*, 221-266.
103. Hübner, M.P.; Townson, S.; Gokool, S.; Tagboto, S.; Maclean, M.J.; Verocai, G.G.; Wolstenholme, A.J.; Frohberger, S.J.; Hoerauf, A.; Specht, S.*, et al.* Evaluation of the in vitro susceptibility of various filarial nematodes to emodepside. *International Journal for Parasitology: Drugs and Drug Resistance* **2021**, *17*, 27-35.
104. Hübner, M.P.; Ehrens, A.; Koschel, M.; Dubben, B.; Lenz, F.; Frohberger, S.J.; Specht, S.; Quirynen, L.; Lachau-Durand, S.; Tekle, F.*, et al.* Macrofilaricidal efficacy of single and repeated oral and subcutaneous doses of flubendazole in *Litomosoides sigmodontis* infected jirds. *PLoS Negl Trop Dis* **2019**, *13*, e0006320.
105. Hübner, M.P.; Martin, C.; Specht, S.; Koschel, M.; Dubben, B.; Frohberger, S.J.; Ehrens, A.; Fendler, M.; Struever, D.; Mitre, E.*, et al.* Oxfendazole mediates macrofilaricidal efficacy against the filarial nematode *Litomosoides sigmodontis* in vivo and inhibits *Onchocerca* spec. Motility in vitro. *PLoS Negl Trop Dis* **2020**, *14*, e0008427.
106. Lacey, E. Mode of action of benzimidazoles. *Parasitol Today* **1990**, *6*, 112-115.
107. Richard-Lenoble, D.; Chandenier, J.; Gaxotte, P. Ivermectin and filariasis. *Fundam Clin Pharmacol* **2003**, *17*, 199-203.
108. Moreno, Y.; Nabhan, J.F.; Solomon, J.; Mackenzie, C.D.; Geary, T.G. Ivermectin disrupts the function of the excretory-secretory apparatus in microfilariae of *Brugia malayi*. *Proc Natl Acad Sci U S A* **2010**, *107*, 20120-20125.
109. Loghry, H.J.; Yuan, W.; Zamanian, M.; Wheeler, N.J.; Day, T.A.; Kimber, M.J. Ivermectin inhibits extracellular vesicle secretion from parasitic nematodes. *J Extracell Vesicles* **2020**, *10*, e12036.
110. Verma, S.; Kashyap, S.S.; Robertson, A.P.; Martin, R.J. Diethylcarbamazine activates trp channels including trp-2 in filaria, *Brugia malayi*. *Commun Biol* **2020**, *3*, 398.
111. Williams, P.D.E.; Kashyap, S.S.; McHugh, M.A.; Brewer, M.T.; Robertson, A.P.; Martin, R.J. Diethylcarbamazine, trp channels and ca(2+) signaling in cells of the ascaris intestine. *Sci Rep* **2022**, *12*, 21317.
112. Tripathi, B.; Roy, N.; Dhingra, N. Introduction of triple-drug therapy for accelerating lymphatic filariasis elimination in india: Lessons learned. *Am J Trop Med Hyg* **2022**, *106*, 29-38.
113. King, C.L.; Suamani, J.; Sanuku, N.; Cheng, Y.C.; Satofan, S.; Mancuso, B.; Goss, C.W.; Robinson, L.J.; Siba, P.M.; Weil, G.J.*, et al.* A trial of a triple-drug treatment for lymphatic filariasis. *N Engl J Med* **2018**, *379*, 1801-1810.
114. Krentel, A.; Basker, N.; Beau de Rochars, M.; Bogus, J.; Dilliott, D.; Direny, A.N.; Dubray, C.; Fischer, P.U.; Ga, A.L.; Goss, C.W.*, et al.* A multicenter, community-based, mixed methods assessment of the acceptability of a triple drug regimen for elimination of lymphatic filariasis. *PLoS Negl Trop Dis* **2021**, *15*, e0009002.
115. Kamgno, J.; Pion, S.D.; Chesnais, C.B.; Bakalar, M.H.; D'Ambrosio, M.V.; Mackenzie, C.D.; Nana-Djeunga, H.C.; Gounoue-Kamkumo, R.; Njitchouang, G.R.; Nwane, P.*, et al.* A test-and-not-treat strategy for onchocerciasis in loa loa-endemic areas. *N Engl J Med* **2017**, *377*, 2044-2052.

116. WHO. Progress in eliminating onchocerciasis in the who region of the americas: Doxycycline treatment as an end-game strategy. *Wkly Epidemiol Rec* **2019**, *94*, 415-419.
117. Debrah, A.Y.; Mand, S.; Specht, S.; Marfo-Debrekyei, Y.; Batsa, L.; Pfarr, K.; Larbi, J.; Lawson, B.; Taylor, M.; Adjei, O.*, et al.* Doxycycline reduces plasma vegf-c/svegfr-3 and improves pathology in lymphatic filariasis. *PLoS Pathog* **2006**, *2*, e92.
118. Debrah, A.Y.; Mand, S.; Marfo-Debrekyei, Y.; Batsa, L.; Albers, A.; Specht, S.; Klarmann, U.; Pfarr, K.; Adjei, O.; Hoerauf, A. Macrofilaricidal activity in *Wuchereria bancrofti* after 2 weeks treatment with a combination of rifampicin plus doxycycline. *J Parasitol Res* **2011**, *2011*, 201617.
119. Hoerauf, A.; Volkmann, L.; Hamelmann, C.; Adjei, O.; Autenrieth, I.B.; Fleischer, B.; Buttner, D.W. Endosymbiotic bacteria in worms as targets for a novel chemotherapy in filariasis. *Lancet* **2000**, *355*, 1242-1243.
120. Https://www.cdc.gov/parasites/loiasis/health_professionals/index.Html#tx. (access: 12.05.2023),
121. Davi, S.D.; Ramharter, M.; Nordmann, T. Loiasis – eine extrem vernachlässigte tropenerkrankung. *Flugmedizin · Tropenmedizin · Reisemedizin - FTR* **2023**, *30*, 15-19.
122. Ta-Tang, T.H.; Crainey, J.L.; Post, R.J.; Luz, S.L.; Rubio, J.M. Mansonellosis: Current perspectives. *Res Rep Trop Med* **2018**, *9*, 9-24.
123. https://www.msdmanuals.com/de-de/profi/infektionskrankheiten/nematoden-rundw%C3%BCrmer/mansonellose (access: 04.07.2023),
124. H, T.s.; Legesse, M. The role of wolbachia bacteria in the pathogenesis of onchocerciasis and prospects for control of the disease. **2007**.
125. Hertig, M.; Wolbach, S.B. Studies on rickettsia-like micro-organisms in insects. *J Med Res* **1924**, *44*, 329-374 327.
126. McLaren, D.J.; Worms, M.J.; Laurence, B.R.; Simpson, M.G. Micro-organisms in filarial larvae (nematoda). *Trans R Soc Trop Med Hyg* **1975**, *69*, 509-514.
127. Kozek, W.J. Transovarially-transmitted intracellular microorganisms in adult and larval stages of *Brugia malayi*. *The Journal of Parasitology* **1977**, *63*, 992.
128. Vincent, A.L.; Ash, L.R.; Frommes, S.P. The ultrastructure of adult *Brugia malayi* (brug, 1927) (nematoda: Filarioidea). *J Parasitol* **1975**, *61*, 499-512.
129. Kozek, W.J.; Marroquin, H.F. Intracytoplasmic bacteria in *Onchocerca volvulus*. *Am J Trop Med Hyg* **1977**, *26*, 663-678.
130. Genchi, C.; Sacchi, L.; Bandi, C.; Venco, L. Preliminary results on the effect of tetracycline on the embryogenesis and symbiotic bacteria (*Wolbachia*) of *Dirofilaria immitis*. An update and discussion. *Parassitologia* **1998**, *40*, 247-249.
131. Bandi, C.; Anderson, T.J.; Genchi, C.; Blaxter, M.L. Phylogeny of *Wolbachia* in filarial nematodes. *Proc Biol Sci* **1998**, *265*, 2407-2413.
132. McCall, J.W.; Jun, J.J.; Bandi, C. *Wolbachia* and the antifilarial properties of tetracycline. An untold story. *Italian Journal of Zoology* **1999**, *66*, 7-10.
133. Bakowski, M.A.; McNamara, C.W. Advances in antiwolbachial drug discovery for treatment of parasitic filarial worm infections. *Trop Med Infect Dis* **2019**, *4*, 108.
134. Hong, W.D.; Benayoud, F.; Nixon, G.L.; Ford, L.; Johnston, K.L.; Clare, R.H.; Cassidy, A.; Cook, D.A.N.; Siu, A.; Shiotani, M.*, et al.* Awz1066s, a highly specific anti-*Wolbachia* drug candidate for a short-course treatment of filariasis. *Proc Natl Acad Sci U S A* **2019**, *116*, 1414-1419.
135. Hubner, M.P.; Koschel, M.; Struever, D.; Nikolov, V.; Frohberger, S.J.; Ehrens, A.; Fendler, M.; Johannes, I.; von Geldern, T.W.; Marsh, K.*, et al.* In vivo kinetics of *Wolbachia* depletion by abbv-4083 in *L. sigmodontis* adult worms and microfilariae. *PLoS Negl Trop Dis* **2019**, *13*, e0007636.

136. Krome, A.K.; Becker, T.; Kehraus, S.; Schiefer, A.; Gutschow, M.; Chaverra-Munoz, L.; Huttel, S.; Jansen, R.; Stadler, M.; Ehrens, A.*, et al.* Corallopyronin a: Antimicrobial discovery to preclinical development. *Nat Prod Rep* **2022**, *39*, 1705-1720.
137. Schiefer, A.; Schmitz, A.; Schaberle, T.F.; Specht, S.; Lammer, C.; Johnston, K.L.; Vassylyev, D.G.; Konig, G.M.; Hoerauf, A.; Pfarr, K. Corallopyronin a specifically targets and depletes essential obligate *Wolbachia* endobacteria from filarial nematodes in vivo. *J Infect Dis* **2012**, *206*, 249-257.
138. Edwards, J.L.; Balthazar, J.T.; Esposito, D.L.A.; Ayala, J.C.; Schiefer, A.; Pfarr, K.; Hoerauf, A.; Alt, S.; Hesterkamp, T.; Grosse, M.*, et al.* Potent in vitro and ex vivo anti-gonococcal activity of the rpob inhibitor corallopyronin a. *mSphere* **2022**, *7*, e0036222.
139. Schiefer, A.; Hubner, M.P.; Krome, A.; Lammer, C.; Ehrens, A.; Aden, T.; Koschel, M.; Neufeld, H.; Chaverra-Munoz, L.; Jansen, R.*, et al.* Corallopyronin a for short-course anti-wolbachial, macrofilaricidal treatment of filarial infections. *PLoS Negl Trop Dis* **2020**, *14*, e0008930.
140. Finkelstein, A.E.; Walz, D.T.; Batista, V.; Mizraji, M.; Roisman, F.; Misher, A. Auranofin. New oral gold compound for treatment of rheumatoid arthritis. *Ann Rheum Dis* **1976**, *35*, 251-257.
141. Katz, W.A.; Alexander, S.; Bland, J.H.; Blechman, W.; Bluhm, G.B.; Bonebrake, R.A.; Falbo, A.; Greenwald, R.A.; Hartman, S.; Hobbs, T.*, et al.* The efficacy and safety of auranofin compared to placebo in rheumatoid arthritis. *J Rheumatol Suppl* **1982**, *8*, 173-178.
142. Bulman, C.A.; Bidlow, C.M.; Lustigman, S.; Cho-Ngwa, F.; Williams, D.; Rascon, A.A., Jr.; Tricoche, N.; Samje, M.; Bell, A.; Suzuki, B.*, et al.* Repurposing auranofin as a lead candidate for treatment of lymphatic filariasis and onchocerciasis. *PLoS Negl Trop Dis* **2015**, *9*, e0003534.
143. Kulke, D.; von Samson-Himmelstjerna, G.; Miltsch, S.M.; Wolstenholme, A.J.; Jex, A.R.; Gasser, R.B.; Ballesteros, C.; Geary, T.G.; Keiser, J.; Townson, S.*, et al.* Characterization of the Ca2+-gated and voltage-dependent K+-channel SLO-1 of nematodes and its interaction with emodepside. *PLoS Negl Trop Dis* **2014**, *8*, e3401.
144. Krucken, J.; Harder, A.; Jeschke, P.; Holden-Dye, L.; O'Connor, V.; Welz, C.; von Samson-Himmelstjerna, G. Anthelmintic cyclcooctadepsipeptides: Complex in structure and mode of action. *Trends Parasitol* **2012**, *28*, 385-394.
145. Bah, G.S.; Schneckener, S.; Hahnel, S.R.; Bayang, N.H.; Fieseler, H.; Schmuck, G.M.; Krebber, R.; Sarr, A.; Terjung, C.; Ngangyung, H.F.*, et al.* Emodepside targets SLO-1 channels of *Onchocerca ochengi* and induces broad anthelmintic effects in a bovine model of onchocerciasis. *PLoS Pathog* **2021**, *17*, e1009601.
146. Krucken, J.; Holden-Dye, L.; Keiser, J.; Prichard, R.K.; Townson, S.; Makepeace, B.L.; Hubner, M.P.; Hahnel, S.R.; Scandale, I.; Harder, A.*, et al.* Development of emodepside as a possible adulticidal treatment for human onchocerciasis-the fruit of a successful industrial-academic collaboration. *PLoS Pathog* **2021**, *17*, e1009682.
147. https://dndi.org/research-development/portfolio/emodepside/ (access: 04.07.2023),
148. Mrimi, E.C.; Welsche, S.; Ali, S.M.; Hattendorf, J.; Keiser, J. Emodepside for *Trichuris trichiura* and hookworm infection. *N Engl J Med* **2023**, *388*, 1863-1875.
149. Gonzalez, A.E.; Codd, E.E.; Horton, J.; Garcia, H.H.; Gilman, R.H. Oxfendazole: A promising agent for the treatment and control of helminth infections in humans. *Expert Rev Anti Infect Ther* **2019**, *17*, 51-56.
150. Hou, Z.J.; Luo, X.; Zhang, W.; Peng, F.; Cui, B.; Wu, S.J.; Zheng, F.M.; Xu, J.; Xu, L.Z.; Long, Z.J.*, et al.* Flubendazole, FDA-approved anthelmintic, targets breast cancer stem-like cells. *Oncotarget* **2015**, *6*, 6326-6340.
151. Canova, K.; Rozkydalova, L.; Rudolf, E. Anthelmintic flubendazole and its potential use in anticancer therapy. *Acta Medica (Hradec Kralove)* **2017**, *60*, 5-11.

152. Zhen, Y.; Zhao, R.; Wang, M.; Jiang, X.; Gao, F.; Fu, L.; Zhang, L.; Zhou, X.L. Flubendazole elicits anti-cancer effects via targeting eva1a-modulated autophagy and apoptosis in triple-negative breast cancer. *Theranostics* **2020**, *10*, 8080-8097.
153. Zhou, X.; Zou, L.; Chen, W.; Yang, T.; Luo, J.; Wu, K.; Shu, F.; Tan, X.; Yang, Y.; Cen, S.*, et al.* Flubendazole, FDA-approved anthelmintic, elicits valid antitumor effects by targeting p53 and promoting ferroptosis in castration-resistant prostate cancer. *Pharmacol Res* **2021**, *164*, 105305.
154. Chen, C.; Ding, Y.; Liu, H.; Sun, M.; Wang, H.; Wu, D. Flubendazole plays an important anti-tumor role in different types of cancers. *Int J Mol Sci* **2022**, *23*, 519.
155. Dominguez-Vazquez, A.; Taylor, H.R.; Greene, B.M.; Ruvalcaba-Macias, A.M.; Rivas-Alcala, A.R.; Murphy, R.P.; Beltran-Hernandez, F. Comparison of flubendazole and diethylcarbamazine in treatment of onchocerciasis. *Lancet* **1983**, *1*, 139-143.
156. Sjoberg, H.T.; Pionnier, N.; Aljayyoussi, G.; Metuge, H.M.; Njouendou, A.J.; Chunda, V.C.; Fombad, F.F.; Tayong, D.B.; Gandjui, N.V.T.; Akumtoh, D.N.*, et al.* Short-course, oral flubendazole does not mediate significant efficacy against *Onchocerca* adult male worms or *Brugia* microfilariae in murine infection models. *PLoS Negl Trop Dis* **2019**, *13*, e0006356.
157. Lachau-Durand, S.; Lammens, L.; van der Leede, B.J.; Van Gompel, J.; Bailey, G.; Engelen, M.; Lampo, A. Preclinical toxicity and pharmacokinetics of a new orally bioavailable flubendazole formulation and the impact for clinical trials and risk/benefit to patients. *PLoS Negl Trop Dis* **2019**, *13*, e0007026.
158. Fischer, C.; Ibiricu Urriza, I.; Bulman, C.A.; Lim, K.C.; Gut, J.; Lachau-Durand, S.; Engelen, M.; Quirynen, L.; Tekle, F.; Baeten, B.*, et al.* Efficacy of subcutaneous doses and a new oral amorphous solid dispersion formulation of flubendazole on male jirds (*Meriones unguiculatus*) infected with the filarial nematode *Brugia pahangi. PLoS Negl Trop Dis* **2019**, *13*, e0006787.
159. Blanton, R.E.; Wachira, T.M.; Zeyhle, E.E.; Njoroge, E.M.; Magambo, J.K.; Schantz, P.M. Oxfendazole treatment for cystic hydatid disease in naturally infected animals. *Antimicrob Agents Chemother* **1998**, *42*, 601-605.
160. Gavidia, C.M.; Gonzalez, A.E.; Lopera, L.; Jayashi, C.; Angelats, R.; Barron, E.A.; Ninaquispe, B.; Villarreal, L.; Garcia, H.H.; Verastegui, M.R.*, et al.* Evaluation of nitazoxanide and oxfendazole efficacy against cystic echinococcosis in naturally infected sheep. *Am J Trop Med Hyg* **2009**, *80*, 367-372.
161. Gomez-Puerta, L.A.; Gavidia, C.; Lopez-Urbina, M.T.; Garcia, H.H.; Gonzalez, A.E.; Cysticercosis Working Group in, P. Efficacy of a single oral dose of oxfendazole against *Fasciola hepatica* in naturally infected sheep. *Am J Trop Med Hyg* **2012**, *86*, 486-488.
162. https://dndi.org/research-development/portfolio/oxfendazole/ (access: 04.07.2023),
163. Bach, T.; Galbiati, S.; Kennedy, J.K.; Deye, G.; Nomicos, E.Y.H.; Codd, E.E.; Garcia, H.H.; Horton, J.; Gilman, R.H.; Gonzalez, A.E.*, et al.* Pharmacokinetics, safety, and tolerability of oxfendazole in healthy adults in an open-label phase 1 multiple ascending dose and food effect study. *Antimicrob Agents Chemother* **2020**, *64*.
164. Specht, S.; Keiser, J. Helminth infections: Enabling the world health organization road map. *Int J Parasitol* **2022**.
165. LeGuennec, M.; Klena, N.; Aeschlimann, G.; Hamel, V.; Guichard, P. Overview of the centriole architecture. *Curr Opin Struct Biol* **2021**, *66*, 58-65.
166. Fennell, B.J.; Naughton, J.A.; Barlow, J.; Brennan, G.; Fairweather, I.; Hoey, E.; McFerran, N.; Trudgett, A.; Bell, A. Microtubules as antiparasitic drug targets. *Expert Opin Drug Dis* **2008**, *3*, 501-518.
167. Brouhard, G.J.; Rice, L.M. Microtubule dynamics: An interplay of biochemistry and mechanics. *Nat Rev Mol Cell Biol* **2018**, *19*, 451-463.

168. Goodson, H.V.; Jonasson, E.M. Microtubules and microtubule-associated proteins. *Cold Spring Harb Perspect Biol* **2018**, *10*, a022608.
169. Liu, P.; Wurtz, M.; Zupa, E.; Pfeffer, S.; Schiebel, E. Microtubule nucleation: The waltz between gamma-tubulin ring complex and associated proteins. *Curr Opin Cell Biol* **2021**, *68*, 124-131.
170. Zupa, E.; Liu, P.; Wurtz, M.; Schiebel, E.; Pfeffer, S. The structure of the gamma-turc: A 25-years-old molecular puzzle. *Curr Opin Struct Biol* **2021**, *66*, 15-21.
171. Liu, P.; Zupa, E.; Neuner, A.; Bohler, A.; Loerke, J.; Flemming, D.; Ruppert, T.; Rudack, T.; Peter, C.; Spahn, C*., et al.* Insights into the assembly and activation of the microtubule nucleator gamma-turc. *Nature* **2020**, *578*, 467-471.
172. Wurtz, M.; Zupa, E.; Atorino, E.S.; Neuner, A.; Bohler, A.; Rahadian, A.S.; Vermeulen, B.J.A.; Tonon, G.; Eustermann, S.; Schiebel, E*., et al.* Modular assembly of the principal microtubule nucleator gamma-turc. *Nat Commun* **2022**, *13*, 473.
173. Winey, M.; O'Toole, E. Centriole structure. *Philos Trans R Soc Lond B Biol Sci* **2014**, *369*, 20130457.
174. Akhmanova, A.; Steinmetz, M.O. Control of microtubule organization and dynamics: Two ends in the limelight. *Nat Rev Mol Cell Biol* **2015**, *16*, 711-726.
175. Ezrahi, S.; Aserin, A.; Garti, N. Basic principles of drug delivery systems - the case of paclitaxel. *Adv Colloid Interface Sci* **2019**, *263*, 95-130.
176. Prota, A.E.; Bargsten, K.; Northcote, P.T.; Marsh, M.; Altmann, K.H.; Miller, J.H.; Diaz, J.F.; Steinmetz, M.O. Structural basis of microtubule stabilization by laulimalide and peloruside a. *Angew Chem Int Ed Engl* **2014**, *53*, 1621-1625.
177. Ravelli, R.B.; Gigant, B.; Curmi, P.A.; Jourdain, I.; Lachkar, S.; Sobel, A.; Knossow, M. Insight into tubulin regulation from a complex with colchicine and a stathmin-like domain. *Nature* **2004**, *428*, 198-202.
178. Gigant, B.; Wang, C.; Ravelli, R.B.; Roussi, F.; Steinmetz, M.O.; Curmi, P.A.; Sobel, A.; Knossow, M. Structural basis for the regulation of tubulin by vinblastine. *Nature* **2005**, *435*, 519-522.
179. Aguayo-Ortiz, R.; Mendez-Lucio, O.; Medina-Franco, J.L.; Castillo, R.; Yepez-Mulia, L.; Hernandez-Luis, F.; Hernandez-Campos, A. Towards the identification of the binding site of benzimidazoles to beta-tubulin of *Trichinella spiralis*: Insights from computational and experimental data. *J Mol Graph Model* **2013**, *41*, 12-19.
180. Aguayo-Ortiz, R.; Cano-Gonzalez, L.; Castillo, R.; Hernandez-Campos, A.; Dominguez, L. Structure-based approaches for the design of benzimidazole-2-carbamate derivatives as tubulin polymerization inhibitors. *Chem Biol Drug Des* **2017**, *90*, 40-51.
181. Ehrlich, P. Chemotherapie von infektionskrankheiten. In *The collected papers of paul ehrlich*, Elsevier: 1960; pp 213-227.
182. Doenhoff, M.J. The immune-dependence of chemotherapy in experimental schistosomiasis. *Mem Inst Oswaldo Cruz* **1989**, *84 Suppl 1*, 31-37.
183. Silva, J.C.S.; Bernardes, M.; Melo, F.L.; Sa, M.; Carvalho, B.M. Praziquantel versus praziquantel associated with immunomodulators in mice infected with *Schistosoma mansoni*: A systematic review and meta-analysis. *Acta Trop* **2020**, *204*, 105359.
184. Zhang, S.; Zhou, Y.; Su, L.; Zhang, X.; Wang, H.; Liu, B. In vivo evaluation of the efficacy of combined albedazole-ifn-alpha treatment for cystic echinococcosis in mice. *Parasitol Res* **2017**, *116*, 735-742.
185. Rahdar, M.; Rafiei, A.; Valipour-Nouroozi, R. The combination of cytokines and albendazole therapy for prophylaxis and treatment of experimental/hydatid cyst. *Acta Trop* **2020**, *201*, 105206.

186. Dvoroznakova, E.; Porubcova, J.; Sevcikova, Z. Immune response of mice with alveolar echinococcosis to therapy with transfer factor, alone and in combination with albendazole. *Parasitol Res* **2009**, *105*, 1067-1076.
187. Murthy, P.K.; Tyagi, K.; Chatterjee, R.K. *Brugia malayi* in *Mastomys natalensis*: Efficacy of mebendazole in combination with freund's complete adjuvant. *Folia Parasitol (Praha)* **1992**, *39*, 51-59.
188. Owais, M.; Misra-Bhattacharya, S.; Haq, W.; Gupta, C.M. Immunomodulator tuftsin augments antifilarial activity of diethylcarbamazine against experimental brugian filariasis. *J Drug Target* **2003**, *11*, 247-251.
189. Du, W.Y.; Liao, J.W.; Fan, C.K.; Su, K.E. Combined treatment with interleukin-12 and mebendazole lessens the severity of experimental eosinophilic meningitis caused by *Angiostrongylus cantonensis* in icr mice. *Infect Immun* **2003**, *71*, 3947-3953.
190. Fatma, N.; Mathur, K.B.; Chatterjee, R.K. Chemotherapy of experimental filariasis: Enhancement of activity profile of ivermectin with immunomodulators. *Acta Trop* **1994**, *57*, 55-67.
191. Risch, F.; Scheunemann, J.F.; Reichwald, J.J.; Lenz, B.; Ehrens, A.; Gal, J.; Fercoq, F.; Koschel, M.; Fendler, M.; Hoerauf, A.*, et al.* The efficacy of the benzimidazoles oxfendazole and flubendazole against *Litomosoides sigmodontis* is dependent on the adaptive and innate immune system. *Front Microbiol* **2023**, *14*, 1213143.
192. Bouchery, T.; Ehrhardt, K.; Lefoulon, E.; Hoffmann, W.; Bain, O.; Martin, C. Differential tissular distribution of *Litomosoides sigmodontis* microfilariae between microfilaremic and amicrofilaremic mice following experimental infection. *Parasite* **2012**, *19*, 351-358.
193. Ajendra, J.; Specht, S.; Neumann, A.L.; Gondorf, F.; Schmidt, D.; Gentil, K.; Hoffmann, W.H.; Taylor, M.J.; Hoerauf, A.; Hubner, M.P. St2 deficiency does not impair type 2 immune responses during chronic filarial infection but leads to an increased microfilaremia due to an impaired splenic microfilarial clearance. *PLoS One* **2014**, *9*, e93072.
194. Hawking, F. The role of the spleen in controlling the number of microfilariae (*Dirofilaria immitis*, *D. repens*, *Litomosoides carinii* and *Dipetalonema witei*) in the blood. *Ann Trop Med Parasitol* **1962**, *56*, 168-172.
195. Cayrol, C.; Girard, J.P. Interleukin-33 (il-33): A critical review of its biology and the mechanisms involved in its release as a potent extracellular cytokine. *Cytokine* **2022**, *156*.
196. Chhabra, N.; Aseri, M.L.; Padmanabhan, D. A review of drug isomerism and its significance. *Int J Appl Basic Med Res* **2013**, *3*, 16-18.
197. Kuehlwein, J.M.; Borsche, M.; Korir, P.J.; Risch, F.; Mueller, A.K.; Hubner, M.P.; Hildner, K.; Hoerauf, A.; Dunay, I.R.; Schumak, B. Protection of batf3-deficient mice from experimental cerebral malaria correlates with impaired cytotoxic t-cell responses and immune regulation. *Immunology* **2020**, *159*, 193-204.
198. Reichwald, J.J.; Risch, F.; Neumann, A.L.; Frohberger, S.J.; Scheunemann, J.F.; Lenz, B.; Ehrens, A.; Strutz, W.; Schumak, B.; Hoerauf, A.*, et al.* ILC2s control microfilaremia during *Litomosoides sigmodontis* infection in *Rag2*(-/-) mice. *Frontiers in Immunology* **2022**, *13*.
199. Scheunemann, J.F.; Risch, F.; Reichwald, J.J.; Lenz, B.; Neumann, A.L.; Garbe, S.; Frohberger, S.J.; Koschel, M.; Ajendra, J.; Rothe, M.*, et al.* Potential of nucleic acid receptor ligands to improve vaccination efficacy against the filarial nematode *Litomosoides sigmodontis*. *Vaccines (Basel)* **2023**, *11*, 966.
200. Hotez, P.J. Ntds v.2.0: "Blue marble health"--neglected tropical disease control and elimination in a shifting health policy landscape. *PLoS Negl Trop Dis* **2013**, *7*, e2570.
201. Hotez, P.J.; Molyneux, D.H.; Fenwick, A.; Kumaresan, J.; Sachs, S.E.; Sachs, J.D.; Savioli, L. Control of neglected tropical diseases. *N Engl J Med* **2007**, *357*, 1018-1027.

202. Le Goff, L.; Lamb, T.J.; Graham, A.L.; Harcus, Y.; Allen, J.E. Il-4 is required to prevent filarial nematode development in resistant but not susceptible strains of mice. *Int J Parasitol* **2002**, *32*, 1277-1284.
203. Martin, C.; Saeftel, M.; Vuong, P.N.; Babayan, S.; Fischer, K.; Bain, O.; Hoerauf, A. B-cell deficiency suppresses vaccine-induced protection against murine filariasis but does not increase the recovery rate for primary infection. *Infect Immun* **2001**, *69*, 7067-7073.
204. Volkmann, L.; Saeftel, M.; Bain, O.; Fischer, K.; Fleischer, B.; Hoerauf, A. Interleukin-4 is essential for the control of microfilariae in murine infection with the filaria litomosoides sigmodontis. *Infect Immun* **2001**, *69*, 2950-2956.
205. Al-Qaoud, K.M.; Fleischer, B.; Hoerauf, A. The xid defect imparts susceptibility to experimental murine filariosis--association with a lack of antibody and il-10 production by B cells in response to phosphorylcholine. *Int Immunol* **1998**, *10*, 17-25.
206. Al-Qaoud, K.M.; Taubert, A.; Zahner, H.; Fleischer, B.; Hoerauf, A. Infection of BALB/c mice with the filarial nematode *Litomosoides sigmodontis*: Role of CD4+ t cells in controlling larval development. *Infect Immun* **1997**, *65*, 2457-2461.
207. Jacquelot, N.; Seillet, C.; Vivier, E.; Belz, G.T. Innate lymphoid cells and cancer. *Nat Immunol* **2022**, *23*, 371-379.
208. Garofalo, C.; Cerantonio, A.; Muscoli, C.; Mollace, V.; Viglietto, G.; De Marco, C.; Cristiani, C.M. Helper innate lymphoid cells-unappreciated players in melanoma therapy. *Cancers (Basel)* **2023**, *15*, 933.
209. Ziegler-Heitbrock, L.; Ohteki, T.; Ginhoux, F.; Shortman, K.; Spits, H. Reclassifying plasmacytoid dendritic cells as innate lymphocytes. *Nat Rev Immunol* **2023**, *23*, 1-2.
210. Reizis, B.; Idoyaga, J.; Dalod, M.; Barrat, F.; Naik, S.; Trinchieri, G.; Tussiwand, R.; Cella, M.; Colonna, M. Reclassification of plasmacytoid dendritic cells as innate lymphocytes is premature. *Nat Rev Immunol* **2023**, *23*, 336-337.
211. Boyd, A.; Killoran, K.; Mitre, E.; Nutman, T.B. Pleural cavity type 2 innate lymphoid cells precede th2 expansion in murine *Litomosoides sigmodontis* infection. *Exp Parasitol* **2015**, *159*, 118-126.
212. Korten, S.; Volkmann, L.; Saeftel, M.; Fischer, K.; Taniguchi, M.; Fleischer, B.; Hoerauf, A. Expansion of NK cells with reduction of their inhibitory ly-49a, ly-49c, and ly-49g2 receptor-expressing subsets in a murine helminth infection: Contribution to parasite control. *Journal of Immunology* **2002**, *168*, 5199-5206.
213. Peng, J.; Siracusa, M.C. Basophils in antihelminth immunity. *Semin Immunol* **2021**, *53*, 101529.
214. Torrero, M.N.; Hubner, M.P.; Larson, D.; Karasuyama, H.; Mitre, E. Basophils amplify type 2 immune responses, but do not serve a protective role, during chronic infection of mice with the filarial nematode *Litomosoides sigmodontis*. *J Immunol* **2010**, *185*, 7426-7434.
215. Hartmann, W.; Linnemann, L.C.; Reitz, M.; Specht, S.; Voehringer, D.; Breloer, M. Basophils are dispensable for the control of a filarial infection. *Immunohorizons* **2018**, *2*, 296-304.
216. Galli, S.J.; Gaudenzio, N.; Tsai, M. Mast cells in inflammation and disease: Recent progress and ongoing concerns. *Annu Rev Immunol* **2020**, *38*, 49-77.
217. Linnemann, L.C.; Reitz, M.; Feyerabend, T.B.; Breloer, M.; Hartmann, W. Limited role of mast cells during infection with the parasitic nematode *Litomosoides sigmodontis*. *PLoS Negl Trop Dis* **2020**, *14*, e0008534.
218. Layland, L.E.; Ajendra, J.; Ritter, M.; Wiszniewsky, A.; Hoerauf, A.; Hubner, M.P. Development of patent *Litomosoides sigmodontis* infections in semi-susceptible C57BL/6 mice in the absence of adaptive immune responses. *Parasit Vectors* **2015**, *8*, 396.
219. Ramakrishnan, L. Revisiting the role of the granuloma in tuberculosis. *Nat Rev Immunol* **2012**, *12*, 352-366.

220. Tamarozzi, F.; Turner, J.D.; Pionnier, N.; Midgley, A.; Guimaraes, A.F.; Johnston, K.L.; Edwards, S.W.; Taylor, M.J. *Wolbachia* endosymbionts induce neutrophil extracellular trap formation in human onchocerciasis. *Sci Rep* **2016**, *6*, 35559.
221. Saeftel, M.; Volkmann, L.; Korten, S.; Brattig, N.; Al-Qaoud, K.; Fleischer, B.; Hoerauf, A. Lack of interferon-gamma confers impaired neutrophil granulocyte function and imparts prolonged survival of adult filarial worms in murine filariasis. *Microbes Infect* **2001**, *3*, 203-213.
222. Attout, T.; Martin, C.; Babayan, S.A.; Kozek, W.J.; Bazzocchi, C.; Oudet, F.; Gallagher, I.J.; Specht, S.; Bain, O. Pleural cellular reaction to the filarial infection *Litomosoides sigmodontis* is determined by the moulting process, the worm alteration, and the host strain. *Parasitology International* **2008**, *57*, 201-211.
223. Al-Qaoud, K.M.; Pearlman, E.; Hartung, T.; Klukowski, J.; Fleischer, B.; Hoerauf, A. A new mechanism for IL-5-dependent helminth control: Neutrophil accumulation and neutrophil-mediated worm encapsulation in murine filariasis are abolished in the absence of il-5. *Int Immunol* **2000**, *12*, 899-908.
224. Remion, E.; Gal, J.; Chaouch, S.; Rodrigues, J.; Lhermitte-Vallarino, N.; Alonso, J.; Kohl, L.; Hubner, M.P.; Fercoq, F.; Martin, C. Unbalanced arginine pathway and altered maturation of pleural macrophages in th2-deficient mice during *Litomosoides sigmodontis* filarial infection. *Front Immunol* **2022**, *13*, 866373.
225. Rivera, A.; Siracusa, M.C.; Yap, G.S.; Gause, W.C. Innate cell communication kick-starts pathogen-specific immunity. *Nat Immunol* **2016**, *17*, 356-363.
226. Hartmann, W.; Brunn, M.L.; Stetter, N.; Gabriel, G.; Breloer, M. Pre-existing helminth infection impairs the efficacy of adjuvanted influenza vaccination in mice. *PLoS One* **2022**, *17*, e0266456.
227. Babayan, S.A.; Read, A.F.; Lawrence, R.A.; Bain, O.; Allen, J.E. Filarial parasites develop faster and reproduce earlier in response to host immune effectors that determine filarial life expectancy. *PLoS Biol* **2010**, *8*, e1000525.
228. Ehrens, A.; Lenz, B.; Neumann, A.L.; Giarrizzo, S.; Reichwald, J.J.; Frohberger, S.J.; Stamminger, W.; Buerfent, B.C.; Fercoq, F.; Martin, C*., et al.* Microfilariae trigger eosinophil extracellular DNA traps in a dectin-1-dependent manner. *Cell Rep* **2021**, *34*, 108621.
229. Attout, T.; Babayan, S.; Hoerauf, A.; Taylor, D.W.; Kozek, W.J.; Martin, C.; Bain, O. Blood-feeding in the young adult filarial worms *Litomosoides sigmodontis. Parasitology* **2005**, *130*, 421-428.
230. Zmora, N.; Bashiardes, S.; Levy, M.; Elinav, E. The role of the immune system in metabolic health and disease. *Cell Metab* **2017**, *25*, 506-521.
231. Perl, A. Review: Metabolic control of immune system activation in rheumatic diseases. *Arthritis Rheumatol* **2017**, *69*, 2259-2270.
232. Levy, M.; Kolodziejczyk, A.A.; Thaiss, C.A.; Elinav, E. Dysbiosis and the immune system. *Nat Rev Immunol* **2017**, *17*, 219-232.
233. Arner, E.N.; Rathmell, J.C. Metabolic programming and immune suppression in the tumor microenvironment. *Cancer Cell* **2023**, *41*, 421-433.
234. Noack, S.; Harrington, J.; Carithers, D.S.; Kaminsky, R.; Selzer, P.M. Heartworm disease - overview, intervention, and industry perspective. *Int J Parasitol Drugs Drug Resist* **2021**, *16*, 65-89.
235. Liu, M.; Guo, S.; Stiles, J.K. The emerging role of CXCL10 in cancer (review). *Oncol Lett* **2011**, *2*, 583-589.
236. Paul, W.E. Interleukin-4: A prototypic immunoregulatory lymphokine. *Blood* **1991**, *77*, 1859-1870.
237. Van Dyken, S.J.; Locksley, R.M. Interleukin-4- and interleukin-13-mediated alternatively activated macrophages: Roles in homeostasis and disease. *Annu Rev Immunol* **2013**, *31*, 317-343.

238. Luzina, I.G.; Keegan, A.D.; Heller, N.M.; Rook, G.A.; Shea-Donohue, T.; Atamas, S.P. Regulation of inflammation by interleukin-4: A review of "alternatives". *J Leukoc Biol* **2012**, *92*, 753-764.
239. Takatsu, K. Interleukin-5. *Curr Opin Immunol* **1992**, *4*, 299-306.
240. Liew, F.Y.; Girard, J.P.; Turnquist, H.R. Interleukin-33 in health and disease. *Nat Rev Immunol* **2016**, *16*, 676-689.
241. Van Oosterhout, A.J.; Fattah, D.; Van Ark, I.; Hofman, G.; Buckley, T.L.; Nijkamp, F.P. Eosinophil infiltration precedes development of airway hyperreactivity and mucosal exudation after intranasal administration of interleukin-5 to mice. *J Allergy Clin Immunol* **1995**, *96*, 104-112.
242. Kraneveld, A.D.; Nijkamp, F.P.; Van Oosterhout, A.J. Role for neurokinin-2 receptor in interleukin-5-induced airway hyperresponsiveness but not eosinophilia in guinea pigs. *Am J Respir Crit Care Med* **1997**, *156*, 367-374.
243. Beckert, H.; Meyer-Martin, H.; Buhl, R.; Taube, C.; Reuter, S. Single and synergistic effects of type 2 cytokines on eosinophils and asthma hallmarks. *J Immunol* **2020**, *204*, 550-558.
244. Diemert, D.J.; Pinto, A.G.; Freire, J.; Jariwala, A.; Santiago, H.; Hamilton, R.G.; Periago, M.V.; Loukas, A.; Tribolet, L.; Mulvenna, J.*, et al.* Generalized urticaria induced by the *Na*-asp-2 hookworm vaccine: Implications for the development of vaccines against helminths. *J Allergy Clin Immunol* **2012**, *130*, 169-176 e166.
245. Wiria, A.E.; Sartono, E.; Supali, T.; Yazdanbakhsh, M. Helminth infections, type-2 immune response, and metabolic syndrome. *PLoS Pathog* **2014**, *10*, e1004140.
246. Herbert, D.R.; Douglas, B.; Zullo, K. Group 2 innate lymphoid cells (ilc2): Type 2 immunity and helminth immunity. *Int J Mol Sci* **2019**, *20*, 2276.
247. Pulendran, B.; Artis, D. New paradigms in type 2 immunity. *Science* **2012**, *337*, 431-435.
248. Iwasaki, A.; Medzhitov, R. Control of adaptive immunity by the innate immune system. *Nat Immunol* **2015**, *16*, 343-353.
249. Ruggeri, M.; Signorini, A.; Caravaggio, S. Casirivimab and imdevimab: Cost-effectiveness analysis of the treatment based on monoclonal antibodies on outpatients with covid-19. *PLoS One* **2023**, *18*, e0279022.
250. Kastner, R.J.; Sicuri, E.; Stone, C.M.; Matwale, G.; Onapa, A.; Tediosi, F. How much will it cost to eradicate lymphatic filariasis? An analysis of the financial and economic costs of intensified efforts against lymphatic filariasis. *PLoS Negl Trop Dis* **2017**, *11*, e0005934.
251. Di Pasquale, A.; Preiss, S.; Tavares Da Silva, F.; Garcon, N. Vaccine adjuvants: From 1920 to 2015 and beyond. *Vaccines (Basel)* **2015**, *3*, 320-343.
252. Mallory, R.M.; Formica, N.; Pfeiffer, S.; Wilkinson, B.; Marcheschi, A.; Albert, G.; McFall, H.; Robinson, M.; Plested, J.S.; Zhu, M.*, et al.* Safety and immunogenicity following a homologous booster dose of a sars-cov-2 recombinant spike protein vaccine (nvx-cov2373): A secondary analysis of a randomised, placebo-controlled, phase 2 trial. *Lancet Infect Dis* **2022**, *22*, 1565-1576.